

ISSN: 3041-0746 (Print)  
ISSN: 3029-2573 (Online)

# International Journal of AI for Materials and Design

Volume 2 • Issue 2  
June 2025

*Rethinking Industrial AI*

**Rethinking industrial artificial intelligence:  
A unified foundation framework**

Jay Lee, Hanqi Su

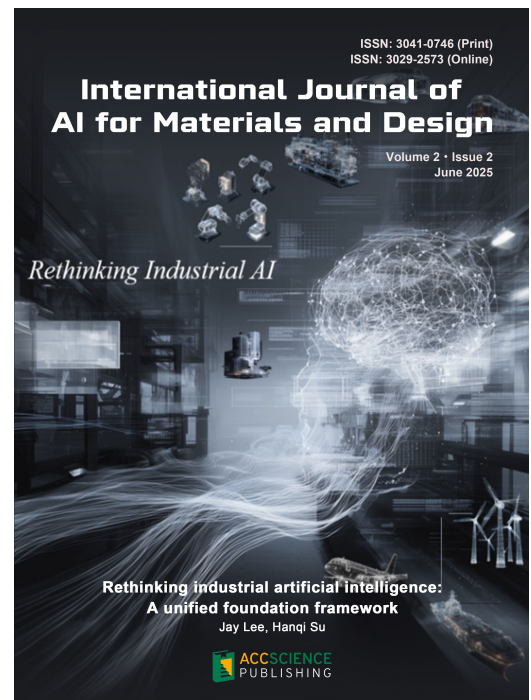
 **ACCSCIENCE**  
PUBLISHING

# International Journal of AI for Materials and Design

Print ISSN: 3041-0746

Online ISSN: 3029-2573

*The International Journal of AI for Material and Design (IJAMD)* is a scholarly publication dedicated to advancing the intersection of artificial intelligence (AI), materials science and design. This peer-reviewed journal provides a platform for researchers, academics, and industry professionals to disseminate cutting-edge research, innovative methodologies, and practical applications that leverage AI techniques to enhance the understanding, development, and optimization of aspects related to materials and design processes. IJAMD seeks to contribute to the advancement of technology, innovation, and sustainability in materials design, engineering disciplines, product manufacturing and process technology.



## About the Publisher

AccScience Publishing is a publishing company based in Singapore. We publish a range of high-quality, open-access, peer-reviewed journals and books from a broad spectrum of disciplines.

### Contact Us

Managing Editor

ijamd.office@accscience.sg

AccScience Publishing

9 Raffles Place, Republic Plaza 1 #06-00 Singapore 048619.

Volume 2 • Issue 2 • June 2025  
ISSN 3041-0746 (print) ISSN 3029-2573 (online)

# INTERNATIONAL JOURNAL OF AI FOR MATERIALS AND DESIGN

**Editor-in-Chief**

**Wai Yee Yeong**

*Nanyang Technological University,  
Singapore*



Access Science Without Barriers

**Full issue copyright © 2025 AccScience Publishing**

All rights reserved. Without permission in writing from the publisher, this full issue publication in its entirety may not be reproduced or transmitted for commercial purposes in any form or by any means, electronic or mechanical, including photocopying, recording, or any information storage and retrieval system. Permissions may be sought from [ijamd.office@accscience.sg](mailto:ijamd.office@accscience.sg).

**Article copyright © Respective Author(s)**

See articles for copyright year. All articles in this full issue publication are open-access. There are no restrictions in the distribution and reproduction of individual articles, provided the original work is properly cited. However, permission to reuse copyrighted materials of an article for commercial purposes is applicable if the article is licensed under Creative Commons Attribution-NonCommercial License. Check the specific license before reusing.

***International Journal of AI for Materials and Design***

ISSN: 3041-0746 (print)

ISSN: 3029-2573 (online)

**Editorial and Production Credits**

Publisher: AccScience Publishing

Managing Editor: Shirley Lu

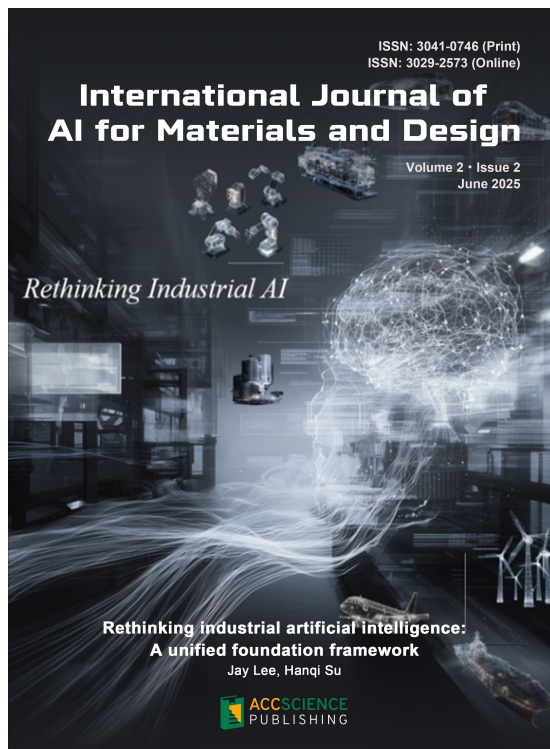
Production Editor: Sharmila Velapasamy

Article Layout and Typeset: Sinjore Technologies (India)

For all advertising queries, contact  
[ijamd.office@accscience.sg](mailto:ijamd.office@accscience.sg).

**Supplementary file**

Supplementary files of articles can be obtained at  
<https://accscience.com/journal/IJAMD/2/2>.



**Disclaimer**

AccScience Publishing is not liable to the statements, perspectives, and opinions contained in the publications. The appearance of advertisements in the journal shall not be construed as a warranty, endorsement, or approval of the products or services advertised and/or the safety thereof. AccScience Publishing disclaims responsibility for any injury to persons or property resulting from any ideas or products referred to in the publications or advertisements. AccScience Publishing remains neutral with regard to jurisdictional claims in published maps and institutional affiliations.

# International Journal of AI for Materials and Design

## Editorial Board

### **Editor-in-Chief**

Wai Yee Yeong, *Singapore*

### **Associate Editor**

Shweta Agarwala, *Denmark*

### **Editorial Board**

#### **Members\***

Antonio Gloria, *Italy*

Faris M. Al-Oqla, *Jordan*

Mehdi Amiri, *USA*

Ruzena Bajcsy, *USA*

Valentina E. Balas, *Romania*

Michail Beliatas, *Denmark*

Filippo Berto, *Italy*

Dermot Brabazon, *Ireland*

Ilaria Cacciotti, *Italy*

Yanlong Cao, *China*

Danni Chang, *China*

Chongdu Cho, *Korea*

Alfredo Cuzzocrea, *Italy*

Gianni D'Angelo, *Italy*

Frédéric Demoly, *France*

Shi Xue Dou, *Australia*

Zhimin Du, *China*

Mohammad Elahinia, *USA*

Gerd Grau, *Canada*

Qi Gu, *China*

Mohammad Heidari-Rarani, *Iran*

Im Doo Jung, *South Korea*

Seong Su Kim, *South Korea*

Hyunwoong Ko, *USA*

A. Senthil Kumar, *Singapore*

Panagiotis Kyratsis, *Greece*

Pascal LORENZ, *France*

Jay Lee, *USA*

Xiaopeng Li, *Australia*

Weifu Li, *China*

Zhong Alan Li, *Hong Kong*

Kaili Lin, *China*

Xu Long, *China*

Jianxi Luo, *Singapore*

Dragan Marinkovic, *Germany*

Abbas Milani, *Canada*

Chilukuri K. Mohan, *USA*

Seung Ki Moon, *Singapore*

Nezih Mrad, *Canada*

Tuhin Mukherjee, *USA*

Roger Narayan, *USA*

Ping Feng Pai, *Taiwan (China)*

Stefanos Papanikolaou, *Poland*

Radu-Emil Precup, *Romania*

Seunghwa Ryu, *South Korea*

Sonal Shreya, *Denmark*

Swee Leong Sing, *Singapore*

Anil Srivastava, *USA*

Tino Stankovic, *Switzerland*

Ephraim Suhir, *USA*

Gyorgy Szekely, *Saudi Arabia*

Jeanne Tan, *China*

Ehsan Toyserkani, *Canada*

Man Pun Wan, *Singapore*

Pan Wang, *Singapore*

Shenghao Wang, *China*

Hao Wang, *China*

Dazhong Wu, *USA*

Kentaro Yaji, *Japan*

W. Hong Yeo, *USA*

Jingjie Yeo, *USA*

Zhen Yuan, *China*

Y. Shrike Zhang, *USA*

Xing Zhang, *China*

Yicha Zhang, *France*

Pai Zheng, *China*

Junxing Zheng, *China*

Hongxiang Zong, *China*

### **Assistant Editors**

Nehru Devabharathi, *India*

Wei Long Ng, *Singapore*

### **Youth Editorial Board**

#### **Members**

Murali Mohan Cheepu, *Korea*

Zhen Liu, *USA*

Faez Masurkar, *UAE*

Haoyuan Shi, *USA*

Jinlong Su, *Singapore*

Yutai Su, *China*

Bijun Tang, *Singapore*

César M. A. Vasques, *Portugal*

### **Co-Guest Editors**

Xiaorui Liu, *USA*

Liming Tan, *China*

Liang Wang, *China*

Kun Zhou, *Singapore*

### **Guest Editor**

Dong Wang, *China*

\*Editorial Board Members as of June 24, 2025

## CONTENTS

### REVIEW ARTICLES

- 1**      **Artificial intelligence-driven material development for additive manufacturing: A critical review**  
*Peijie Shangguan, Huifei Zhou, Xi Huang, Jinlong Su, Wai Yee Yeong, Swee Leong Sing*
- 27**     **Advancing intelligent additive manufacturing: Machine learning approaches for process optimization and quality control**  
*Hayeol Kim, Kyung-Hwan Kim, Jiyun Jeong, Hongryung Jeon, Im Doo Jung*

### PERSPECTIVE ARTICLE

- 56**     **Rethinking industrial artificial intelligence: A unified foundation framework**  
*Jay Lee, Hanqi Su*

### ORIGINAL RESEARCH ARTICLES

- 69**     **Prediction of the lack-of-fusion defect of laser powder bed fusion based on deep learning**  
*Lidong Wang*
- 79**     **Automated fruit sorting system integrating image processing and support vector machine techniques**  
*Babatunde Olayinka Oyefeso, Oluwaseun Emmanuel Oyewande, John Audu*

## REVIEW ARTICLE

Artificial intelligence-driven material  
development for additive manufacturing: A  
critical reviewPeijie Shangguan<sup>1</sup>, Huifei Zhou<sup>1</sup>, Xi Huang<sup>2</sup>, Jinlong Su<sup>1\*</sup>,  
Wai Yee Yeong<sup>2</sup>, and Swee Leong Sing<sup>1\*</sup><sup>1</sup>Department of Mechanical Engineering, College of Design and Engineering, National University of Singapore, Singapore<sup>2</sup>School of Mechanical and Aerospace Engineering, Nanyang Technological University, Singapore(This article belongs to *Special Issue: Artificial Intelligence Applications in Additive Manufacturing and 3D Printing*)

## Abstract

Additive manufacturing (AM) has revolutionized material fabrication by enabling the production of complex structures with enhanced design flexibility and material efficiency. However, the development of AM-specific materials remains a critical challenge due to the unique process characteristics of AM. Recent advancements in artificial intelligence (AI), for example, machine learning and deep learning, have emerged as powerful tools in accelerating material discovery, optimizing process parameters, and improving material performance for AM. This review provides a comprehensive overview of AI-driven material development for AM, focusing on metals, polymers, and bioinks/biomaterial inks. The discussion encompasses AI techniques applied to material development, including predictive modeling, generative algorithms, and intelligent optimization methods. Data collection and pre-processing methodologies for AI applications in AM are discussed. In addition, the applications of AI in material development in AM are also reviewed. Finally, the review highlights emerging trends, such as AI-driven high-throughput material screening, integration of AI with multiscale high-fidelity simulations, the use of digital twins for real-time process control, and active learning strategies for optimizing material compositions. By summarizing recent advancements and outlining future directions, this review provides insights into the evolving intersection of AI and AM, paving the way for more intelligent and efficient material development in the next generation of manufacturing.

**Keywords:** Artificial intelligence; Additive manufacturing; Machine learning; Material design; Performance optimization; Bioprinting

## 1. Introduction

Additive manufacturing (AM) has revolutionized modern manufacturing by enabling the layer-by-layer fabrication of complex structures with high precision and design flexibility.<sup>1</sup> This approach minimizes or even eliminates the need for extensive

**\*Corresponding authors:**Jinlong Su  
(jinlongsu96@foxmail.com)  
Swee Leong Sing  
(sweeleong.sing@nus.edu.sg)**Citation:** Shangguan P, Zhou H, Huang X, Su J, Yeong WY, Sing SL. Artificial intelligence-driven material development for additive manufacturing: A critical review. *Int J AI Mater Design*. 2025;2(2):1-26. doi: 10.36922/IJAMD025100007**Received:** March 5, 2025**1st revised:** April 3, 2025**2nd revised:** April 11, 2025**Accepted:** April 16, 2025**Published online:** May 5, 2025**Copyright:** © 2025 Author(s). This is an Open-Access article distributed under the terms of the Creative Commons Attribution License, permitting distribution, and reproduction in any medium, provided the original work is properly cited.**Publisher's Note:** AccScience Publishing remains neutral with regard to jurisdictional claims in published maps and institutional affiliations.

machining, thereby significantly improving material utilization efficiency.<sup>2</sup> As a general term encompassing various techniques, AM has been adopted across multiple industries, including aerospace, biomedical, and automotive sectors. Each AM technique, whether designed for metals, polymers, or bioinks/biomaterial inks, operates under distinct processing principles that influence the manufacturability and performance of fabricated components.<sup>3,4</sup>

Designing and optimizing materials for AM remains a challenging task, as it has traditionally relied on heuristic-driven trial-and-error methods that are both time-consuming and resource-intensive. These conventional approaches struggle to efficiently navigate the complex and non-linear relationships between processing conditions, microstructure evolution, and resulting material properties. Moreover, most existing materials were originally developed for conventional manufacturing techniques and are often not suitable for AM, leading to issues such as poor printability, defect formation, and variability in mechanical performance.<sup>5,6</sup> The growing need for AM-specific materials with tailored functionalities demands a paradigm shift in how materials are discovered and developed. In this context, artificial intelligence (AI) offers powerful capabilities to handle high-dimensional datasets, identify hidden patterns, and accelerate the design process by predicting material performance based on compositional and process parameters. By moving beyond empirical heuristics, AI-driven methods enable more systematic and scalable exploration of the vast design space, offering a promising alternative to traditional approaches.

In recent years, AI has demonstrated remarkable success in media applications based on image and voice big data, and it has recently expanded into diverse fields, such as medicine, education, and engineering.<sup>7,8</sup> Its ability to analyze vast datasets, identify complex patterns, and make predictive decisions has also positioned AI as a powerful tool in scientific and industrial applications, including materials science. In particular, AI has emerged as a transformative tool in accelerating materials development for AM. By leveraging data-driven approaches, AI enables the prediction of material properties, optimization of alloy compositions, and exploration of new material spaces with reduced experimental effort. AI-driven methods facilitate the rapid identification of processable materials with tailored properties, improving the efficiency of AM applications across metals, polymers, and bioinks/biomaterial inks. As AM continues to evolve toward more sophisticated and customized applications, AI-driven material development plays an increasingly vital role in bridging the gap between

computational design and experimental realization. The increasing research interest in this field is reflected in the growing number of AI-driven AM publications over the past decade, as illustrated in [Figure 1](#).

Given the growing importance of AI in materials discovery for AM, this review aims to provide a critical assessment of recent advancements in AI-driven material development across different AM material categories. Unlike many existing reviews that predominantly focus on *in situ* monitoring, process control, or the printability assessment of feedstock materials using AI,<sup>9</sup> this review specifically emphasizes AI-driven material development. We adopt a narrow definition of material development, which centers on the design and optimization of material properties or compositions, excluding applications solely related to manufacturability, defect detection, or geometry control. This focused perspective highlights the unique role of AI in accelerating the discovery and tailoring of materials for AM. The framework of the review is presented in [Figure 2](#). The discussion covers data collection and pre-processing methods, AI-enabled material development strategies, and key applications in AM. By summarizing recent progress and highlighting existing challenges, this review seeks to offer insights into the evolving intersection of AI and AM materials development, paving the way for future innovations in this field.

## **2. Overview of various AM techniques and the need for material development**

There are various AM techniques that enable the fabrication of complex structures. Each AM technique imposes distinct material requirements, influencing processing feasibility and final part performance. This section provides a concise description of seven key AM techniques ([Figure 3](#)), their material requirements, and challenges in material development.

### **2.1. Vat photopolymerization (VPP)**

The VPP process is an AM technology based on a liquid photosensitive resin, which is cured layer by layer using a light source, resulting in a solid 3D part. Several variations of VPP exist, including stereolithography, digital light processing, two-photon polymerization, and volumetric 3D printing.<sup>11</sup> Commonly employed light sources include laser, digital light projection, and LED systems, offering varying resolutions and processing speeds.<sup>12</sup> VPP is capable of achieving micron- to nanometer-scale resolution, making it well-suited for manufacturing components requiring high dimensional accuracy and superior surface quality.<sup>13</sup> This technique has been widely applied

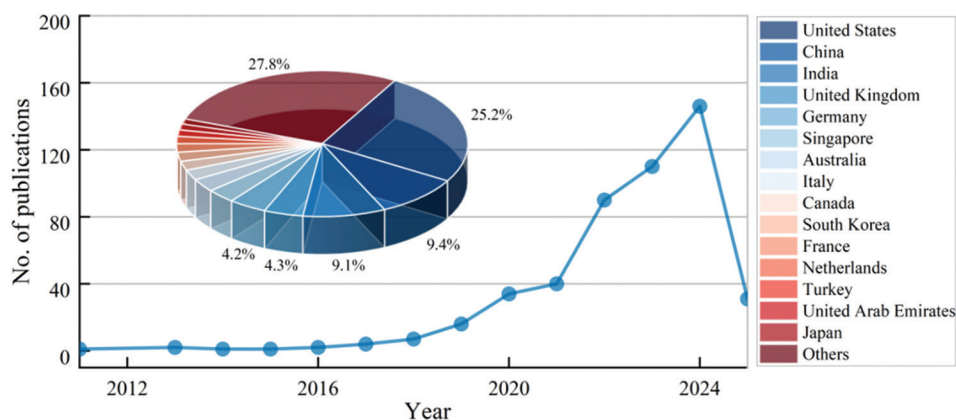


Figure 1. Research and development trends are reflected by the number of publications in the field of machine learning for material design of AM (data acquired from the Scopus database)

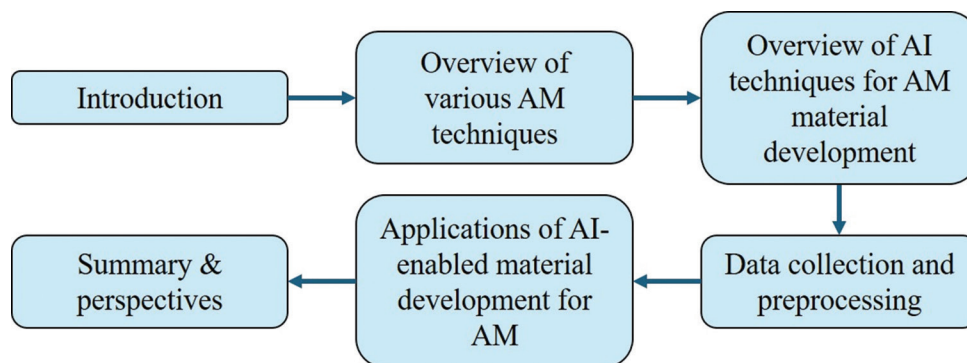


Figure 2. The framework of this work  
Abbreviations: AI: Artificial intelligence; AM: Additive manufacturing.

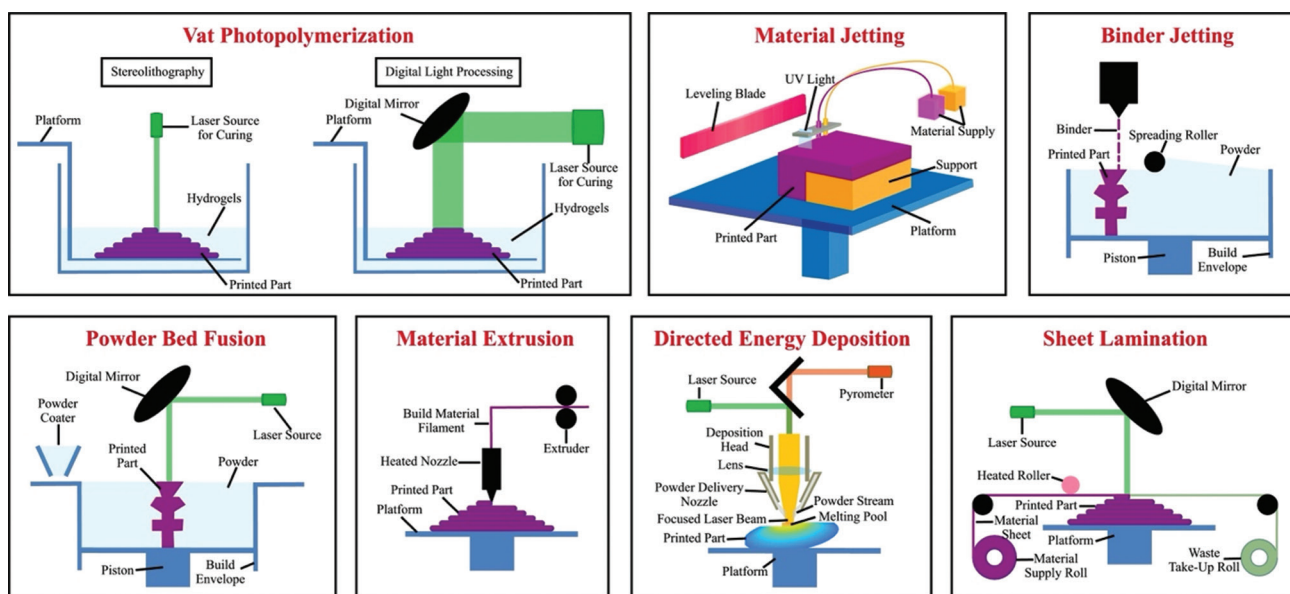


Figure 3. Categories of additive manufacturing techniques. Reproduced from Jin *et al.*<sup>10</sup>

in industrial engineering, regenerative medicine, smart materials, and both nano- and micro-scale manufacturing.

It also holds significant promise for emerging applications such as 4D printing and bioprinting.<sup>12</sup>

## 2.2. Material jetting (MJT)

MJT operates similarly to inkjet printing, where liquid materials are deposited as microdroplets through a print head and cured by ultraviolet light to build a structure.<sup>14</sup> The process utilizes two types of materials: Build material, which forms the final part, and support material, which provides structural integrity during printing and is later removed through dissolution. MJT technology has the advantages of high resolution, multi-material printing capability,<sup>15</sup> and the ability to fabricate intricate geometries, surpassing material extrusion (MEX), binder jetting (BJT), and powder bed fusion (PBF) in surface accuracy.<sup>16</sup> It is widely applied in aerospace, biomedical, dental, and mechanical engineering.<sup>16</sup>

## 2.3. BJT

BJT constructs 3D structures by selectively depositing a liquid binder onto a powder bed, gradually bonding the material to form the desired shape. Unlike other AM methods, BJT does not require a heat source, such as a laser or electron beam, making it a more cost-effective approach.<sup>17</sup> BJT-printed parts are self-supporting, eliminating the need for support structures and enabling the simultaneous fabrication of multiple components.<sup>13</sup> However, the printed parts often exhibit lower mechanical strength, necessitating post-processing treatments, such as sintering or infiltration, to improve material performance.<sup>13</sup> BJT is widely applied in biomedical engineering,<sup>18</sup> mold casting,<sup>19</sup> and food technology.<sup>20</sup>

## 2.4. PBF

PBF is a widely adopted AM process, primarily used for metals<sup>21</sup> and polymers,<sup>22</sup> with limited applications in ceramics and composites.<sup>13</sup> It has several different terms, including selective laser sintering, electron beam melting, selective laser melting, and direct metal laser sintering. PBF utilizes a powder bed, where the material is selectively fused using a laser or electron beam, with layer deposition and fusion repeating until the final structure is formed. An inert gas-protective environment is often needed to prevent oxidation.

Despite its widespread use, materials used for PBF still primarily derive from commercially available materials, which were not originally designed for AM, leading to several key challenges.<sup>23</sup> Many existing commercial alloys (e.g., 7075Al alloy, H13 tool steel, Inconel718 nickel-based superalloy, and CoCrFeMnNi Cantor high-entropy alloy) are prone to hot cracking and defect formation, compromising part integrity and limiting their applicability. In addition, controlling microstructure evolution remains a critical issue, as rapid solidification

and complex thermal histories have a critical influence on grain structure, dislocation evolution, and phase transformation behavior. To overcome these limitations, advancements in AM-specific material development are essential to optimize phase stability, enhance mechanical properties, and, in particular, ensure reproducibility.

## 2.5. Material extrusion

In MEX, a material is first heated to its melting point, then extruded as a filament, and finally deposited to form a structure. Two common MEX methods include fused deposition modeling (FDM) and direct ink writing (DIW). FDM relies on thermoplastic filaments that are melted and extruded, making it widely used for rapid prototyping, educational applications, and engineering part fabrication due to its low cost, ease of handling, and ability to print with multiple materials. In contrast, DIW involves extruding high-viscosity inks, pastes, or gels, enabling the fabrication of soft materials, ceramics, and bioprinted structures. Due to its low cost, ease of handling, and capability for multi-material printing, MEX is well-suited for rapid prototyping, educational applications, and engineering part fabrication.<sup>13</sup> However, its relatively low resolution limits its suitability for small-scale or highly detailed components. At present, the MEX process is widely used in medical modeling, engineering parts, prototyping, tissue engineering, and bioprinting devices.<sup>24</sup>

## 2.6. Directed energy deposition (DED)

DED melts and deposits materials simultaneously using a high-energy heat source, such as a laser beam or arc.<sup>13</sup> The process utilizes powder or wire as feedstock, with material introduced into a molten pool during printing. Multi-axis motion control enables complex geometries, making DED suitable for metallic multi-materials, functional gradient materials, composite fabrication, and component repair.<sup>25</sup> Notably, DED is primarily used for metallic materials and offers a significantly higher deposition rate than PBF, making it favorable for large-format component fabrication.

Despite its versatility, DED material design remains complex because the rapid solidification leads to non-equilibrium microstructures, affecting phase stability, residual stress, and mechanical performance.<sup>25</sup> Similar to PBF, most alloys used in DED are legacy alloys originally designed for conventional manufacturing methods, limiting the full exploration of DED's potential. This underscores the critical need for developing AM-specific materials to fully leverage the capabilities of these AM techniques.

## 2.7. Sheet lamination (SHL)

SHL constructs 3D parts by stacking and bonding material layers, which are cut using laser or mechanical

cutters. The process follows two main approaches: Bond-then-form and form-then-bond.<sup>13</sup> Compared to other AM techniques, SHL offers cost-effective material usage and rapid processing, making it particularly suited for large and thick components.<sup>26</sup> In addition, SHL does not require support structures, enabling the fabrication of complex geometries directly.<sup>26</sup> SHL has also shown various applications in aerospace,<sup>27</sup> automotive,<sup>28</sup> medical,<sup>29</sup> and bioengineering fields.<sup>30</sup>

### 3. Overview of AI techniques for AM material development

The advancement of AI has significantly influenced traditional manufacturing, enhancing the productivity, efficiency, and flexibility of AM.<sup>31</sup> This section explores three major categories of AI techniques for material development, analyzing their applications in materials

development, as illustrated in Figure 4. Table 1 summarizes the common AI methods employed across different stages of AM, including their typical applications, strengths, and limitations.

#### 3.1. Machine learning (ML)

ML, a subset of AI, is primarily categorized into supervised learning, unsupervised learning, and reinforcement learning, enabling computers to learn from data without explicit programming.<sup>32</sup> Common ML methods include k-nearest neighbor and support vector machine.

ML has been increasingly applied to conventional materials development. For example, Dang *et al.*<sup>33</sup> used the support vector regression model to predict the fatigue life of titanium alloys by analyzing their microstructural characteristics, including the stress intensity near the holes and the type of holes. Besides, Ling *et al.*<sup>34</sup> used the

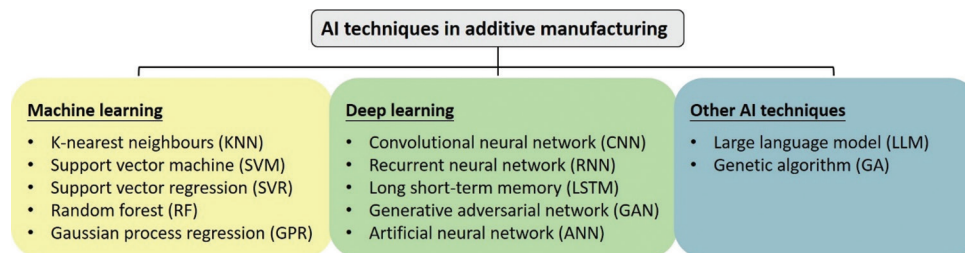


Figure 4. Categories of AI techniques in additive manufacturing  
Abbreviation: AI: Artificial intelligence.

Table 1. Summary of common AI methods, applications, strengths, and limitations across key AM steps

AM steps	Common AI methods	Typical applications	Strengths	Limitations
AM design	RF, SVM, NNs, Lasso/elastic net regression, GA, feed-forward NN, Bayesian inference, hierarchical clustering	Feature recommendation, part mass, and cost prediction, build time estimation, topology design, thermal compensation, shape deviation prediction	RF is robust to noisy data; SVM is effective with small datasets; GA enables global search; NNs capture complex non-linear relations	NNs require large datasets and long training; SVMs are sensitive to kernel settings; GA can be time-consuming; RF may bias toward dominant features
AM process and performance optimization	Back propagation NN, SOM, LS-SVM, GPR, Kriging, GA	Melt pool depth/width prediction, powder spreading, strength/hardness estimation, porosity and density prediction	NNs capture complex non-linearities; GPR provides uncertainty quantification; GA is good for multi-objective optimization	GPR scales poorly; NNs are data-hungry; GA performance depends on parameter tuning
<i>In situ</i> process monitoring and control	NN, SVM, Naive Bayes clustering, CNNs, deep belief networks (deep learning), K-means	Porosity and defect detection, anomaly detection, spatter classification, acoustic emission analysis, multi-sensor fusion, CT-aided defect identification	Probabilistic models handle uncertainty; CNNs/deep belief networks are excellent for sensor/image data; clustering helps early-stage pattern recognition	Deep models are computationally demanding; clustering accuracy may be low; Naive Bayes assumes feature independence
Testing and validation	Sparse representation, KNN, Naive Bayes clustering, SVM, decision trees	Point cloud-based dimensional analysis, defect classification (e.g., porosity)	KNN is simple and intuitive; SVMs are robust; sparse models are suited to high-dimensional data	KNN suffers in high dimensions; decision trees overfit easily; sparse models require careful tuning

Abbreviations: CNN: Convolutional neural network; CT: Computed tomography; GA: Genetic algorithm; GPR: Gaussian process regression; KNN: K-nearest neighbor; NNs: Neural networks; LS-SVM: Least squares support vector machine; RF: Random forest; SOM: Self-organizing map; SVM: Support vector machine; AI: Artificial intelligence; AM: Additive manufacturing.

random forest (RF) algorithm to predict the fatigue life of a steel sample by analyzing a fatigue test dataset of 439 steels containing nine alloying elements, and from the 437 possible combinations to select the composition and treatment of steel with the best fatigue life. In addition, Navarrete *et al.*<sup>35</sup> used ML models to predict the static yield stress of mixed cement pastes containing supplementary cementitious materials by collecting datasets from previous experimental work, and have compared the prediction accuracies of different ML models, including multilayer perceptron, RF, and support vector regression.

These studies, although not related to AM, have demonstrated the capabilities of ML in material property prediction and process optimization. By extracting complex relationships from extensive experimental datasets, ML models improve decision-making, process efficiency, and reliability. As ML techniques continue to evolve, their integration with computational modeling and experimental validation will further accelerate the design of next-generation materials and enhance manufacturing intelligence.

### 3.2. Deep learning (DL)

DL leverages multilayer neural networks to extract features, identify patterns, and model complex relationships in high-dimensional data.<sup>36</sup> Compared to traditional ML methods, DL excels in automatic feature learning, making it particularly effective for image-based analysis, sequential data modeling, and generative design. Common DL architectures include convolutional neural networks (CNNs), recurrent neural networks, long short-term memory, generative adversarial networks (GANs), and artificial neural networks (ANNs).

DL extends data-driven approaches in material development, playing a key role in microstructure-property correlation, process design, and automated material discovery. For example, Gu *et al.*<sup>37</sup> used DL for the design of layered materials and trained a finite element analysis (FEA) model to obtain high-performance materials. Specifically, CNN was used to predict the mechanical properties of composites and combined it with a self-learning algorithm to optimize the design of the materials. Li *et al.*<sup>38</sup> investigated the joint effects of the size, depth, distribution, and orientation of defects on the fatigue life of AM-built Ti-6Al-4V alloys by constructing an ANN-based model, revealing how these factors interact with each other, which in turn affects the durability of the Ti-6Al-4V alloy. Shen and Buehler<sup>39</sup> developed a novel unsupervised GANs (specifically StyleGAN) approach, trained with input unlabeled data, to construct a latent space that is free to be explored for material design without

human intervention. Lee *et al.*<sup>40</sup> used the GAN model to generate additional data to solve the problem of insufficient samples, which successfully improved the accuracy of the phase prediction of high-entropy alloys and revealed the key design parameters, providing a new insight for the design and discovery of high-entropy alloys.

### 3.3. Other AI techniques

Large language models (LLMs) are a class of AI models extensively applied in natural language processing. LLMs capture complex linguistic patterns and structures, enabling multilingual processing and contextual understanding. Their capabilities extend beyond language applications, with emerging studies demonstrating their potential in materials science and engineering. For example, Buehler<sup>41</sup> developed MechGPT, an LLM-based framework designed to simulate and analyze mechanical behavior and failure mechanisms, improving the predictive accuracy of material properties and supporting the design of novel materials.

Genetic algorithms (GA) provide an effective strategy for global optimization, employing selection, mutation, and crossover to explore complex solution spaces. In the study of Shen and Buehler,<sup>39</sup> they used GA to further optimize the microstructure of the model-designed materials to improve their mechanical properties. Nazar *et al.*,<sup>42</sup> on the other hand, combined GA with the gene expression concept to develop a new gene expression programming model to predict the plastic viscosity and yield stress of fresh concrete used for the MEX process by analyzing six key factors, such as cement, sand, water, different sizes of coarse aggregate, and superplasticizers, to improve the accuracy and efficiency of predicting the rheological parameters of concrete.

## 4. Data collection and pre-processing

A typical workflow of AI-driven material development in AM is illustrated in [Figure 5](#). The workflow begins with the collection of raw data from various sources, such as simulations, experiments, literature, and databases. The raw data undergoes pre-processing to refine it for AI applications. Subsequently, AI algorithms are applied to train models that predict material behavior or suggest optimal material compositions. The workflow iteratively integrates feedback from experiments and simulations to refine the dataset and improve prediction accuracy.

Data collection and pre-processing are fundamental to the successful implementation of this workflow. High-quality and comprehensive datasets enable AI models to identify underlying correlations and outliers that would be difficult to discern through traditional analysis. However, the heterogeneity and complexity of data sources –

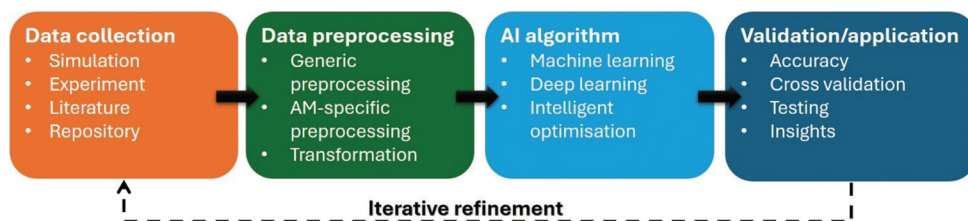


Figure 5. Workflow for artificial intelligence-driven material development in additive manufacturing

ranging from atomic-scale simulations to experimental measurements – present significant challenges. These challenges include inconsistencies in data formats, missing and noisy values, and variability in measurement techniques. Pre-processing mitigates these issues by standardizing and transforming raw data, ensuring its compatibility with AI algorithms.

### 4.1. Data collection

Data for material development are primarily derived from simulations and/or physical experiments. Overall, the types of datasets for material development can be broadly categorized into scalar, time-series, spectral, image, categorical, and spatial data. Scalar data represents single-value material properties, such as tensile strength and elastic modulus. Time-series data captures changes over time, such as stress-strain behavior during tensile testing. Spectral data reveals material composition and structure through techniques, such as X-ray diffraction. Image data mainly includes microstructure images, while categorical data describes qualitative attributes, such as phase and defect types. Spatial data represents geometries and positional relationships, including crystallographic texture. Table 2 summarizes the common types of data obtained through simulations and experiments.

Simulation plays a critical role in AI-driven material development by providing high-fidelity datasets that capture complex material behaviors and properties. These simulations are favorable for generating datasets that can support predictive modeling and validate AI-driven solutions. Commonly employed modeling methods include density functional theory (DFT), FEA, and computer coupling of phase diagrams and thermochemistry (CALPHAD). DFT is widely used for predicting electronic structures and thermodynamic properties. FEA focuses on macroscopic phenomena, such as stress-strain behavior and thermal conductivity under various conditions. CALPHAD, on the other hand, is instrumental in phase diagram calculations and thermodynamic modeling. Complementing simulation, experimental measurements provide essential data that capture the real-world behavior and performance of materials. These measurements not only validate simulation results but also offer unique

Table 2. Common data types and sources in material development

Data source	Data type	Examples
Experiment	Scalar	Ultimate tensile strength, hardness, relative density, and thermal conductivity
	Time-series	Stress-strain curve and thermography
	Spectral	X-ray diffraction, X-ray dispersive spectroscopy, X-ray photoelectron spectroscopy, and Raman spectroscopy
	Image	Scanning electron microscopy, transmission electron microscopy, and atomic force microscopy
	Categorical	Phase and defect
Simulation	Spatial	Crystallographic texture, pore distribution, and filler dispersion
	Scalar	Total energy (DFT), Gibbs free energy (CALPHAD), elastic modulus (DFT, FEM), and stress/strain (FEM)
	Time-series	Displacement evolution (FEM)
	Spectral	Density of states (DFT)
	Image	Charge density maps (DFT) and stress/strain field (FEM)
	Categorical	Phase regions (CALPHAD) and failure regions (FEM)
Spatial	Atomic position (DFT)	

Abbreviations: CALPHAD: Calculation of phase diagrams; DFT: Density functional theory; FEM: Finite element method.

empirical insights. Common techniques include property testing, microscopy, and spectroscopy.

In material development for AM, datasets are often sourced from literature, online databases, or experiments.<sup>43</sup> Table 3 summarizes the commonly used online data repositories. While online material databases provide valuable resources for material development, most existing repositories are primarily built upon data obtained through traditional manufacturing processes. Key aspects of AM, such as the rapid solidification, residual stresses, and complex microstructural evolution characteristics, are typically not captured. As a result, applying data from these repositories directly to AM may lead to inaccuracies,

**Table 3. Online repositories of materials**

Name	Description	Material	Source	Availability
AFLOWLIB.ORG <sup>44</sup>	High-throughput computational database for material properties, focusing on thermodynamics and electronic structures	Metals	DFT	<a href="http://aflow.org/">http://aflow.org/</a> (Free access)
Alloy database	Focused on structure and enthalpy of formation for alloy systems, including stable and metastable phases	Metals	DFT	<a href="http://alloy.phys.cmu.edu/">http://alloy.phys.cmu.edu/</a> (Free access)
ASM database	Comprehensive database on material properties, phase diagrams, and processing data	Metals, polymers	Experiment, CALPHAD	<a href="https://www.asminternational.org/">https://www.asminternational.org/</a> (License required)
CINDAS LLC	Provides critically evaluated databases for thermal, mechanical, electrical, and physical properties of materials, including aerospace alloys	Metals	Experiment	<a href="https://cindasdata.com/">https://cindasdata.com/</a> (License required)
Computational materials repository	Open platform for accessing materials property datasets derived from simulations, including thermodynamic and mechanical properties	Metals	DFT, MD	<a href="https://cmr.fysik.dtu.dk/">https://cmr.fysik.dtu.dk/</a> (Free access)
Crystallography open database <sup>45</sup>	Open-access collection of crystal structures of organic, inorganic, metal-organic compounds, and minerals	Metals	Experiment	<a href="http://www.crystallography.net/">http://www.crystallography.net/</a> (Free access)
Inorganic crystal structure database <sup>46</sup>	Curated database of crystallographic data for inorganic compounds; provides high-quality structural information for metals, ceramics, and minerals, with additional crystallographic parameters calculated	Metals	Experiment	<a href="https://icsd.fiz-karlsruhe.de/">https://icsd.fiz-karlsruhe.de/</a> (License required)
Joint Automated repository for various integrated simulations <sup>47</sup>	Comprehensive platform supporting the Materials Genome Initiative, designed to accelerate materials discovery for energy, electronics, and mechanical applications	Metals, polymers	DFT, MD, experiment	<a href="https://jarvis.nist.gov/">https://jarvis.nist.gov/</a> (Free access)
Knovel database	Engineering materials database covering properties, such as mechanical strength, thermal stability, and chemical behavior	Metals, polymers	Experiment	<a href="https://app.knovel.com/">https://app.knovel.com/</a> (License required)
Matmatch	Interactive platform designed for material selection, offering comprehensive datasets on material properties and enabling comparisons for engineering and design applications	Metals, polymers	Experiment	<a href="https://matmatch.com/">https://matmatch.com/</a> (Free access)
Materials-cloud <sup>48</sup>	Open-access platform for computational materials science, serving as a “repository of repositories” similar to GitHub; provides data sharing, simulation workflows, and educational resources to support reproducibility and collaboration	Metals	DFT	<a href="https://www.materialscloud.org/">https://www.materialscloud.org/</a> (Free access)
MatNavi	Comprehensive materials database platform featuring sub-databases for polymers (chemical structures, processing properties, and NMR spectra), inorganic materials (crystal structures, phase diagrams, and physical properties), metallic materials (density, elastic constants, and creep characteristics), and computational electronic structure data (band structures from first-principles calculations)	Metals, polymers	Experiment, CALPHAD, DFT	<a href="https://mits.nims.go.jp/">https://mits.nims.go.jp/</a> (Free access)
MatWeb	Searchable database providing detailed material property data for a wide range of engineering materials	Metals, polymers	Experiment	<a href="http://www.matweb.com/">http://www.matweb.com/</a> (Free access)

(Cont'd...)

Table 3. (Continued)

Name	Description	Material	Source	Availability
NIST DATA	Comprehensive repository offering experimental and computational material property data, including phase diagrams, thermophysical properties, and structural information	Metals, polymers	DFT, CALPHAD, MD, Monte Carlo, FEA, experiment	<a href="https://www.nist.gov/data/">https://www.nist.gov/data/</a> (License required for some datasets)
NOMAD repository <sup>49</sup>	Platform for computational materials science providing FAIR (Findable, Accessible, Interoperable, Reusable) data sharing; includes the world's largest repository of computational raw data, normalized into a code-independent format, enabling data mining and machine learning for materials discovery	Metals	DFT	<a href="https://nomad-lab.eu/">https://nomad-lab.eu/</a> (Free access)
NREL MatDB	Computational materials database with a specific focus on materials for renewable energy applications, including, but not limited to, photovoltaic materials, materials for photo-electrochemical water splitting, and thermoelectric	Metals	DFT	<a href="https://materials.nrel.gov/">https://materials.nrel.gov/</a> (Free access)
OpenKIM <sup>50</sup>	Curated repository of interatomic potentials and analytics for making classical molecular simulations of materials reliable, reproducible, and accessible	Metals	DFT, experiment	<a href="https://openkim.org/">https://openkim.org/</a> (Free access)
Predictive integrated structural materials science	Repository combining materials science data, models, and workflows to support advanced simulations	Metals	DFT, CALPHAD, experiment	<a href="http://www.prisms-center.org/">http://www.prisms-center.org/</a> (Free access)
The materials project <sup>51</sup>	Open-access platform for computational materials science that uses high-throughput calculations to compute and disseminate properties of materials; provides structural, electronic, and thermodynamic properties for accelerating materials discovery and design	Metals	DFT	<a href="https://materialsproject.org/">https://materialsproject.org/</a> (Free access)
Total material	Comprehensive materials information platform providing access to data on over 540,000 metallic and non-metallic materials; includes extensive mechanical and physical property data, global standards and equivalencies, stress-strain, and fatigue properties	Metals, polymers	Experiment	<a href="https://www.totalmateria.com/">https://www.totalmateria.com/</a> (License required)
The open quantum materials database <sup>52</sup>	High-throughput database containing over 200,000 DFT calculations of crystal structures and formation energies; serves as a resource for materials discovery, providing thermodynamic stability analysis, chemical potential data, and datasets for training machine learning models	Metals	DFT	<a href="https://oqmd.org/">https://oqmd.org/</a> (Free access)

Abbreviations: CALPHAD: Calculation of phase diagrams; DFT: Density functional theory; FEA: Finite element analysis; MD: Molecular dynamics.

particularly when predicting material performance under AM-specific conditions. However, these traditional datasets can still serve as initial guidance for material selection and composition screening. By integrating such data with AM-specific experimental results and process parameters (e.g., laser power, scan speed, and cooling rates), AI models can be adapted to better reflect the unique processing-structure-property relationships in AM. Developing specialized AM databases that incorporate both material composition and AM process conditions

remains an essential step for advancing AI-driven material development in this field.

#### 4.2. Data pre-processing

Data pre-processing is for ensuring that raw data are systematically refined into a structured format suitable for computational analysis and model training. Given the inherent imperfections in raw datasets, such as noise, inconsistencies, and incomplete records, pre-processing plays a crucial role in mitigating these issues. The presence

of unprocessed data can significantly compromise the accuracy and reliability of AI models, necessitating robust pre-processing methodologies to enhance data quality and ensure compatibility with ML algorithms. A well-designed pre-processing pipeline ensures that datasets are not only internally consistent but also scalable and representative of the underlying material properties and behaviors. Furthermore, it facilitates bias mitigation, minimizes redundancy, and enhances predictive accuracy.

#### 4.2.1. Fundamental data pre-processing techniques

Data pre-processing typically begins with data cleaning, a process that involves handling missing values, detecting and correcting inconsistencies, and eliminating outliers. In AI-based material research, missing values can arise from incomplete experimental records or sensor failures during process monitoring. Various imputation strategies can be applied depending on data type and structure. For numerical variables, mean or median imputation is commonly used, whereas categorical data are often addressed using the most frequent category or probabilistic imputation techniques<sup>53</sup>

Feature encoding is another critical step, particularly when dealing with categorical attributes, such as material compositions, process parameters, and classification labels. Conventional encoding techniques, such as one-hot encoding, enable categorical variables to be represented numerically without introducing unintended ordinal relationships. Feature scaling follows as a necessary step to ensure comparability across different feature dimensions. Common approaches include min-max normalization, which scales features to a defined range, and standardization (Z-score normalization), which transforms features to have zero mean and unit variance, mitigating the effects of disproportionate feature magnitudes on model training.

#### 4.2.2. Pre-processing strategies for data in AM

Unlike conventional structured datasets, datasets in AM are inherently multimodal, encompassing tabular datasets, high-resolution imaging, time-series process data, and three-dimensional geometric representations. As a result, pre-processing strategies must be adapted to accommodate these diverse data formats while ensuring cross-modality compatibility.

One of the key challenges in AM data pre-processing is data registration, which aligns information obtained from different stages of the manufacturing process. For example, ensuring that *in situ* monitoring data is correctly mapped to corresponding microstructural characterization results is essential for accurate process–property correlations. This alignment is particularly relevant in AM, where variations

in process parameters directly influence material structure and mechanical performance.

In addition, AM datasets are often structured across multiple spatial and temporal scales. Multiscale data integration is necessary to harmonize information collected at different levels, such as individual powder particles, melt pools, printed layers, and entire components. This requires the standardization of spatial resolutions and temporal sampling rates to enable meaningful feature extraction and pattern recognition.

Feature extraction is a particularly critical aspect of pre-processing in AM, as raw sensor data often requires transformation before it can be effectively utilized in AI models. For example, three-dimensional data derived from X-ray, computed tomography (CT) scans,<sup>54</sup> or microstructure imaging may be converted into structured representations through voxelization. Similarly, time-series data from thermal sensors or acoustic emission monitoring may be analyzed using the Fourier<sup>55</sup> or Wavelet<sup>56</sup> transforms to extract frequency-based features relevant to defect detection and process stability. Dimensionality reduction techniques, such as principal component analysis, are frequently applied to condense high-dimensional feature sets while preserving essential information.<sup>57</sup>

## 5. Applications of AI-enabled material development for AM

The development of materials with optimized properties is a central objective, driving advancements in structural, functional, and high-performance materials. The pursuit of improved mechanical strength, thermal stability, electrical conductivity, and biocompatibility has led to extensive research into metals, polymers, and bioinks/biomaterial inks.

This section explores the applications of AI in material development for AM, with a particular focus on metals, polymers, and bioinks/biomaterial inks. For metals and polymers, the discussion is structured into two key aspects: Material design and performance optimization. In the material design section, we examine how AI-driven methods facilitate the discovery and optimization of novel compositions/structures tailored for AM processes. The performance optimization section extends this analysis by establishing a link between AM process parameters and material performance (Figure 6), leveraging AI to refine microstructural features and mechanical properties. For bioinks and biomaterial inks, the focus is on AI-assisted formulation optimization, where balancing printability, rheological properties, biocompatibility, and mechanical integrity is crucial for ensuring successful bioprinting outcomes.

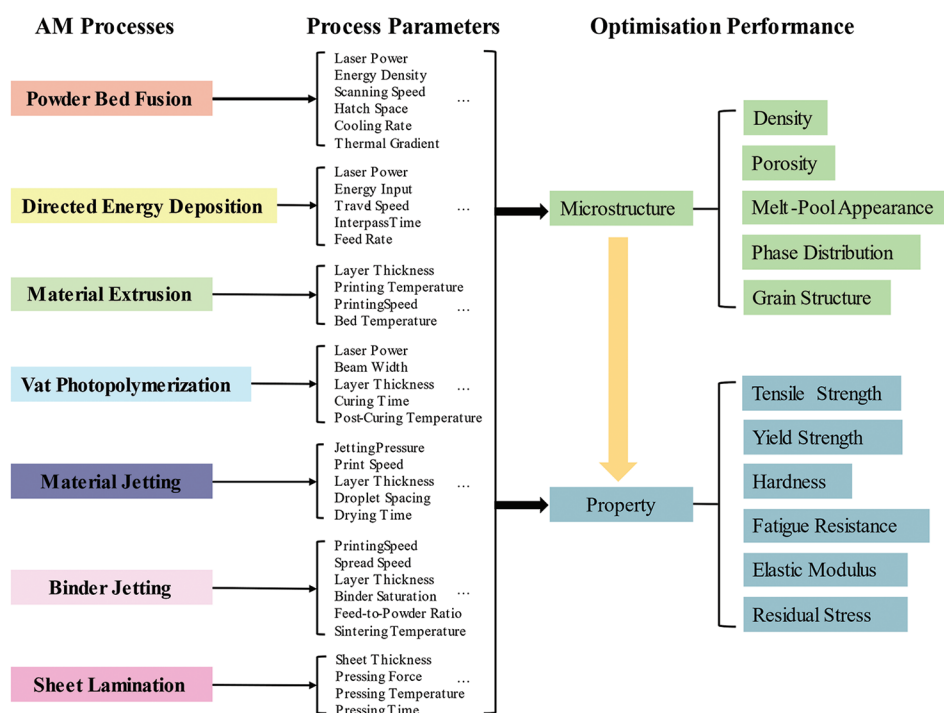


Figure 6. Link between additive manufacturing process parameters and material microstructure and properties. Adapted from Jin *et al.*<sup>10</sup>

## 5.1. Metallic materials for AM

Table 4 presents a summary of AI applications related to metal materials in AM. The following sections will explore representative examples to elucidate how AI facilitates material design and performance optimization.

### 5.1.1. Alloy design for metal AM

A prominent success of AI-driven alloy design is its application in phase prediction for high-entropy alloys. Due to their multi-principal element nature, high-entropy alloys exhibit a vast range of possible phase structures, which directly influence their mechanical, thermal, and chemical properties.<sup>67</sup> A variety of ML models have been employed to classify high-entropy alloy phases, employing diverse feature sets to improve prediction accuracy. Commonly used models include ANNs,<sup>68-70</sup> RF,<sup>71,72</sup> support vector machine,<sup>73,74</sup> logistic regression,<sup>75</sup> gradient-boosted trees,<sup>76</sup> and Gaussian process classification.<sup>77</sup> These models utilize input features, such as atomic size difference ( $\delta$ ), valence electron concentration, mixing enthalpy ( $H_{mix}$ ), and entropy parameters, to predict phase formation, including face-centered cubic, body-centered cubic, hexagonal close-packed, and multiphase structures.

Beyond high-entropy alloys, AI has also been employed to optimize the composition of green maraging steels for AM. As seen in Figure 7, Tan *et al.*<sup>58</sup> employed ML

algorithms to optimize the composition of Fe–Ni–Ti–Al maraging steel, tailoring it for AM. Specifically, this study utilized thermodynamic simulations to generate a dataset, which was subsequently integrated with RF, decision trees, AdaBoost, and k-nearest neighbor to predict the formation of Ni<sub>3</sub>Ti precipitates and Laves phases during AM. Based on these predictions, the concentrations of Ni, Ti, and Al were adjusted to enhance precipitation strengthening while mitigating the formation of detrimental phases, thereby improving microstructural stability and mechanical properties. Finally, the newly developed maraging steel exhibits exceptional mechanical properties, achieving a tensile strength of 1,538 MPa and a uniform elongation of 8.1%, validating the effectiveness of the AI-driven material development approach.

Overall, while AI-driven methodologies have demonstrated significant potential in alloy design, the direct application of AI in AM-specific alloy design is still rare. Most studies still focus on general material design, where AI is primarily employed for composition optimization<sup>78</sup> and phase prediction,<sup>79</sup> without explicitly considering the constraints imposed by AM processing. To enhance the applicability of AI-driven alloy design for AM, it is essential to further integrate it with process-aware models that account for rapid solidification, thermal cycling, and process-induced defects.

Table 4. Summary of AI applications for metal materials for AM

AM process	Material	Optimization type	AI method	Target	Model performance	References
DED	Fe-Ni-Ti-Al	Design	RF	Composition optimization	R2=0.998 MAE=0.292	Tan <i>et al.</i> <sup>58</sup>
PBF	SS316L	Performance	Adaptive Neuro-Fuzzy Inference System (ANFIS)	Fatigue life prediction	RMS=14.66%	Zhang <i>et al.</i> <sup>59</sup>
PBF	Zr52.5Cu17.9Ni14.6Al10Ti	Performance	HGP	Materials characteristics prediction	RMSE=2.58%	Chernyavsky <i>et al.</i> <sup>60</sup>
PBF	AlSi10Mg	Performance	GPR	Tensile property optimization (YS and elongation)	-	He <i>et al.</i> <sup>61</sup>
PBF	AlSi10Mg	Performance	GPR	Density variations and microstructural characteristics prediction	-	Liu <i>et al.</i> <sup>62</sup>
PBF	Ti-6Al-4V	Performance	MML	Fatigue strength design	-	Awd <i>et al.</i> <sup>63</sup>
PBF	Ti-6Al-4V	Performance	ANN	Tensile property optimization (YS, UTS, and elongation)	R2: YS=0.9887, UTS=0.9921, elongation=0.9917	Maleki <i>et al.</i> <sup>64</sup>
PBF	Ti-6Al-4V	Performance	RSM+GA	Energy absorption optimization	R2=0.9431	Meng <i>et al.</i> <sup>65</sup>
DED	Ti-Mn alloy	Performance	GPR	YS and modulus optimization	MAPE: YS=6.26%, E=2.02%	Gong <i>et al.</i> <sup>66</sup>

Abbreviations: ANN: Artificial neural networks; DED: Directed energy deposition; E: Elastic modulus; GA: Genetic algorithms; GPR: Gaussian process regression; HGP: Heteroscedastic Gaussian process; MAE: Mean absolute error; MML: Mechanistic machine learning; PBF: Powder bed fusion; RF: Random forest; RMS: Root mean square; RMSE: Root mean square error; RSM: Response surface methodology; UTS: Ultimate tensile strength; YS: Yield strength; AI: Artificial intelligence; AM: Additive manufacturing.

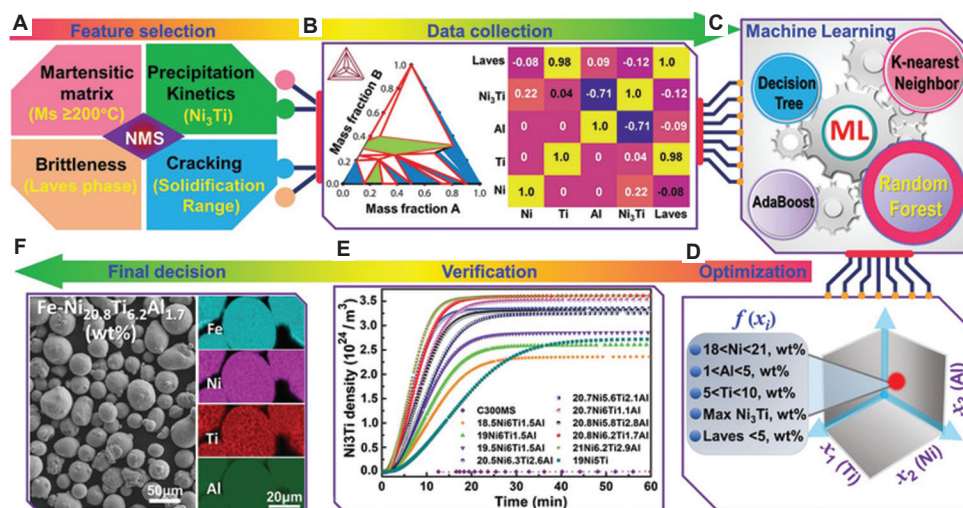


Figure 7. The schematic of ML-assisted composition design of Fe-Ni-Ti-Al NMS. (A) Feature selections in the design of NMS. (B) Data collections from Thermo-Calc software and the correlation matrix of the input composition (Ni, Ti, and Al) and output (Ni<sub>3</sub>Ti precipitate and Laves phase weight fractions) in the surrogate models. (C) ML by various algorithms (random forest is the most accurate one). (D) Composition optimization for the allowable range of alloying elements. (E) Time-dependent dynamic precipitation behaviors of different compositions at 490°C (the balance is Fe). (F) Optimal composition Fe-20.8Ni-6.2Ti-1.7Al (wt%) along with the morphology and elemental mapping of the produced powder. Reproduced from Tan *et al.*<sup>58</sup>

Abbreviations: NMS: Novel maraging steel; ML: Machine learning.

### 5.1.2. Performance optimization in metal AM

Alloy performance optimization includes both microstructural optimization and mechanical property

optimization. Microstructural optimization focuses on the regulation of grain size, phase distribution, precipitate morphology, and porosity to achieve improved

structural homogeneity and stability. Mechanical property optimization, on the other hand, primarily focuses on the enhancement of properties, including strength, hardness, ductility, and fracture toughness, which are typically realized through appropriate microstructural and process control.

Recent advancements in AI-driven methodologies have enabled the establishment of correlations between processing parameters and microstructural characteristics in AM. By leveraging ML models trained on experimental and computational datasets, AI enables more accurate predictions of microstructural evolution and mechanical properties under varying process conditions. For example, Awd *et al.*<sup>63</sup> integrated mechanistic ML with physics-based models to predict and optimize the fatigue strength of AM-fabricated metamaterials. Their approach combines electronic structure calculations, stochastic process modeling, and microstructural characterization to establish process-structure-property (PSP) relationships. Through  $\mu$ -CT imaging and defect quantification, they demonstrated how AI-driven methodologies can enhance fatigue damage modeling, enabling more accurate predictions of material performance under cyclic loading. Similarly, Liu *et al.*<sup>62</sup> employed Gaussian process regression (GPR) to model the complex relationships between processing parameters, microstructure, and mechanical properties in laser powder bed fusion (LPBF)-fabricated AlSi10Mg. GPR was utilized to predict density variations and microstructural characteristics based on key process parameters. Their study demonstrated that GPR effectively captures non-linear dependencies

within PSP relationships, allowing for improved process parameter selection to minimize defects and enhance mechanical performance. The model showed strong agreement with experimental results, suggesting reliable prediction accuracy.

In addition, Gaussian process-based models have been explored to optimize process parameters for improved mechanical performance. Tapia *et al.*<sup>80</sup> developed a Gaussian process-based surrogate modeling framework to predict melt pool depth in LPBF of 316L stainless steel, thereby identifying processing windows that enhance part quality. Their approach enabled the classification of conduction-mode and keyhole-mode melting regimes, which directly affect the microstructure and, consequently, the mechanical properties of AM components. Chernyavsky *et al.*<sup>60</sup> introduced a Heteroscedastic Gaussian process (HGP) model to predict the amorphicity of a Zr-based glass-forming alloy fabricated through LPBF. This model effectively establishes a quantitative link between LPBF conditions and microstructural evolution. Figure 8 illustrates the predictive capability of the HGP model, covering amorphicity distribution (Figure 7A), uncertainty quantification (Figure 7B), and prediction accuracy (Figure 7C). These results highlight the model's robustness in not only delivering accurate amorphicity predictions but also in assessing dataset reliability and identifying underlying physical mechanisms governing glass formation in AM.

The integration of AI-driven methodologies in alloy performance optimization has significantly advanced the understanding and prediction of PSP relationships.

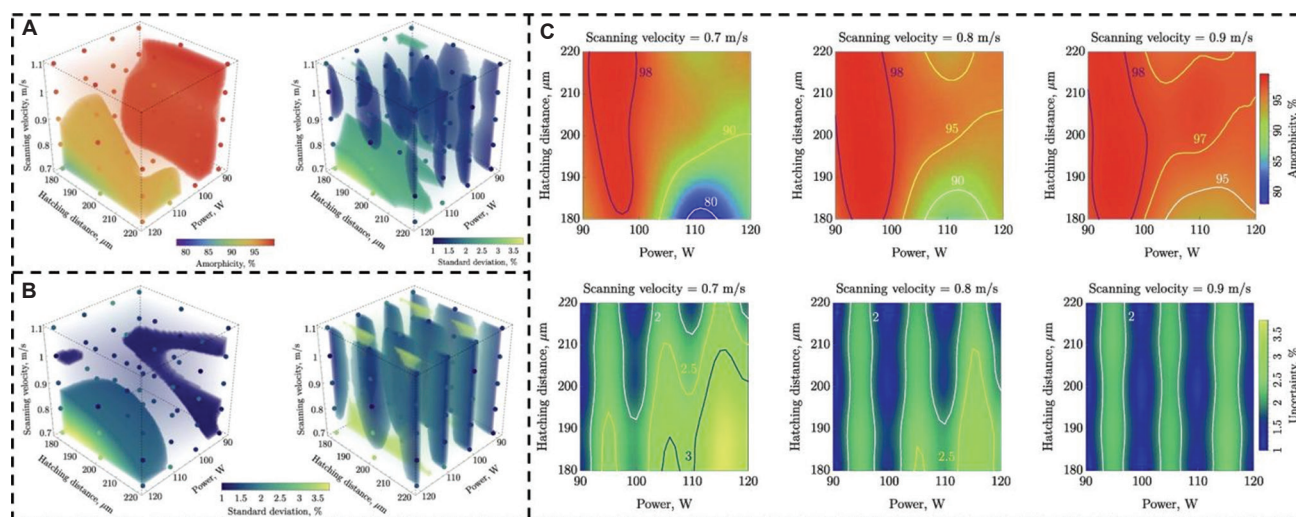


**Figure 8.** Predicted amorphicity distributions and associated uncertainty for alloys fabricated through laser powder bed fusion. (A) HGP model predictions for mean values of amorphicity and its total uncertainty. (B) Position-resolved aleatoric and epistemic uncertainties predicted by the HGP model. (C) Two-dimensional contour maps of HGP model predictions for mean values of amorphicity and its total uncertainty. Reproduced from Chernyavsky *et al.*<sup>60</sup> Abbreviation: HGP: Heteroscedastic Gaussian process.

From fatigue strength modeling to process parameter optimization, AI has proven to be a powerful tool in enhancing microstructural control and mechanical property refinement. Despite these advancements, challenges remain in data completeness, model interpretability, and generalization across different AM processes and material systems. The continued development of hybrid AI approaches, integrating physics-based models with data-

driven learning, will be essential for further improving predictive accuracy and expanding the applicability of AI in AM alloy design.

## 5.2. Polymer materials for AM

Table 5 compiles a range of AI-driven strategies applied to polymer AM, covering both compositional design and property improvement.

**Table 5. Summary of artificial intelligence applications for polymer materials for additive manufacturing**

AM process	Material	Optimization type	AI method	Target	Model performance	References
PBF	Multi-material	Design	GMM and PCR	Elastic property optimization	Poisson's ratio error≈16%	Chen <i>et al.</i> <sup>81</sup>
VPP	RPU+SilDN	Design	VAE and BO	Elastic moduli tailoring (Young's modulus and Poisson's ratio)	Poisson's ratio error≈6.4%, E error≈11.3%	Xue <i>et al.</i> <sup>82</sup>
VPP	TPU	Design	MLP	Novel metamaterial with variable compression properties design	-	Fleisch <i>et al.</i> <sup>83</sup>
MET	PLA	Performance	Bayesian ML	Super-compressibility and recoverability design	R2≈0.988	Bessa <i>et al.</i> <sup>84</sup>
MET	PLA	Performance	RF, KNN, ADA, DT, and LSTM	Tensile and flexural strength prediction and optimization	LSTM achieved best performance: R <sup>2</sup> =0.9169, MAPE=2.85%, RMSE=2.44; other models (RF, KNN, ADA, DT) showed R <sup>2</sup> <0.75 and MAPE >5%.	Sharma <i>et al.</i> <sup>85</sup>
MET	Technomelt PA 6910	Performance	LiR, GPR, RR, and KNN	Tensile property prediction (Young's modulus, yield stress, yield strain, tensile stress, and tensile strain)	LiR/RR best: <10% error	Nasrin <i>et al.</i> <sup>86</sup>
MET	ABS	Performance	LiR, DT, RF, and ADA	Hardness prediction	RF best: R <sup>2</sup> ≈ 0.91, RMSE≈0.99, AdaBoost close: R <sup>2</sup> ≈ 0.90, RMSE≈1.09 LR & DT lower: R <sup>2</sup> ≈ 0.84 & 0.77	Veeman <i>et al.</i> <sup>87</sup>
MET	PLA	Performance	CNN and RF	Process parameters–property correlation (TS and hardness)	RF accuracy: 94% (TS), 89% (hardness); CNN 88% (TS), 88% (hardness)	Butt and Mohaghegh <sup>88</sup>
MET	PLA	Performance	LSTM	TS prediction	R <sup>2</sup> =89.4%	Zhang <i>et al.</i> <sup>89</sup>
VPP	Resin	Performance	GA+NN	Modulus and strength optimization	R <sup>2</sup> =0.9978	Lee <i>et al.</i> <sup>90</sup>
MJT	Multi-material	Performance	GA	Tunable deformation and antibacterial performance	-	He <i>et al.</i> <sup>91</sup>
MJT	Multi-material		ANN and RSM	Shore hardness and compressive modulus optimization	ANN: MSE=0.36% (Shore A), 0.98% (E); RSM: MSE=1.3% (Shore A), 4.4% (E)	Goh <i>et al.</i> <sup>92</sup>

Abbreviations: ABS: Acrylonitrile butadiene styrene; ADA: Adaptive design algorithm; ANN: Artificial neural network; BO: Bayesian optimization; CNN: Convolutional neural network; DT: Decision trees; GA: Genetic algorithms; GMM: Gaussian mixture model; GPR: Gaussian process regression; KNN: K-nearest neighbors; LiR: Linear regression; LSTM: Long short-term memory; MAPE: Mean absolute percentage error; MET: Multi-exponential theory; MJT: Material jetting; ML: Machine learning; MLP: Multilayer perceptron; MSE: Mean squared error; NN: Neural network; PBF: Powder bed fusion; PCR: Principal component regression; PLA: Polylactic acid; RF: Random forest; RMSE: Root mean square error; RPU: A commercial hard polyurethane; RR: Ridge regression; RSM: Response surface methodology; SilDN: A custom soft silicone; TPU: Thermoplastic polyurethane; TS: Tensile strength; VAE: Variational autoencoder; VPP: Vat photopolymerization.

### 5.2.1. Material design for polymer AM

In polymer AM, material design primarily revolves around structural engineering rather than composition optimization, as modifying polymer composition is far less feasible compared to metals. To date, very few studies have employed AI for the targeted optimization of polymer feedstock composition or molecular-level properties. Unlike metals, where alloying elements can be systematically adjusted to tailor phase stability, mechanical properties, and processing behavior, polymer properties are largely dictated by their intrinsic chemical structures, molecular weight distributions, and polymerization mechanisms, making composition-based optimization significantly more constrained. In addition, synthesizing new printable polymers often requires extensive chemical modifications and rigorous processing validation, further limiting rapid material innovation. As a result, this review focuses on the AI-assisted design of mechanical metamaterials in polymer AM – an emerging direction where structural architecture, rather than chemistry, defines material performance. These metamaterials achieve properties such as auxetic behavior (negative Poisson's ratio),<sup>93</sup> programmable mechanical responses,<sup>94</sup> controlled buckling behavior,<sup>95</sup> shape morphing,<sup>96</sup> and acoustic band gap<sup>97</sup> through precise structural design rather than relying solely on material composition. By integrating computational modeling, ML, and multi-objective optimization, AI facilitates the design of next-generation metamaterials tailored for specific AM applications.

In polymer AM, VPP techniques are particularly well-suited for fabricating metamaterials due to their high resolution, surface quality, and processing speed. However, traditional design methodologies based on prior knowledge and intuition are increasingly inadequate for achieving next-generation metamaterial designs with optimized performance. In addition, the computational cost associated with exploring extensive lattice configurations using FEA presents a significant bottleneck, further restricting design innovation. To overcome these limitations, AI-driven approaches have been increasingly employed to automate the design process and optimize metamaterial architectures. By efficiently navigating the vast design space, AI enables the discovery of novel lattice structures with optimized properties while reducing reliance on computationally expensive simulations. This integration of AI with polymer AM facilitates the rapid development of high-performance metamaterials tailored for advanced applications. Chen *et al.*<sup>81</sup> developed an AI-driven computational approach for the automated discovery of mechanical metamaterials with extreme properties. Experimental validation confirms its effectiveness in discovering auxetic structures with

negative Poisson's ratios, covering a broad range of elastic properties. This scalable framework extends to multiphysics metamaterials, advancing the AI-driven automated design of high-performance materials.

Similarly, Xue *et al.*<sup>82</sup> proposed an AI-driven optimization framework for the automated design of composite mechanical metamaterials. Their approach utilized a variational autoencoder to encode representative volume element images into a latent space, enabling efficient exploration of material distributions. Bayesian optimization (BO) was then employed to identify optimal representative volume element configurations that achieve target macroscopic elastic moduli. The optimized designs were fabricated using multi-material 3D printing and experimentally validated, demonstrating the framework's reliability in generating high-performance metamaterials.

Bessa *et al.*<sup>84</sup> extended AI-driven metamaterial design to brittle polymers, employing a Bayesian ML framework to develop super-compressible metamaterials. As seen in Figure 9, their approach employed sparse Gaussian processes to model uncertainty and identify recoverable structures with extreme deformation capabilities. By systematically adapting designs to different length scales and material constraints, they demonstrated the potential of AI-driven approaches in creating lightweight, tunable, and highly deformable metamaterials.

### 5.2.2. Performance optimization in polymer AM

Beyond metamaterial design, AI-driven approaches play a central role in optimizing process parameters and predicting material performance for polymer AM. These methods enable data-driven decision-making, significantly improving the efficiency and accuracy of mechanical performance predictions.<sup>88,98</sup> For example, Zhang *et al.*<sup>89</sup> employed a long short-term memory neural network, a DL algorithm adept at handling sequential data, to predict the tensile strength of polylactic acid components based on in-process sensor data. The model captured layer-wise temporal dependencies in FDM and achieved higher predictive accuracy than traditional ML models, underscoring the advantage of DL in time-series analysis for polymer AM.

In a generative design context, Lee *et al.*<sup>90</sup> applied AI-based optimization using Bézier curve manipulation and finite element simulations to design polymer lattice structures with superior mechanical performance. Their approach involved iteratively adjusting lattice beam geometries and evaluating mechanical responses, effectively shortening design cycles and outperforming human-guided design in terms of both modulus and strength.

Extending this approach to multi-material systems, He *et al.*<sup>91</sup> integrated GA with multi-material-inkjet 3D printing (MM-IJ3DP) and voxel-level finite element modeling. The GA served as a global search tool to explore the vast design space, enabling customizable stiffness gradients and improved biofilm resistance. As illustrated in Figure 10, their framework integrates MM-IJ3DP with FEA and GA to tailor material properties at the voxel level. Experimental validation confirmed that their approach enables the fabrication of customizable polymer composites with tunable stiffness and enhanced biofilm resistance, demonstrating the potential of AI in multifunctional material optimization.

In addition to mechanical performance, AI has been applied to enhance the biofunctional properties of polymeric AM materials.<sup>99</sup> In bioprinting applications, optimizing process parameters can improve biocompatibility and cell viability, while in medical implants and antimicrobial materials development, tailoring surface properties can reduce bacterial adhesion and mitigate infection risks. Magennis *et al.*<sup>100</sup> utilized high-throughput screening to identify polymeric materials capable of effectively resisting bacterial attachment, presenting new opportunities for biomedical AM. Figure 11 shows that their study systematically analyzed the relationship between polymer chemistry and bacterial adhesion by

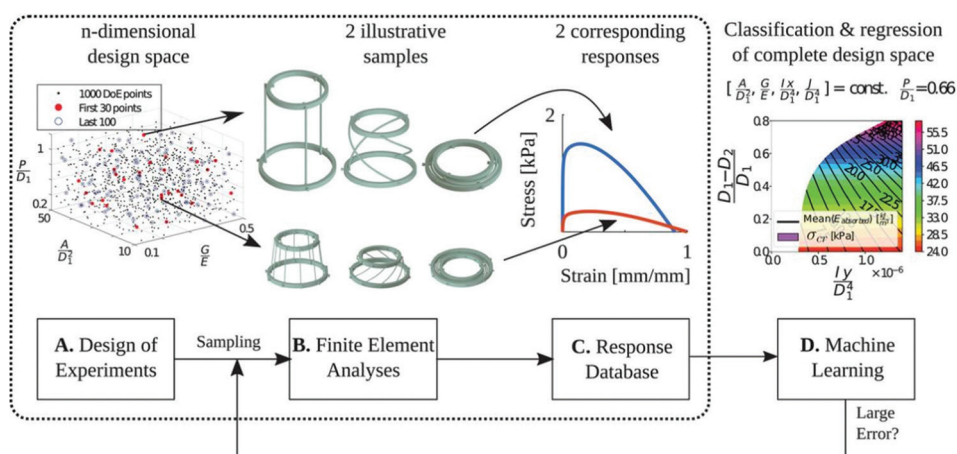


Figure 9. Bayesian machine learning framework for the design of super-compressible metamaterials in brittle polymers. Reproduced from Bessa *et al.*<sup>84</sup>

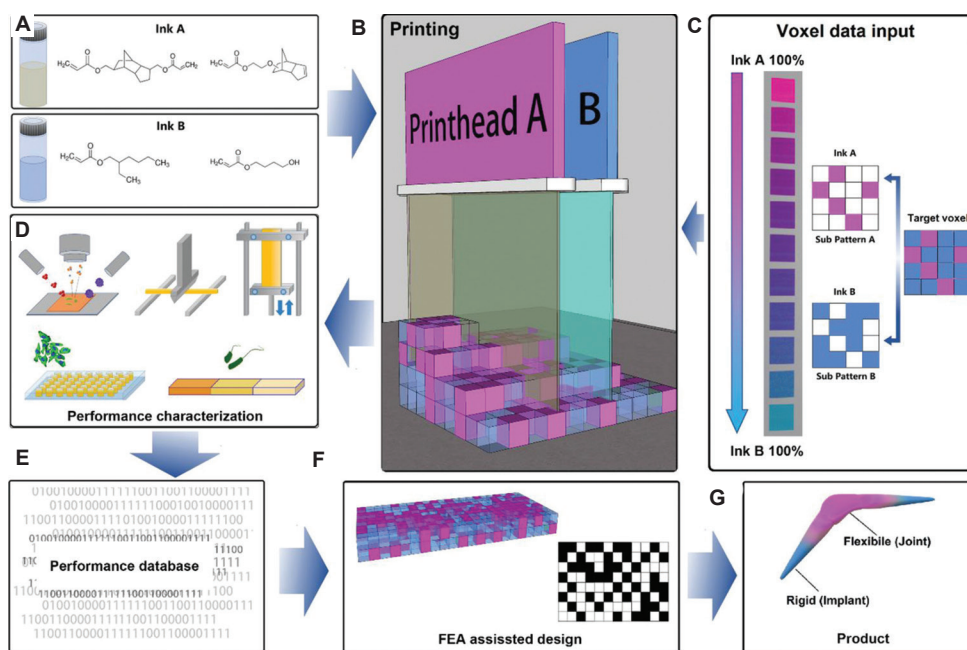


Figure 10. Artificial intelligence-driven generative design framework for multi-material 3D-printed composites. Reproduced from He *et al.*<sup>91</sup> Abbreviation: FEA: Finite element analysis.

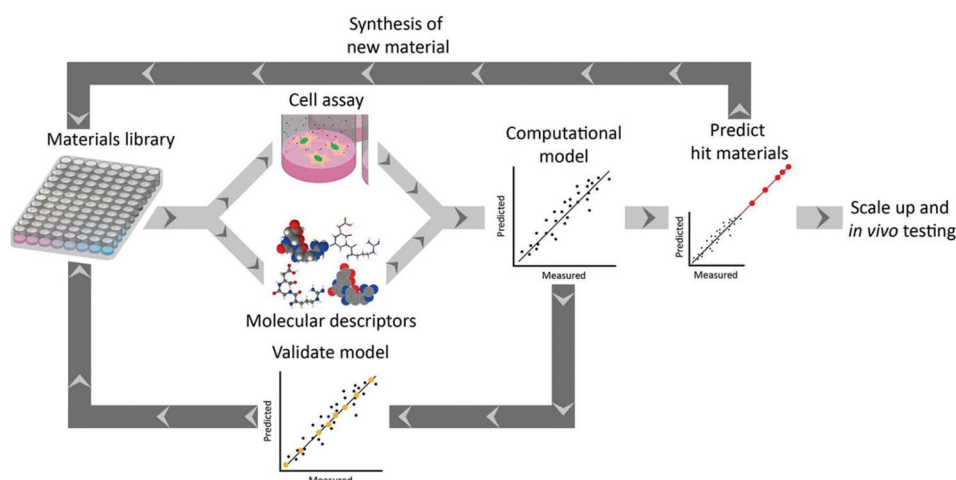


Figure 11. Process of computational modeling for the generation of novel biomaterials. Reproduced from Magennis *et al.*<sup>100</sup>

screening a large material library in combination with computational modeling. As a result, they identified a class of polymers with outstanding antimicrobial properties that can inhibit biofilm formation, thereby enhancing the safety of medical devices and bioprinted scaffolds. This study highlights the potential of AI and data-driven approaches in the optimization of multifunctional AM materials, demonstrating their applicability not only for mechanical enhancement but also for the improvement of biofunctional properties.

### 5.3. Bioink and biomaterial ink for AM

The design of bioinks and biomaterial inks is fundamental in bioprinting, as these materials form the basis for creating functional, 3D biological structures. Bioinks consist of living cells embedded within a biocompatible matrix, whereas biomaterial inks may not contain living cells but are used to construct scaffolds or structures that support cellular activities.<sup>101</sup> Both types of inks must be carefully formulated so that their biological and mechanical properties are compatible with bioprinting and suitable for their intended purpose after the printing process. Crafting an ideal bioink is a multi-objective problem, requiring a delicate balance of various properties, such as printability, biocompatibility, biomimicry, mechanical integrity and stability, and biodegradability.<sup>102,103</sup> For instance, enhancing mechanical integrity and stability often results in reduced biocompatibility, and vice versa. To discover an optimal formulation, a large number of different compositions must be tested, each representing a different trade-off between competing objectives. This is where AI becomes invaluable, significantly improving the efficiency of material search and development by helping navigate the complex multidimensional space of possible formulations.

AI approaches commonly employed in bioink and biomaterial ink design include supervised learning and reinforcement learning. In supervised learning, models are trained to predict the properties of inks in advance, allowing researchers to evaluate potential formulations quickly. Meanwhile, reinforcement learning enables models to explore the search space and identify optimal ink formulations in minimal steps, effectively learning from iterative experimentation.

On the prediction side, Qavi *et al.*<sup>104</sup> examined the relationship between rheological properties and printability in multi-material bioinks for extrusion-based bioprinting (EBB). Using a design of experiment approach coupled with response surface methodology, the study optimized bioink formulations containing sodium alginate, gelatin, and laponite, focusing on parameters, such as zero shear viscosity and storage modulus. By training an ANN on the obtained dataset, the relationships between the parameters were generalized, achieving a maximum mean absolute error of 6.3% in predicting the printability of the bioink formulations.

Lee *et al.*<sup>105</sup> addressed the challenges in designing biocompatible 3D-printable bioinks by developing an ML-based method to create viable bioinks using collagen, hyaluronic acid, and fibrin. They established a relationship between ink mechanical properties and printability, highlighting that a high elastic modulus enhances shape fidelity while extrusion remains feasible below the critical yield stress. Using multiple regression analysis, they developed a model to predict whether a composition has a high elastic modulus and low yield stress. Various bioink formulations were designed to maximize shape fidelity, leading to successful 3D constructs with viable and proliferative cells.

Xu *et al.*<sup>106</sup> introduced an ML framework to predict the viscosity of heterogeneous bioink compositions. Traditional models, such as the Cross model; fall short in this domain due to the non-Newtonian nature of bioinks. Their approach leveraged BO to work with sparse datasets, employing a mask technique to define feasible parameter spaces based on domain expertise. By balancing the exploration of new possibilities and exploitation of existing data, their AI-guided BO framework effectively reduced experimental workload and streamlined the building of the surrogate model for viscosity prediction.

Qiao *et al.*<sup>107</sup> explored the application of AI in bioink development for cryobioprinting, which integrates extrusion bioprinting and cryopreservation to enhance bioink shelf availability without using dimethyl sulfoxide due to its potential toxicity. They developed a gelatin methacryloyl (GelMA)-based bioink incorporating cryoprotective agents (CPAs) and assessed two CPA formulations, finding that ethylene glycol outperformed glycerol. Using this dataset, they established four ML models, with the ANN showing the highest predictive accuracy. This ANN model was successfully applied to predict outcomes for various CPA-based formulations, showcasing the potential of ML in the development of effective cryoprotective bioinks for cryobioprinting.

In reinforcement learning applications, Ruberu *et al.*<sup>108</sup> demonstrated how BO can quantitatively evaluate and optimize the printability of biomaterial inks, such as GelMA and hyaluronic acid methacrylate, by adjusting GelMA composition, ink reservoir temperature, pressure, speed, and platform temperature. They significantly reduced the number of experiments required for 3D bioprinting optimization from 10,000 to an order of 10. Hashemi *et al.*<sup>109</sup> also explored the development of a chitosan-gelatin-agarose biomaterial ink optimized for extrusion-based 3D bioprinting through BO. The study focused on achieving desirable mechanical properties, biocompatibility, and precise printability. The optimized ink composition (27% agarose, 53% chitosan, and 20% gelatin) showed promise for fabricating complex 3D tissue constructs. The optimized biomaterial ink exhibited sufficient viscosity for reliable printing while maintaining shape integrity in 3D structures. Biological evaluations involving bone marrow mesenchymal stem/stromal cells revealed that the ink supported favorable cell adhesion, growth, and viability.

However, a major challenge in applying AI to bioprinting is the slow collection of biologically relevant datasets, such as cell viability. A small sample size can hinder the development of robust models. To mitigate this issue, AI can be applied for fast measurement of crucial

parameters using AI-driven sensors, as well as enabling rapid optimization of print parameters. For example, Huang *et al.*<sup>110</sup> introduced an ML-based model to predict cell numbers in bioprinted droplets by analyzing droplet velocity. Utilizing a non-destructive optical system, the study accurately detected the presence and quantity of cells in droplets. Among the evaluated models, RF regression achieved 80% accuracy for single droplet cell presence, while extra tree regression had the lowest error at 12% for cell number predictions across multiple droplets. Besides, the gel fraction of hydrogel during bioprinting can be measured with the ML or DL model through *in situ* measurement of the hydrogel's ultraviolet transmissivity.<sup>111</sup>

Moreover, reinforcement learning-based rapid print parameter optimization can increase sample count and efficiency. Bonatti *et al.*<sup>112</sup> proposed a DL-based control system to reduce the trial-and-error in EBB. The authors collected a high-resolution video dataset of various EBB parameters and trained a CNN to optimize print parameters and monitor the process in real time. This control loop halted erroneous prints to conserve resources and time while integrating the ML model with existing mathematical models, demonstrating the potential of ML to automate and ensure quality in EBB. Chen *et al.*<sup>113</sup> introduced an AI-assisted high-throughput printing-condition-screening system (AI-HTPCSS) to enhance the optimization of printing conditions for 3D bioprinting. This system integrated a programmable pneumatic extrusion printer with an AI-driven image-analysis algorithm to efficiently screen conditions for printing uniformly structured hydrogel scaffolds. The optimized conditions achieved through AI-HTPCSS led to scaffolds with favorable mechanical properties, improved *in vitro* biological performance, and effectiveness in enhancing diabetic wound healing *in vivo*.

The integration of AI into bioprinting has advanced bioink design by optimizing formulation properties, such as printability and biocompatibility. However, the field is still emerging, challenged by the lack of extensive datasets necessary for robust AI models. In the future, AI has the potential to revolutionize bioprinting further by enabling real-time process monitoring and adaptive control, thereby enhancing the precision and functionality of bioink development.

## 6. Summary

As summarized in [Figure 12](#), this review examines how AI is transforming material development for AM, with a focus on material design and performance optimization. The integration of AI with AM processes has facilitated

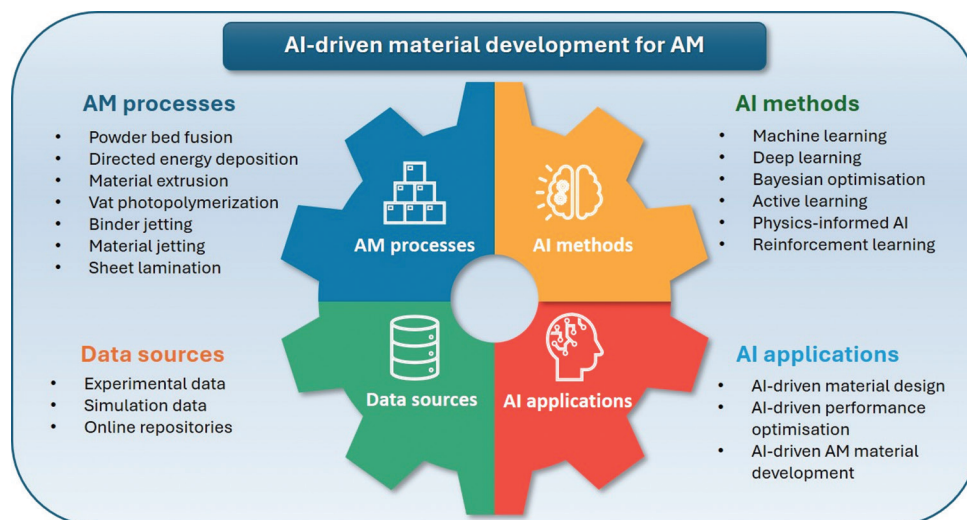


**Figure 12.** An overview of AI-driven material development for AM  
Abbreviations: AM: Additive manufacturing; AI: Artificial intelligence.

predictive modeling, data-driven material discovery, and process optimization, significantly improving efficiency and material performance.

This review highlights the transformative role of AI in material development for AM, with particular emphasis on material design and performance optimization. Traditional trial-and-error approaches are inefficient and costly, whereas AI – particularly ML and DL – enables predictive modeling of material behavior, composition optimization, and microstructural tailoring. The integration of AI with physics-based methods, such as DFT, CALPHAD, and FEA, further enhances the accuracy and efficiency of material development workflows.

The success of AI-driven approaches depends critically on the availability of high-quality datasets. These datasets can be obtained through experimental measurements, physics-based simulations, and structured online repositories. However, most existing databases have been developed for conventional manufacturing and do not capture the process-specific features required for AM. This limitation is particularly evident under conditions involving rapid solidification and non-equilibrium phase transformations. To address this gap, there is a pressing need to construct AM-oriented datasets and apply rigorous data pre-processing procedures.

AI applications in AM material development span metals, polymers, and bioprinting. In metal AM, AI facilitates alloy design, phase prediction, and microstructure control, which helps improve printability and enhance mechanical properties. In polymer AM, AI-guided generative design supports the development of mechanical metamaterials with improved structural performance. In the context of

bioprinting, AI plays a critical role in optimizing bioink formulations by balancing printability, biocompatibility, and mechanical integrity. It has also been applied to adjust extrusion parameters through reinforcement learning, thereby improving reproducibility and promoting cell viability in printed constructs. Across these domains, AI efforts are directed toward intrinsic material development, with a focus on selecting compositions, controlling phase evolution, and enhancing functional performance. This emphasis distinguishes material-centric strategies from broader manufacturing optimization. Moreover, AI improves the understanding of complex PSP relationships, which enables the design of materials with reliable and tailored properties for AM applications.

In conclusion, AI offers a paradigm shift in AM-oriented material development by accelerating the design of materials with tailored compositions and microstructures, aligned with the specific requirements of AM processes. Future progress depends on improved data availability, closer integration between AI and physical modeling, and a sustained focus on the core material properties that define performance.

## 7. Concluding remarks and perspectives

As discussed above, the continued advancement of AI is expected to revolutionize material development in AM by significantly enhancing predictive capabilities. By integrating AI with AM, researchers can accelerate material discovery, optimize processing conditions, and improve overall performance. Looking ahead, several key advancements are poised to shape the future of AI-driven AM materials development, as presented below.

### 7.1. AI-driven high-throughput material development for AM

Traditional material development for AM relies on time-consuming experimental trials and computational simulations, limiting the speed of new material discovery. AI-driven high-throughput material development offers a transformative approach by leveraging automated workflows that integrate ML, combinatorial synthesis, and rapid characterization techniques:

- (i) AI-guided experimental design: ML models can predict optimal material compositions and processing conditions, reducing the need for extensive experimental iterations. By incorporating experimental data in real time, AI refines its predictions to enhance material discovery efficiency.
- (ii) Automated high-throughput screening: AI has the potential to accelerate the evaluation of new alloys, polymers, and ceramics through high-throughput experimentation and combinatorial approaches, enabling the rapid assessment of microstructural stability and mechanical properties.
- (iii) Inverse materials design: The prediction capacity of AI facilitates inverse materials design, allowing researchers to specify desired properties and identify compositions that meet these criteria efficiently. This approach has the potential to significantly shorten the material development lifecycle.

### 7.2. Integration with multiscale high-fidelity simulation with AI

While AI has demonstrated strong predictive capabilities, its full potential in AM material development requires integration with multiscale, high-fidelity simulations to improve physical accuracy and interpretability. AI can enhance and accelerate simulations in the following ways:

- (i) Surrogate modeling for computational efficiency: AI-based surrogate models can approximate high-fidelity simulations (e.g., FEA, molecular dynamics, and CALPHAD) with significantly reduced computational cost, enabling rapid exploration of process–composition–microstructure relationships. For complex-shaped parts, accelerating simulations through AI should be a key research and development focus. A promising approach is to first identify defect-sensitive regions and then strategically adjust process parameters in these susceptible areas to mitigate defects.
- (ii) Multiscale modeling for process optimization: AI can bridge different lengths and time scales in AM simulations, integrating macro-scale thermal simulations with microstructural evolution models to predict final part properties more accurately.

- (iii) Data-driven augmentation of physics-based models: By learning from simulation outputs and experimental validation, AI improves the predictive power of physical models, correcting deviations and refining underlying assumptions. The synergy between AI and physics-based simulations will enable more accurate predictions of AM material behavior, improving process optimization and material performance forecasting.

### 7.3. Integration of digital twins and closed-loop design and manufacturing

The concept of digital twins – real-time virtual replicas of physical AM systems – offers new opportunities for AI-driven material design and process control. The integration of digital twins with AI enables closed-loop adaptive manufacturing, where real-time data informs continuous optimization:

- (i) Real-time process monitoring and defect prediction: AI-powered digital twins integrate sensor data, *in situ* monitoring, and ML models to predict and mitigate defects such as porosity, cracking, and residual stress in AM-fabricated components.
- (ii) Adaptive process control: AI-driven control systems dynamically adjust process parameters (e.g., laser power and scan speed) based on real-time feedback to optimize microstructure formation and mechanical properties.
- (iii) Virtual prototyping and predictive maintenance: Digital twins enable virtual prototyping of materials and components, allowing for iterative design refinements before fabrication. In addition, predictive maintenance models help extend machine lifespan and reduce production downtime.

### 7.4. Active learning-driven material composition optimization for AM

One of the major challenges in AI-driven material development for AM is the scarcity of high-quality experimental data. Active learning, a branch of ML that selects the most informative data points for labeling, provides an efficient solution by minimizing experimental efforts while maximizing predictive performance:

- (i) Efficient exploration of composition space: Active learning strategies guide experimental design by focusing on unexplored or high-uncertainty regions of material composition space, accelerating the discovery of optimized AM-compatible materials.
- (ii) Iterative AI-experimental feedback loops: AI models dynamically update as new experimental data is acquired, refining their predictions and continuously improving the efficiency of material optimization.

(iii) BO for multi-objective design: Active learning combined with BO enables the efficient optimization of material properties while balancing trade-offs between competing factors (e.g., strength versus ductility and toughness versus printability).

## Acknowledgments

None.

## Funding

This work is fully supported by the Advanced Research and Technology Innovation Centre (ARTIC), National University of Singapore, under the grant (project number: ADT-RP1).

## Conflict of interest

Wai Yee Yeong is an Editorial Board Member of this journal, but was not in any way involved in the editorial and peer-review process conducted for this paper, directly or indirectly. Swee Leong Sing serves as an Editorial Board Member of the journal and as the Guest Editor for the Special Issue to which this paper belongs, but he was not involved in the editorial or peer-review process for this manuscript, either directly or indirectly. Jinlong Su is a Youth Editorial Board Member of the journal and serves as a Co-Guest Editor for the same Special Issue, but similarly had no involvement in the editorial handling or peer-review of this paper. Separately, other authors declared that they have no known competing financial interests or personal relationships that could have influenced the work reported in this paper.

## Author contributions

*Conceptualization:* Swee Leong Sing, Jinlong Su

*Funding acquisition:* Swee Leong Sing

*Supervision:* Swee Leong Sing, Wai Yee Yeong

*Visualization:* Peijie Shangguan

*Writing – original draft:* Peijie Shangguan, Huifei Zhou, Xi Huang

*Writing – review & editing:* Jinlong Su, Swee Leong Sing, Wai Yee Yeong

## Ethics approval and consent to participate

Not applicable.

## Consent for publication

Not applicable.

## Availability of data

Not applicable.

## References

1. Tan C, Li R, Su J, *et al.* Review on field assisted metal additive manufacturing. *Int J Mach Tools Manuf.* 2023;189:104032. doi: 10.1016/j.ijmachtools.2023.104032
2. Su J, Jiang F, Teng J, *et al.* Recent innovations in laser additive manufacturing of titanium alloys. *Int J Extreme Manuf.* 2024;6(3):032001. doi: 10.1088/2631-7990/ad2545
3. Liu Y, Sing SL. A review of advances in additive manufacturing and the integration of high-performance polymers, alloys, and their composites. *Mater Sci Addit Manuf.* 2023;2(3):1587. doi: 10.36922/msam.1587
4. Su J, Ng WL, An J, Yeong WY, Chua CK, Sing SL. Achieving sustainability by additive manufacturing: A state-of-the-art review and perspectives. *Virtual Phys Prototyp.* 2024;19(1):e2438899. doi: 10.1080/17452759.2024.2438899
5. Mondal S, Shubhra Goswami S. Machine learning techniques for quality assurance in additive manufacturing processes. *Int J AI Mater Des.* 2024;1(2):21. doi: 10.36922/ijamd.3455
6. Su JL, Jiang FL, Teng J, *et al.* Laser additive manufacturing of titanium alloys: Process, materials and post-processing. *Rare Met.* 2024;43(12):6288-6328. doi: 10.1007/s12598-024-02685-x
7. Seo E, Sung H, Jeon H, *et al.* Laser powder bed fusion for AI assisted digital metal components. *Virtual Phys Prototyp.* 2022;17(4):806-820. doi: 10.1080/17452759.2022.2068804
8. Kim T, Kim JG, Park S, *et al.* Virtual surface morphology generation of Ti-6Al-4V directed energy deposition via conditional generative adversarial network. *Virtual Phys Prototyp.* 2023;18(1):e2124921. doi: 10.1080/17452759.2022.2124921
9. Zhang J, Yin C, Xu Y, Sing SL. Machine learning applications for quality improvement in laser powder bed fusion: A state-of-the-art review. *Int J AI Mater Des.* 2024;1(1):26. doi: 10.36922/ijamd.2301
10. Jin L, Zhai X, Wang K, *et al.* Big data, machine learning, and digital twin assisted additive manufacturing: A review. *Mater Des.* 2024;244:113086. doi: 10.1016/j.matdes.2024.113086
11. Al Rashid A, Ahmed W, Khalid MY, Koç M. Vat photopolymerization of polymers and polymer composites: Processes and applications. *Addit Manuf.* 2021;47:102279. doi: 10.1016/j.addma.2021.102279

12. Pagac M, Hajnys J, Ma QP, *et al.* A review of vat photopolymerization technology: Materials, applications, challenges, and future trends of 3D printing. *Polymers*. 2021;13(4):598.  
doi: 10.3390/polym13040598
13. Gibson I, Rosen D, Stucker B, Khorasani M. *Additive Manufacturing Technologies*. Berlin: Springer International Publishing; 2021.  
doi: 10.1007/978-3-030-56127-7
14. Elkaseer A, Chen KJ, Janhsen JC, Refle O, Hagenmeyer V, Scholz SG. Material jetting for advanced applications: A state-of-the-art review, gaps and future directions. *Addit Manuf*. 2022;60:103270.  
doi: 10.1016/j.addma.2022.103270
15. Chou WH, Gamboa A, Morales JO. Inkjet printing of small molecules, biologics, and nanoparticles. *Int J Pharm*. 2021;600:120462.  
doi: 10.1016/j.ijpharm.2021.120462
16. Gülcan O, Günaydın K, Tamer A. The state of the art of material jetting-a critical review. *Polymers (Basel)*. 2021;13(16):2829.  
doi: 10.3390/polym13162829
17. Sachs E, Cima M, Williams P, Brancazio D, Cornie J. Three dimensional printing: Rapid tooling and prototypes directly from a CAD model. *J Eng Ind*. 1992;114(4):481-488.  
doi: 10.1115/1.2900701
18. Naitoh M, Kubota Y, Katsumata A, Ohsaki C, Arijii E. Dimensional accuracy of a binder jet model produced from computerized tomography data for dental implants. *J Oral Implantol*. 2006;32(6):273-276.  
doi: 10.1563/1548-1336(2006)32[273:DAOAB]2.0.CO;2
19. Deng C, Kang J, Shangguan H, Hu Y, Huang T, Liu Z. Effects of hollow structures in sand mold manufactured using 3D printing technology. *J Mater Process Technol*. 2018;255:516-523.
20. Holland S, Foster T, Tuck C. Creation of food structures through binder jetting. In: *Fundamentals of 3D Food Printing and Applications*. Elsevier; 2019. p. 257-288. Available from: <https://www.sciencedirect.com/science/article/pii/B9780128145647000092> [Last accessed on 2024 Dec 16].
21. Su J, Li Q, Teng J, *et al.* Programmable mechanical properties of additively manufactured novel steel. *Int J Extreme Manuf*. 2025;7(1):015001.  
doi: 10.1088/2631-7990/ad88bc
22. Priyadarshini BM, Kok WK, Dikshit V, Feng S, Li KHH, Zhang Y. 3D printing biocompatible materials with Multi Jet Fusion for bioreactor applications. *Int J Bioprinting*. 2022;9(1):623.  
doi: 10.18063/ijb.v9i1.623
23. Singh R, Gupta A, Tripathi O, *et al.* Powder bed fusion process in additive manufacturing: An overview. *Mater Today Proc*. 2020;26:3058-3070.  
doi: 10.1016/j.matpr.2020.02.635
24. Gharraei R, Bergstrom DJ, Chen X. Extrusion bioprinting from a fluid mechanics perspective. *Int J Bioprinting*. 2024;10(6):3973.  
doi: 10.36922/ijb.3973
25. Svetlizky D, Das M, Zheng B, *et al.* Directed energy deposition (DED) additive manufacturing: Physical characteristics, defects, challenges and applications. *Mater Today*. 2021;49:271-295.  
doi: 10.1016/j.mattod.2021.03.020
26. Kumar A, Dixit AR, Sreenivasa S. Mechanical properties of additively manufactured polymeric composites using sheet lamination technique and fused deposition modeling: A review. *Polym Adv Technol*. 2024;35(4):e6396.  
doi: 10.1002/pat.6396
27. Tepylo N, Huang X, Patnaik PC. Laser-based additive manufacturing technologies for aerospace applications. *Adv Eng Mater*. 2019;21(11):1900617.  
doi: 10.1002/adem.201900617
28. Hofstätter T, Pedersen DB, Tosello G, Hansen HN. State-of-the-art of fiber-reinforced polymers in additive manufacturing technologies. *J Reinf Plast Compos*. 2017;36(15):1061-1073.  
doi: 10.1177/0731684417695648
29. Kussmaul R, Biedermann M, Pappas GA, *et al.* Individualized lightweight structures for biomedical applications using additive manufacturing and carbon fiber patched composites. *Des Sci*. 2019;5:e20.
30. Li Y, Feng Z, Huang L, *et al.* Additive manufacturing high performance graphene-based composites: A review. *Compos Part Appl Sci Manuf*. 2019;124:105483.
31. Wang B, Tao F, Fang X, Liu C, Liu Y, Freiheit T. Smart manufacturing and intelligent manufacturing: A comparative review. *Engineering*. 2021;7(6):738-757.
32. Xiao S, Li J, Wang Z, Chen Y, Tofighi S. Advancing additive manufacturing through machine learning techniques: A state-of-the-art review. *Future Internet*. 2024;16:419.
33. Dang L, He X, Tang D, Li Y, Wang T. A fatigue life prediction approach for laser-directed energy deposition titanium alloys by using support vector regression based on pore-induced failures. *Int J Fatigue*. 2022;159:106748.
34. Ling J, Hutchinson M, Antono E, Paradiso S, Meredig B. High-dimensional materials and process optimization using data-driven experimental design with well-calibrated uncertainty estimates. *Integr Mater Manuf Innov*. 2017;6:207-217.
35. Navarrete I, Fé-Perdomo IL, Ramos-Grez JA, Lopez M.

- Predicting the evolution of static yield stress with time of blended cement paste through a machine learning approach. *Constr Build Mater.* 2023;371:130632.  
doi: 10.1016/j.conbuildmat.2023.130632
36. Khurana D, Koli A, Khatter K, Singh S. Natural language processing: State of the art, current trends and challenges. *Multimed Tools Appl.* 2023;82(3):3713-3744.  
doi: 10.1007/s11042-022-13428-4
37. Gu GX, Chen CT, Richmond DJ, Buehler MJ. Bioinspired hierarchical composite design using machine learning: Simulation, additive manufacturing, and experiment. *Mater Horiz.* 2018;5(5):939-945.  
doi: 10.1039/C8MH00653A
38. Li J, Yang Z, Qian G, Berto F. Machine learning based very-high-cycle fatigue life prediction of Ti-6Al-4V alloy fabricated by selective laser melting. *Int J Fatigue.* 2022;158:106764.
39. Shen SC, Buehler MJ. Nature-inspired architected materials using unsupervised deep learning. *Commun Eng.* 2022;1(1):37.
40. Lee SY, Byeon S, Kim HS, Jin H, Lee S. Deep learning-based phase prediction of high-entropy alloys: Optimization, generation, and explanation. *Mater Des.* 2021;197:109260.  
doi: 10.1016/j.matdes.2020.109260
41. Buehler MJ. MechGPT, a language-based strategy for mechanics and materials modeling that connects knowledge across scales, disciplines, and modalities. *Appl Mech Rev.* 2024;76(2):021001.  
doi: 10.1115/1.4063843
42. Nazar S, Yang J, Faisal Javed M, Khan K, Li L, Liu QF. An evolutionary machine learning-based model to estimate the rheological parameters of fresh concrete. *Structures.* 2023;48:1670-1683.  
doi: 10.1016/j.istruc.2023.01.019
43. Hu M, Tan Q, Knibbe R, et al. Recent applications of machine learning in alloy design: A review. *Mater Sci Eng R Rep.* 2023;155:100746.  
doi: 10.1016/j.mser.2023.100746
44. Curtarolo S, Setyawan W, Wang S, et al. AFLOWLIB.ORG: A distributed materials properties repository from high-throughput ab initio calculations. *Comput Mater Sci.* 2012;58:227-235.  
doi: 10.1016/j.commatsci.2012.02.002
45. Gražulis S, Daškevič A, Merkys A, et al. Crystallography open database (COD): An open-access collection of crystal structures and platform for world-wide collaboration. *Nucleic Acids Res.* 2012;40(D1):D420-D427.  
doi: 10.1093/nar/gkr900
46. Belsky A, Hellenbrandt M, Karen VL, Luksch P. New developments in the Inorganic Crystal Structure Database (ICSD): Accessibility in support of materials research and design. *Acta Crystallogr B.* 2002;58(3):364-369.  
doi: 10.1107/S0108768102006948
47. Choudhary K, Garrity KF, Reid ACE, et al. The joint automated repository for various integrated simulations (JARVIS) for data-driven materials design. *NPJ Comput Mater.* 2020;6(1):173.  
doi: 10.1038/s41524-020-00440-1
48. Talirz L, Kumbhar S, Passaro E, et al. Materials cloud, a platform for open computational science. *Sci Data.* 2020;7(1):299.  
doi: 10.1038/s41597-020-00637-5
49. Draxl C, Scheffler M. NOMAD: The FAIR concept for big data-driven materials science. *MRS Bull.* 2018;43(9):676-682.  
doi: 10.1557/mrs.2018.208
50. Tadmor EB, Elliott RS, Sethna JP, Miller RE, Becker CA. The potential of atomistic simulations and the knowledgebase of interatomic models. *JOM.* 2011;63(7):17.  
doi: 10.1007/s11837-011-0102-6
51. Jain A, Ong SP, Hautier G, et al. Commentary: The materials project: A materials genome approach to accelerating materials innovation. *APL Mater.* 2013;1(1):011002.  
doi: 10.1063/1.4812323
52. Saal JE, Kirklin S, Aykol M, Meredig B, Wolverton C. Materials design and discovery with high-throughput density functional theory: The open quantum materials database (OQMD). *JOM.* 2013;65(11):1501-1509.  
doi: 10.1007/s11837-013-0755-4
53. Lakshminarayan K, Harp SA, Goldman R, Samad T. Imputation of Missing Data Using Machine learning Techniques. In: *Simoudis E, Han J, Fayyad UM, editors. Proceedings - 2<sup>nd</sup> International Conference on Knowledge Discovery and Data Mining, KDD 1996.* AAAI Press; 1996. p. 140-5.
54. Mahato V, Chatterjee S, Nyabadza A, Caputo A, Brabazon D. Layer porosity in powder-bed fusion prediction using regression machine learning models and time-series features. *Int J AI Mater Des.* 2024;1(3):33-49.  
doi: 10.36922/ijamd.4812
55. Montazeri M, Nassar AR, Dunbar AJ, Rao P. In-process monitoring of porosity in additive manufacturing using optical emission spectroscopy. *IISE Trans.* 2020;52(5):500-515.  
doi: 10.1080/24725854.2019.1659525
56. Wasmer K, Le-Quang T, Meylan B, Shevchik S. A. *In situ* quality monitoring in AM using acoustic emission: A reinforcement learning approach. *J Mater Eng Perform.*

- 2019;28(2):666-672.  
doi: 10.1007/s11665-018-3690-2
57. Jolliffe IT, Cadima J. Principal component analysis: A review and recent developments. *Philos Trans R Soc Math Phys Eng Sci.* 2016;374(2015):20150202.  
doi: 10.1098/rsta.2015.0202
58. Tan C, Li Q, Yao X, *et al.* Machine learning customized novel material for energy-efficient 4D printing. *Adv Sci.* 2023;10(10):2206607.  
doi: 10.1002/advs.202206607
59. Zhang M, Sun CN, Zhang X, *et al.* High cycle fatigue life prediction of laser additive manufactured stainless steel: A machine learning approach. *Int J Fatigue.* 2019;128:105194.  
doi: 10.1016/j.ijfatigue.2019.105194
60. Chernyavsky D, Kononenko DY, Han JH, Kim HJ, Van Den Brink J, Kosiba K. Machine learning for additive manufacturing: Predicting materials characteristics and their uncertainty. *Mater Des.* 2023;227:111699.  
doi: 10.1016/j.matdes.2023.111699
61. He P, Liu Q, Kruzic JJ, Li X. Machine-learning assisted additive manufacturing of a TiCN reinforced AlSi10Mg composite with tailorable mechanical properties. *Mater Lett.* 2022;307:131018.  
doi: 10.1016/j.matlet.2021.131018
62. Liu Q, Wu H, Paul MJ, *et al.* Machine-learning assisted laser powder bed fusion process optimization for AlSi10Mg: New microstructure description indices and fracture mechanisms. *Acta Mater.* 2020;201:316-328.  
doi: 10.1016/j.actamat.2020.10.010
63. Awd M, Saeed L, Münstermann S, Faes M, Walther F. Mechanistic machine learning for metamaterial fatigue strength design from first principles in additive manufacturing. *Mater Des.* 2024;241:112889.  
doi: 10.1016/j.matdes.2024.112889
64. Maleki E, Bagherifard S, Guagliano M. Application of artificial intelligence to optimize the process parameters effects on tensile properties of Ti-6Al-4V fabricated by laser powder-bed fusion. *Int J Mech Mater Des.* 2022;18(1):199-222.  
doi: 10.1007/s10999-021-09570-w
65. Meng L, Zhao J, Lan X, Yang H, Wang Z. Multi-objective optimisation of bio-inspired lightweight sandwich structures based on selective laser melting. *Virtual Phys Prototyp.* 2020;15(1):106-119.  
doi: 10.1080/17452759.2019.1692673
66. Gong X, Yabansu Y, Collins P, Kalidindi S. Evaluation of Ti-Mn alloys for additive manufacturing using high-throughput experimental assays and gaussian process regression. *Materials.* 2020;13(20):4641.  
doi: 10.3390/ma13204641
67. Miracle DB, Senkov ON. A critical review of high entropy alloys and related concepts. *Acta Mater.* 2017;122:448-511.  
doi: 10.1016/j.actamat.2016.08.081
68. Huang W, Martin P, Zhuang HL. Machine-learning phase prediction of high-entropy alloys. *Acta Mater.* 2019;169:225-236.  
doi: 10.1016/j.actamat.2019.03.012
69. Beniwal D, Ray PK. Learning phase selection and assemblages in High-Entropy Alloys through a stochastic ensemble-averaging model. *Comput Mater Sci.* 2021;197:110647.  
doi: 10.1016/j.commatsci.2021.110647
70. Krishna YV, Jaiswal UK, Rahul MR. Machine learning approach to predict new multiphase high entropy alloys. *Scr Mater.* 2021;197:113804.  
doi: 10.1016/j.scriptamat.2021.113804
71. Kaufmann K, Vecchio KS. Searching for high entropy alloys: A machine learning approach. *Acta Mater.* 2020;198:178-222.  
doi: 10.1016/j.actamat.2020.07.065
72. Choudhury A, Konnur T, Chattopadhyay PP, Pal S. Structure prediction of multi-principal element alloys using ensemble learning. *Eng Comput.* 2019;37(3):1003-1022.  
doi: 10.1108/EC-04-2019-0151
73. Lee K, Ayyasamy MV, Delsa P, Hartnett TQ, Balachandran PV. Phase classification of multi-principal element alloys via interpretable machine learning. *NPJ Comput Mater.* 2022;8(1):25.  
doi: 10.1038/s41524-022-00704-y
74. Zhang L, Chen H, Tao X, *et al.* Machine learning reveals the importance of the formation enthalpy and atom-size difference in forming phases of high entropy alloys. *Mater Des.* 2020;193:108835.  
doi: 10.1016/j.matdes.2020.108835
75. Dai D, Xu T, Wei X, *et al.* Using machine learning and feature engineering to characterize limited material datasets of high-entropy alloys. *Comput Mater Sci.* 2020;175:109618.  
doi: 10.1016/j.commatsci.2020.109618
76. Kim G, Diao H, Lee C, *et al.* First-principles and machine learning predictions of elasticity in severely lattice-distorted high-entropy alloys with experimental validation. *Acta Mater.* 2019;181:124-138.  
doi: 10.1016/j.actamat.2019.09.026
77. Pei Z, Yin J, Hawk JA, Alman DE, Gao MC. Machine-learning informed prediction of high-entropy solid solution formation: Beyond the Hume-Rothery rules. *NPJ Comput Mater.* 2020;6(1):50.

- doi: 10.1038/s41524-020-0308-7
78. Liu S, Kappes BB, Amin-Ahmadi B, Benafan O, Zhang X, Stebner AP. Physics-informed machine learning for composition-process-property design: Shape memory alloy demonstration. *Appl Mater Today*. 2021;22:100898.  
doi: 10.1016/j.apmt.2020.100898
79. Li Z, Pradeep KG, Deng Y, Raabe D, Tasan CC. Metastable high-entropy dual-phase alloys overcome the strength-ductility trade-off. *Nature*. 2016;534(7606):227-230.  
doi: 10.1038/nature17981
80. Tapia G, Khairallah S, Matthews M, King WE, Elwany A. Gaussian process-based surrogate modeling framework for process planning in laser powder-bed fusion additive manufacturing of 316L stainless steel. *Int J Adv Manuf Technol*. 2018;94(9-12):3591-3603.  
doi: 10.1007/s00170-017-1045-z
81. Chen D, Skouras M, Zhu B, Matusik W. Computational discovery of extremal microstructure families. *Sci Adv*. 2018;4(1):eaao7005.  
doi: 10.1126/sciadv.aao7005
82. Xue T, Wallin TJ, Menguc Y, Adriaenssens S, Chiaramonte M. Machine learning generative models for automatic design of multi-material 3D printed composite solids. *Extreme Mech Lett*. 2020;41:100992.  
doi: 10.1016/j.eml.2020.100992
83. Fleisch M, Thalhamer A, Meier G, et al. Functional mechanical metamaterial with independently tunable stiffness in the three spatial directions. *Mater Today Adv*. 2021;11:100155.  
doi: 10.1016/j.mtadv.2021.100155
84. Bessa MA, Glowacki P, Houlder M. Bayesian machine learning in metamaterial design: Fragile becomes supercompressible. *Adv Mater*. 2019;31(48):1904845.  
doi: 10.1002/adma.201904845
85. Sharma S, Gupta V, Mudgal D, Srivastava V. Predicting biomechanical properties of additively manufactured polydopamine coated poly lactic acid bone plates using deep learning. *Eng Appl Artif Intell*. 2023;124:106587.  
doi: 10.1016/j.engappai.2023.106587
86. Nasrin T, Pourali M, Pourkamali-Anaraki F, Peterson AM. Active learning for prediction of tensile properties for material extrusion additive manufacturing. *Sci Rep*. 2023;13(1):11460.  
doi: 10.1038/s41598-023-38527-6
87. Veeman D, Sudharsan S, Surendhar GJ, Shanmugam R, Guo L. Machine learning model for predicting the hardness of additively manufactured acrylonitrile butadiene styrene. *Mater Today Commun*. 2023;35:106147.  
doi: 10.1016/j.mtcomm.2023.106147
88. Butt J, Mohaghegh V. Combining digital twin and machine learning for the fused filament fabrication process. *Metals*. 2022;13(1):24.  
doi: 10.3390/met13010024
89. Zhang J, Wang P, Gao RX. Deep learning-based tensile strength prediction in fused deposition modeling. *Comput Ind*. 2019;107:11-21.  
doi: 10.1016/j.compind.2019.01.011
90. Lee S, Zhang Z, Gu GX. Generative machine learning algorithm for lattice structures with superior mechanical properties. *Mater Horiz*. 2022;9(3):952-960.  
doi: 10.1039/D1MH01792F
91. He Y, Abdi M, Trindade GF, et al. Exploiting generative design for 3D printing of bacterial biofilm resistant composite devices. *Adv Sci*. 2021;8(15):2100249.  
doi: 10.1002/advs.202100249
92. Goh GD, Sing SL, Lim YF, et al. Machine learning for 3D printed multi-materials tissue-mimicking anatomical models. *Mater Des*. 2021;211:110125.  
doi: 10.1016/j.matdes.2021.110125
93. Veerabagu U, Palza H, Quero F. Review: Auxetic polymer-based mechanical metamaterials for biomedical applications. *ACS Biomater Sci Eng*. 2022;8(7):2798-2824.  
doi: 10.1021/acsbmaterials.2c00109
94. Sinha P, Mukhopadhyay T. Programmable multi-physical mechanics of mechanical metamaterials. *Mater Sci Eng R Rep*. 2023;155:100745.  
doi: 10.1016/j.mser.2023.100745
95. Jiao P, Chen T, Xie Y. Self-adaptive mechanical metamaterials (SMM) using shape memory polymers for programmable postbuckling under thermal excitations. *Compos Struct*. 2021;256:113053.  
doi: 10.1016/j.compstruct.2020.113053
96. Zhang Z, Krushynska AO. Programmable shape-morphing of rose-shaped mechanical metamaterials. *APL Mater*. 2022;10(8):080701.  
doi: 10.1063/5.0099323
97. Chen Y, Wang L. Periodic co-continuous acoustic metamaterials with overlapping locally resonant and Bragg band gaps. *Appl Phys Lett*. 2014;105(19):191907.  
doi: 10.1063/1.4902129
98. Belei C, Pommer R, Amancio-Filho ST. Optimization of additive manufacturing for the production of short carbon fiber-reinforced polyamide/Ti-6Al-4V hybrid parts. *Mater Des*. 2022;219:110776.  
doi: 10.1016/j.matdes.2022.110776

99. Khan ZN, Albalawi HI, Valle-Pérez AU, *et al.* From 3D printed molds to bioprinted scaffolds: A hybrid material extrusion and vat polymerization bioprinting approach for soft matter constructs. *Mater Sci Addit Manuf.* 2022;1(1):7.  
doi: 10.18063/msam.v1i1.7
100. Magennis EP, Hook AL, Davies MC, Alexander C, Williams P, Alexander MR. Engineering serendipity: High-throughput discovery of materials that resist bacterial attachment. *Acta Biomater.* 2016;34:84-92.  
doi: 10.1016/j.actbio.2015.11.008
101. Groll J, Burdick JA, Cho DW, *et al.* A definition of bioinks and their distinction from biomaterial inks. *Biofabrication.* 2018;11(1):013001.  
doi: 10.1088/1758-5090/aaec52
102. Chimene D, Lennox KK, Kaunas RR, Gaharwar AK. Advanced bioinks for 3D printing: A materials science perspective. *Ann Biomed Eng.* 2016;44(6):2090-2102.  
doi: 10.1007/s10439-016-1638-y
103. Zhang Z, Jin Y, Yin J, *et al.* Evaluation of bioink printability for bioprinting applications. *Appl Phys Rev.* 2018;5(4):041304.  
doi: 10.1063/1.5053979
104. Qavi I, Halder S, Tan G. Optimization of printability of bioinks with multi-response optimization (MRO) and artificial neural networks (ANN). *Prog Addit Manuf.* 2024.  
doi: 10.1007/s40964-024-00828-1
105. Lee J, Oh SJ, An SH, Kim WD, Kim SH. Machine learning-based design strategy for 3D printable bioink: Elastic modulus and yield stress determine printability. *Biofabrication.* 2020;12(3):035018.  
doi: 10.1088/1758-5090/ab8707
106. Xu Y, Sarah R, Habib A, Liu Y, Khoda B. Constraint based Bayesian optimization of bioink precursor: A machine learning framework. *Biofabrication.* 2024;16(4):045031.  
doi: 10.1088/1758-5090/ad716e
107. Qiao Q, Zhang X, Yan Z, *et al.* The use of machine learning to predict the effects of cryoprotective agents on the GelMA-based bioinks used in extrusion cryobioprinting. *Bio-Des Manuf.* 2023;6(4):464-477.  
doi: 10.1007/s42242-023-00244-4
108. Ruberu K, Senadeera M, Rana S, *et al.* Coupling machine learning with 3D bioprinting to fast track optimisation of extrusion printing. *Appl Mater Today.* 2021;22:100914.  
doi: 10.1016/j.apmt.2020.100914
109. Hashemi A, Ezati M, Zumberg I, *et al.* Characterization and optimization of a biomaterial ink aided by machine learning-assisted parameter suggestion. *Mater Today Commun.* 2024;40:109777.  
doi: 10.1016/j.mtcomm.2024.109777
110. Huang X, Ng WL, Yeong WY. Predicting the number of printed cells during inkjet-based bioprinting process based on droplet velocity profile using machine learning approaches. *J Intell Manuf.* 2024;35(5):2349-2364.  
doi: 10.1007/s10845-023-02167-4
111. Huang X, Wong YX, Goh GL, Gao X, Lee JM, Yeong WY. Machine learning-driven prediction of gel fraction in conductive gelatin methacryloyl hydrogels. *Int J AI Mater Des.* 2024;1(2):61-75.  
doi: 10.36922/ijamd.3807
112. Bonatti AF, Vozzi G, Chua CK, Maria CD. A deep learning quality control loop of the extrusion-based bioprinting process. *Int J Bioprinting.* 2022;8(4):620.  
doi: 10.18063/ijb.v8i4.620
113. Chen B, Dong J, Ruelas M, *et al.* Artificial intelligence-assisted high-throughput screening of printing conditions of hydrogel architectures for accelerated diabetic wound healing. *Adv Funct Mater.* 2022;32(38):2201843.  
doi: 10.1002/adfm.202201843

## REVIEW ARTICLE

# Advancing intelligent additive manufacturing: Machine learning approaches for process optimization and quality control

Hayeol Kim<sup>1</sup> , Kyung-Hwan Kim<sup>1</sup> , Jiyun Jeong<sup>1</sup> , Hongryung Jeon<sup>1</sup> , and Im Doo Jung<sup>1,2\*</sup> 

<sup>1</sup>Department of Mechanical Engineering, Ulsan National Institute of Science and Technology, Ulsan, Republic of Korea

<sup>2</sup>Artificial Intelligence Graduate School, Ulsan National Institute of Science and Technology, Ulsan, Republic of Korea

(This article belongs to the *Special Issue: Artificial Intelligence Applications in Additive Manufacturing and 3D Printing*)

## Abstract

Additive manufacturing (AM) has revolutionized modern fabrication by enabling complex geometries, material efficiency, and customized production. However, process variability, material inconsistencies, and defect formation remain critical challenges, limiting scalability and industrial adoption. Machine learning (ML) has emerged as a powerful tool to address these limitations by enabling data-driven optimization, defect detection, material property prediction, and real-time process control. This review provides a comprehensive analysis of ML applications in AM, spanning polymers, metals, ceramics, and carbon-based materials, with a focus on process optimization, quality assurance, and predictive modeling. Specifically, this review examines real-time defect detection through vision-based ML techniques, printing parameter optimization using supervised and reinforcement learning, and predictive modeling of material properties—laying the groundwork for deeper exploration of key methodologies such as deep learning and physics-informed models. Key ML methodologies, including deep learning, reinforcement learning, and hybrid physics-informed models, are explored in the context of enhancing print precision, mechanical performance, and functional properties. Despite significant advancements, challenges such as data scarcity, model generalization, and real-time integration into AM workflows persist. Emerging trends, including multimodal sensor fusion, *in situ* monitoring, and cloud-based predictive analytics, are discussed as potential pathways toward fully autonomous and intelligent manufacturing. By consolidating recent developments and outlining future directions, this review provides essential insights for researchers, engineers, and industry professionals looking to harness ML in AM, facilitating advancements in process efficiency, quality control, and overall manufacturing reliability.

**Keywords:** Additive manufacturing; Machine learning; Process optimization; Defect detection; Quality assurance; Material property; Real-time monitoring; Data-driven manufacturing

### \*Corresponding author:

Im Doo Jung  
 (idjung@unist.ac.kr)

**Citation:** Kim H, Kim K, Jeong J, Jeon H, Jung ID. Advancing intelligent additive manufacturing: Machine learning approaches for process optimization and quality control. *Int J AI Mater Design*. 2025;2(2):27-55.  
 doi: 10.36922/IJAMD025130010

**Received:** March 24, 2025

**Revised:** May 20, 2025

**Accepted:** May 23, 2025

**Published online:** June 11, 2025

**Copyright:** © 2025 Author(s). This is an Open-Access article distributed under the terms of the Creative Commons Attribution License, permitting distribution, and reproduction in any medium, provided the original work is properly cited.

**Publisher's Note:** AccScience Publishing remains neutral with regard to jurisdictional claims in published maps and institutional affiliations.

## 1. Introduction

Additive manufacturing (AM), commonly known as 3D printing, has transformed modern manufacturing by enabling the production of complex geometries with high design flexibility and material efficiency. Unlike traditional subtractive manufacturing, which removes material to shape a final product, AM constructs objects layer by layer from digital models, significantly reducing material waste and enabling the fabrication of intricate structures that would be challenging or impossible to achieve through conventional methods.<sup>1,2</sup> Beyond material efficiency, AM eliminates many constraints associated with traditional manufacturing, such as the need for assembly and joining, and accelerates the prototyping process, reducing development time and costs.<sup>3,4</sup> In addition, AM facilitates the integration of multifunctional structures and multi-material designs, expanding its applicability across various industries, including aerospace, automotive, healthcare, and consumer goods.<sup>5-11,12</sup>

Despite these advantages, AM still faces critical challenges that hinder its scalability and widespread industrial adoption. The manufacturing process is highly sensitive to variations in processing parameters, material properties, and environmental conditions, leading to inconsistencies in part quality.<sup>13,14</sup> Defects such as porosity, residual stresses, warping, and poor interlayer bonding frequently occur, necessitating rigorous post-processing to ensure structural integrity.<sup>15</sup> Moreover, optimizing AM processes for different materials and geometries remains a complex and computationally intensive task, as each combination requires precise tuning of parameters such as laser power, scanning speed, layer thickness, and cooling rates to achieve the desired mechanical properties and surface finish.<sup>16-19</sup> These challenges underscore the need for advanced methodologies to enhance the reliability, efficiency, and precision of AM processes.

To address these issues, data-driven approaches leveraging machine learning (ML) have gained significant attention as a means to optimize AM workflows. ML techniques enable predictive modeling, real-time process monitoring, and adaptive control, providing a systematic approach to improving manufacturing consistency and efficiency. Early research in this field, initiated over a decade ago, demonstrated the feasibility of applying basic ML models, such as support vector machines (SVMs) and Gaussian process (GP) regression, to process AM data. For instance, GP-based surrogate models were employed to predict defect formation and porosity from process parameters in metal AM, while SVM classifiers were used to construct process maps and identify stable fabrication regimes.<sup>20,21</sup> Although these pioneering studies validated

the potential of data-driven approaches in understanding complex process-property relationships, their impact was limited by small datasets and issues related to model generalization.<sup>22</sup> Subsequent developments have since advanced beyond these early efforts, leveraging more sophisticated algorithms and larger datasets to achieve robust and scalable ML solutions in AM.

Key ML applications in AM include process parameter optimization, where ML models identify optimal printing conditions to minimize defects and enhance part performance; *in situ* process monitoring and real-time feedback, which utilize sensor data to detect anomalies and adjust parameters dynamically; and quality assessment and defect prediction, allowing for early identification of suboptimal parts before post-processing.<sup>23,24</sup> These ML-driven strategies not only minimize reliance on empirical trial-and-error experimentation but also reduce production time, material consumption, and overall costs while improving repeatability and part quality. Moreover, ML has facilitated advancements that were previously unattainable using conventional process control methods, further demonstrating its potential to revolutionize AM.<sup>25-27</sup>

Given the rapid evolution of ML applications in AM, a comprehensive and up-to-date review is needed to consolidate existing knowledge and identify emerging trends. Although several related reviews have been published, many are limited in scope—often focusing on specific materials, algorithms, or AM techniques—leaving a gap in the broader understanding of ML integration across diverse AM platforms.<sup>24,28-34</sup> In contrast, this review offers a holistic examination of ML-driven strategies for optimizing AM processes, encompassing all major material classes, including polymers, metals, ceramics, and carbon-based composites. By analyzing recent advancements across these material systems, the review aims to provide a structured overview of how ML is being applied to enhance printing efficiency, material utilization, and product quality. Furthermore, it addresses critical challenges such as data scarcity, model generalization, and the integration of real-time control mechanisms. Emerging directions, including physics-informed ML models and multimodal *in situ* monitoring, are also highlighted to offer a forward-looking perspective. The insights presented in this work are intended to support researchers, engineers, and industry professionals in leveraging ML to advance the reliability, scalability, and intelligence of AM technologies.

## 2. AM and ML method

### 2.1. AM

Unlike conventional subtractive methods, which remove material to create a final product, this advanced

manufacturing approach builds objects layer by layer from digital models, maximizing material efficiency and enabling intricate geometries. Its ability to offer exceptional design flexibility has made it a transformative technology in industries such as aerospace, healthcare, and automotive, where lightweight, customized, and functionally optimized structures are essential for innovation and performance. The ASTM standard classifies AM into seven categories, with material extrusion, vat photopolymerization, powder bed fusion (PBF), binder jetting, and directed energy deposition (DED) being the most widely adopted.<sup>35</sup> While AM technologies offer significant advantages over conventional manufacturing, each method presents unique processing requirements and challenges depending on the material type.

Polymer-based AM technologies, such as material extrusion and vat photopolymerization, are widely used due to their cost-effectiveness and broad material availability. Material extrusion, exemplified by fused deposition modeling (FDM) and direct ink writing (DIW), is one of the most accessible and scalable AM techniques. FDM, which utilizes thermoplastic filaments such as acrylonitrile butadiene styrene (ABS) and polylactic acid (PLA), is commonly used for rapid prototyping and functional components. However, FDM parts often suffer from anisotropic mechanical properties and limited resolution, requiring post-processing or parameter optimization to enhance quality.<sup>36</sup> DIW, in contrast, is particularly advantageous for soft and bioinspired materials, such as hydrogels and elastomers, but demands precise rheological control to maintain printing accuracy.<sup>37</sup> Vat photopolymerization, which includes stereolithography (SLA) and digital light processing (DLP), enables high-resolution fabrication with smooth surface finishes, making it particularly beneficial for biomedical applications, dental prosthetics, and microfluidic devices. However, photopolymer-based materials often exhibit brittleness and require post-curing, which may limit their mechanical performance in load-bearing applications.<sup>38</sup>

Metal and ceramic-based AM technologies, such as PBF, binder jetting, and DED, are essential for high-performance applications that require superior mechanical properties and thermal resistance. PBF processes, including selective laser sintering (SLS) for polymers and selective laser melting or electron beam melting for metals, utilize high-energy sources to selectively fuse powdered materials, enabling the production of complex, high-strength components. These techniques are widely used in aerospace, automotive, and medical implants, where precision and material integrity are critical. However, strict control of powder properties, high energy consumption, and extensive post-processing

requirements remain key challenges.<sup>39,40</sup> Binder jetting, which selectively deposits a liquid binding agent onto a powder bed, offers a low-temperature alternative to PBF, making it particularly useful for ceramic and metal-based applications.<sup>41,42</sup> This method enables high-speed, cost-effective large-scale fabrication, but the resulting parts often require sintering or infiltration post-processing to achieve full density and mechanical strength. DED, which directly deposits molten or semi-molten material using a focused energy source such as a laser or plasma arc, is commonly used for metal repair, aerospace component restoration, and large-scale manufacturing. While DED provides greater material efficiency and repair capabilities, it typically results in lower resolution and surface quality compared to PBF, necessitating additional post-processing to improve dimensional accuracy.<sup>43</sup> While AM technologies continue to advance, optimizing process parameters, improving material performance, and addressing scalability challenges remain critical for industrial adoption. Recent advancements in ML have demonstrated significant potential in enhancing process efficiency, real-time monitoring, and defect prediction, as summarized in [Figure 1](#).

## 2.2. ML approaches

ML techniques have become increasingly integral to AM process optimization, defect detection, and quality control. ML approaches in AM are broadly classified

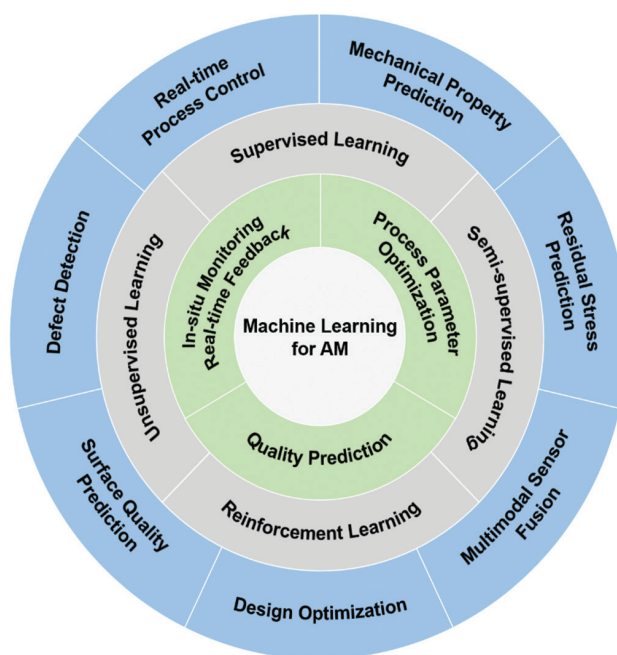


**Figure 1.** Overview of machine learning for additive manufacturing. Machine learning applications, learning types, and key roles in process optimization, quality prediction, and real-time monitoring.

into supervised learning, unsupervised learning, semi-supervised learning, and reinforcement learning, each offering distinct advantages depending on the nature of the available data and the specific manufacturing objectives. A visual summary of the major ML categories, representative models, and their applications across various AM processes and materials is provided in Figure 2, highlighting how different learning paradigms contribute to process, property, and design optimization.

Supervised learning relies on labeled datasets to establish relationships between input parameters and output quality metrics, enabling predictive modeling and automated defect classification. Commonly used algorithms such as SVM, random forests (RF), artificial neural networks (ANN), and convolutional neural networks (CNN) have been applied in AM for tasks such as predicting mechanical properties, optimizing printing parameters, and identifying defects through image-based analysis.<sup>31,44</sup> Unsupervised learning, which identifies patterns in unlabeled data, is particularly useful for clustering process variations and

detecting anomalies. Techniques such as k-means clustering and principal component analysis have been employed to analyze sensor data and monitor inconsistencies in layer formation and material distribution.<sup>45</sup>

Semi-supervised learning, which leverages a combination of labeled and unlabeled data, has proven particularly advantageous in AM, where acquiring large labeled datasets for defect classification can be time-intensive and costly. Methods such as self-training and generative adversarial networks (GANs) have been explored to augment datasets, improve defect detection accuracy, and enhance model robustness.<sup>31</sup> Reinforcement learning, which enables an agent to learn optimal strategies through trial-and-error interactions with the environment, has been increasingly applied in AM for real-time process control and adaptive optimization. Deep Q-networks and proximal policy optimization algorithms have been utilized to dynamically adjust laser power in PBF and extrusion rates in FDM, leading to improved process stability and reduced defect formation.<sup>16</sup>

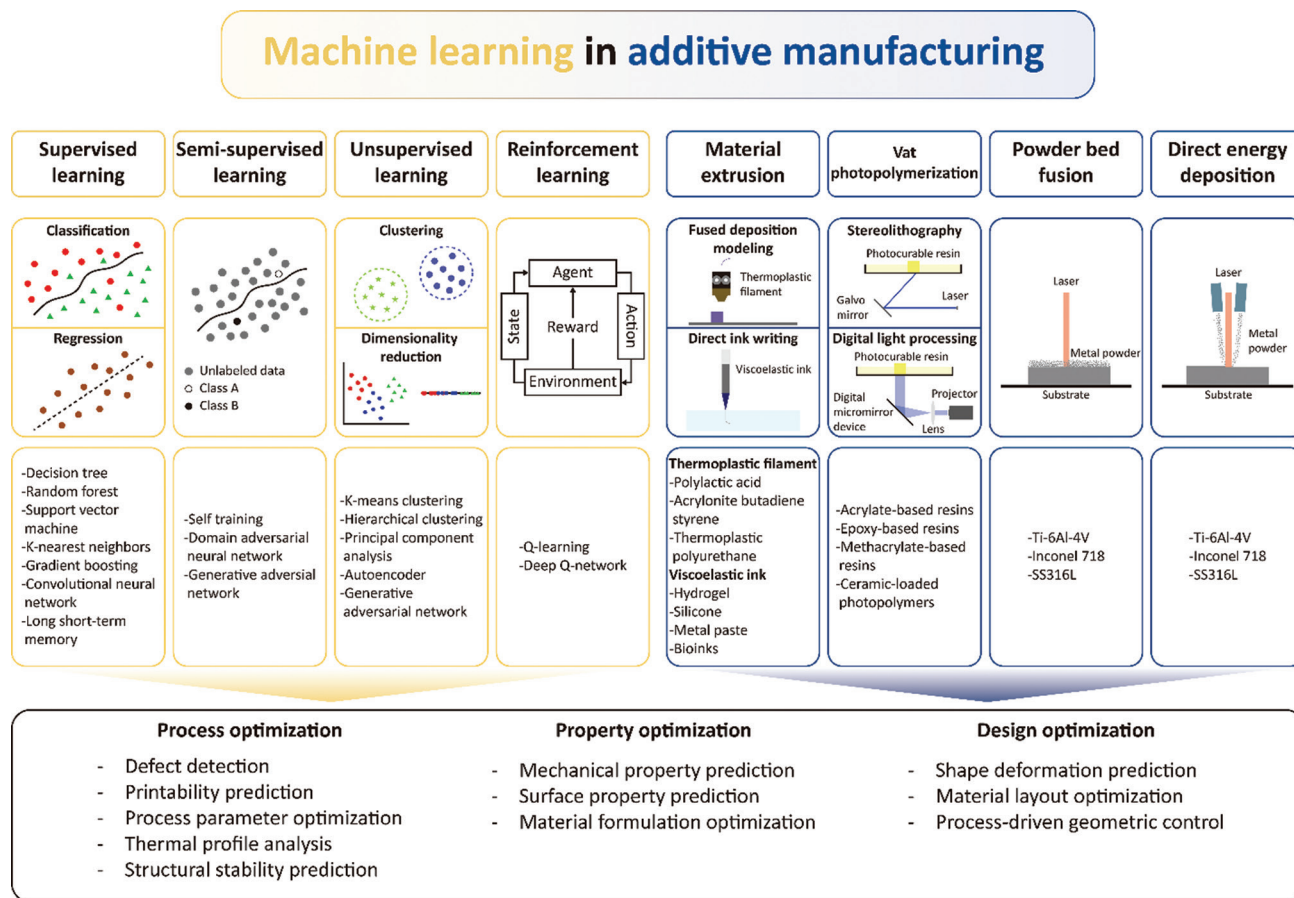


**Figure 2.** Summary of machine learning (ML) and additive manufacturing (AM) techniques commonly used for process optimization. ML approaches and representative models are shown on the left, while AM technologies, materials, and composites are displayed on the right. ML-driven optimization tasks in AM include process optimization, property prediction, and design optimization.

Each ML paradigm presents specific strengths and trade-offs in terms of predictive accuracy, data efficiency, and implementation complexity. Supervised learning generally achieves high accuracy when sufficient labeled data are available, but it requires extensive data collection and careful parameter tuning. In contrast, unsupervised learning offers greater data efficiency by leveraging unlabeled datasets. However, its outputs, such as clusters or anomaly scores, may lack the precision of supervised models due to the absence of ground-truth labels. Semi-supervised learning offers a compromise by combining limited labeled data with abundant unlabeled data to improve learning efficiency. For example, even a small number of labeled defect images can significantly boost detection accuracy when incorporated into a largely unlabeled dataset. Reinforcement learning is particularly suited to sequential decision-making tasks, such as real-time process control, but its application in AM remains relatively limited due to the complexity of reward design and the need for extensive experimentation. In practice, supervised CNN-based models have demonstrated over 90% accuracy in classifying FDM defects when trained with sufficient data, while unsupervised methods can still effectively flag anomalies without any labels. Reinforcement learning, although promising for adaptive control, has thus far been primarily explored in experimental setups.

In addition to purely data-driven methods, hybrid approaches that integrate physical modeling and ML—often referred to as physics-informed or physics-based ML—have gained attention for enhancing prediction reliability and reducing data requirements. For instance, physics-informed neural networks have been applied in fused filament fabrication to incorporate thermal behavior into property prediction models.<sup>46</sup> In addition, physics-based simulations such as finite element analysis (FEA), computational fluid dynamics, and phase-field modeling have been combined with ML to predict microstructure evolution,<sup>47</sup> residual stress formation,<sup>48</sup> and melt pool geometry in metal and ceramic AM processes.<sup>49</sup> These approaches ensure physical consistency in ML predictions and offer scalable solutions for complex modeling processes in AM.

The effectiveness of ML in AM largely depends on the quality and availability of training data. Data generated by AM can be categorized into process data, material data, quality data, and geometric design data, each playing a crucial role in model development and validation. Process data include sensor-based measurements such as temperature, pressure, humidity, and real-time monitoring of melt pool dynamics in metal AM processes. These data points are critical for tracking process stability, detecting

deviations, and predicting potential defects.<sup>32</sup> Material data, encompassing parameters such as composition, viscosity, and thermal properties, influences printability, microstructure evolution, and final part performance. For instance, in vat photopolymerization, resin viscosity and photoinitiator concentration affect curing dynamics, whereas in PBF, powder morphology and packing density determine layer fusion and mechanical strength.<sup>50,51</sup> Quality data, such as surface roughness, porosity, and mechanical properties, are typically obtained through non-destructive evaluation techniques, including X-ray computed tomography (CT) and ultrasonic testing, providing ground truth for ML model validation. Geometric and design data derived from computer-aided design (CAD) models and G-code instructions facilitate the analysis of layer-wise deviations, part distortions, and structural integrity.<sup>23</sup>

Identifying which data types serve as input features versus prediction targets is essential for designing effective ML workflows in AM. In most applications, process and design data—such as machine sensor readings, processing parameters, and CAD files—serve as input features. In contrast, quality metrics (e.g., porosity and mechanical strength) typically serve as the output targets for prediction or classification. Material data can play either role depending on context, for example, known properties may be used as inputs for performance prediction, or they may serve as outputs in formulation design tasks. In a defect detection task, *in situ*, sensor images and environmental data constitute the input, while defect presence or severity, verified by inspection, serves as the output. For property prediction, inputs may include process conditions and material composition, with outputs being target values such as tensile strength or elasticity. Proper alignment of input–output structure helps guide algorithm selection and ensures that the ML approach is suited to the intended application, be it predictive modeling, real-time anomaly detection, or parameter optimization.

To extract meaningful insights from these datasets, various ML-driven data analysis techniques have been adopted. Image processing and computer vision models, including CNNs and You Only Look Once (YOLO) networks, have been employed for real-time defect detection in FDM by analyzing nozzle-near images.<sup>51</sup> Time-series analysis models, such as long short-term memory (LSTM) networks, have been used to predict process drift in PBF by analyzing laser scan data across multiple layers.<sup>52</sup> Hybrid approaches that combine ML with physics-based simulations, such as FEA, have been developed to predict residual stress formation and optimize support structures in metal AM.<sup>53</sup> Furthermore, Bayesian optimization has been widely explored for process parameter tuning, reducing

reliance on traditional empirical trial-and-error methods.<sup>54</sup> These ML-driven strategies significantly enhance process control, reduce production time and material waste, and improve overall manufacturing reliability.

### 3. ML-based 3D printing optimizations

#### 3.1. Polymers

Polymers are macromolecules composed of covalently bonded repeating units, forming long chains that exhibit diverse rheological properties. Such chain structures endow polymers with low density, flexibility, and—in certain cases—viscoelastic behavior.<sup>34</sup> Their physicochemical properties can also be tuned during synthesis and processing to meet specific requirements. Owing to these adaptable characteristics, polymers are widely employed as elastomer matrices in soft robotics,<sup>55–57</sup> soft actuators,<sup>58,59</sup> and soft sensors.<sup>8,60,61</sup>

Because of their tunability and ease of processing, polymers are well-suited for various 3D printing techniques.<sup>62</sup> Material extrusion techniques like FDM typically use thermoplastic filaments such as ABS and PLA,<sup>63</sup> while DIW prints polymer-based materials, including hydrogels and elastomers.<sup>37</sup> Recent studies have leveraged ML-based approaches to optimize DIW parameters, especially for bioinks and hydrogels used in biomedical applications.<sup>37</sup> Key rheological behaviors—such as apparent viscosity, shear-yielding, and shear-thinning—are typically considered for DIW formulations.<sup>8,34,64,65</sup> A summary of recent ML applications and model types used for polymer-based 3D printing is presented in [Table 1](#).

In addition, vat photopolymerization techniques such as SLA and DLP enable high-resolution printing for biomedical<sup>66,67</sup> and electronics<sup>68,69</sup> applications. During the printing process, photosensitive resins must maintain a low viscosity to accommodate continuous layer-by-layer fabrication and be formulated to exhibit optimal reactivity within the targeted wavelength range of the photoinitiation system. While acrylate- and epoxy-based monomers are commonly employed,<sup>68–71</sup> other photosensitive formulations may be used for specialized applications. For example, photocurable hydrogels are frequently considered for bioprinting.<sup>67,71,72</sup>

##### 3.1.1. Process optimization

Despite the advantages of polymer-based 3D printing, process parameters can significantly influence printing quality and yield. In FDM, parameters such as nozzle temperature, layer height, printing speed, build orientation, and infill settings often affect part integrity, potentially causing interlayer delamination and uneven stress distributions.<sup>73–77</sup> With the rapid development

of ML models, numerous studies have attempted to monitor and control defects that emerge during FDM printing. In parallel, experimental approaches based on physical sensing techniques have been used to measure process-induced deformation. For example, Kantaros and Karalekas utilized fiber Bragg grating (FBG) sensors to measure residual strains in ABS parts fabricated via FDM, offering a physics-based understanding of internal stresses through thermo-optic and strain-optic coefficients.<sup>78</sup>

A common approach involves *in situ* monitoring of image data.<sup>51,77–82</sup> For instance, capturing the top view of an FDM part printed with ABS or PLA at certain build stages and then applying image-processing techniques combined with SVM to detect the presence or absence of defects has been reported.<sup>79</sup> Similarly, CNN have been employed to classify defects from top-view images of partially completed prints.<sup>80</sup> Moreover, FDM processes are highly sensitive to environmental conditions, which may drift over time (so-called “drift” in process parameters).<sup>81</sup> Such domain shifts can degrade the performance of previously trained diagnostic models. To mitigate this, a deep learning-based defect detection system has been developed that utilizes top-view images of PLA-printed samples.<sup>54</sup> The training data were balanced using a conditional GAN (CGAN), and domain adversarial neural networks (DANN) were employed to adapt to parameter drift. This system achieved a classification accuracy of 91.01% in detecting various FDM defects. Nevertheless, relying solely on top-view images can pose challenges in detecting flaws on vertical surfaces. Complementing purely data-driven approaches, hybrid models that incorporate physics-based knowledge into ML frameworks have also been proposed. Kapusuzoglu and Mahadevan<sup>46</sup> demonstrated a physics-informed ML model for fused filament fabrication, which integrates thermal and mechanical principles to improve prediction accuracy and reduce the data dependency often seen in conventional ML models.

Beyond defect detection, real-time process compensation offers a more proactive strategy. One study used a CNN-based classifier to analyze nozzle-near images in real-time, detecting under-extrusion or over-extrusion and automatically adjusting extrusion flow rates.<sup>82</sup> By incorporating a feedback loop, the system reduced corrective action times to 8.6 s for under-extrusion and 9.8 s for over-extrusion—faster than human intervention. Another work further automated process correction by modifying G-code based on defect types.<sup>51</sup> Using a YOLO object detection model, under- and over-extrusions were identified in real-time, and flow rates or recent G-code commands were updated accordingly. A streamlined

Table 1. Summary of ML models for polymer-based 3D printing

Motivation	Materials	AM method	ML model	Model inputs	Remarks	References
Process optimization	ABS, PLA	FDM	SVM	Image data from semi-finished printed parts at checkpoints	Real-time defect detection using image processing and ML	84
	ABS, PLA	FDM	CNN	Top-view images from a static camera during printing	Detecting infill pattern in real-time	85
	PLA	FDM	CGAN, DANN	Top-view grayscale images of printed layers	Fault diagnosis under process parameter drift	81
	PLA	FDM	CNN (ResNet-50)	Real-time images from a nozzle-mounted camera	Autonomous <i>in situ</i> correction of under- and over- extrusion	87
	PLA	FDM	YOLOv3-Tiny, YOLOv4-Tiny, ONNX-optimized YOLO	Real-time nozzle-near images	Automated defect detection and G-code correction for <i>in situ</i> extrusion compensation	54
	ABS	FDM	Reinforcement learning	Printing speed, flow rate multiplier, cooling fan, surface quality images	Online-learning based defect mitigation	57
	PLA	FDM	XceptionTime	Temperature, humidity, air pressure, gas particle concentration	Real-time classification of FDM process states using environmental sensor data	88
	GelMA and alginate	DIW (bioprinting)	CNN (ResNeXt-50)	Layer images, interlayer continuity, uniformity metrics	Real-time anomaly detection in bioprinting	90
	16 biomaterials	DIW (bioprinting)	DT, RF, ANN	Bioink composition ratios, printability labels	Predicting the printability of bioink formulations	91
	GelMA with encapsulated cells	DLP (bioprinting)	U-Net-based master-slave neural network	Light scattering patterns, corrected exposure masks	Generating optimized correction masks to mitigate cell-induced light scattering	97
Epoxy acrylate resin+commercial photopolymer resin	DLP (grayscale)	RNN with LSTM layers, EA	Per-pixel grayscale values, deformed structure data	Predicting deformation and optimizing grayscale distribution for enhanced print accuracy	55	
Acrylate photopolymer resin	DLP	LSTM	Temperature data, UV exposure time, layer thickness	Optimizing DLP printing via real-time temperature prediction	99	
Three commercial photopolymer resins	DLP	U-Net, CGAN	Grayscale pixel data, boundary images	Improving printing resolution and reducing jagged edges	100	
Commercial photopolymer resin	DLP	RF with EWMA p-control chart	Strain gauge data, UV exposure levels	Real-time detection of part detachment and automatic process halting	104	
Commercial photopolymer resin	DLP	MLP	Prediction feature region, layer geometry	Predicting optimal idle time for resin drainage	107	
Photopolymer resin	SLA	CNN, Two-stream CNN	FEA-generated stress distributions, geometry data	Predicting layer-wise stress distribution to improve print reliability	56	
Commercial photopolymer resin	DLP	RF	UV exposure time, light intensity, layer thickness	Predicting print accuracy and optimizing printing parameters	106	
Property optimization	PLA	FDM	RF, SVM, K-NN	Layer height, printing speed, printing temperature	Optimizing mechanical properties by predicting tensile strength	108

(Cont'd...)

Table 1. (Continued)

Motivation	Materials	AM method	ML model	Model inputs	Remarks	References
	ABS	FDM	LR, DT, RF, AdaBoost	Infill density, layer thickness, print orientation, raster orientation	Predicting and optimizing hardness	109
	Polydopamine-coated PLA	FDM	RF, K-NN, AdaBoost, DT, LSTM	Infill density, submersion time, shaker speed, coating solution concentration	Predicting mechanical strength (tensile and bending) of PDM-coated PLA structures	110
	PLA	FDM	LSTM	Infrared temperature, thermocouple, accelerometer, printing parameters (extruder temperature, printing speed, layer height)	Predicting tensile strength of PLA parts using process and sensor data	112
	PLA	FDM	Ensemble learning (RF, AdaBoost, CART, SVR, RR, RVFL)	Layer thickness, extruder temperature, print speed, infrared sensor, thermocouple, accelerometer data	Predicting surface roughness	113
	Acrylate photopolymer resin	DLP	GPR, BO, AL	Monomer composition ratios, Young's modulus, peak stress, ultimate strain, Shore A hardness	Optimizing photopolymer resin formulations using active learning and Bayesian optimization	117
	Acrylate photopolymer resin	DLP	Ensemble learning (K-NN, GPR, KR, RF, MLP)	Resin composition ratios, hardness, tensile strength, elongation at break	Predicting multiple mechanical properties of photopolymers	118
Design optimization	Acrylate photopolymer resin	DLP	RNN+EA	Material distribution (binary voxelized structure)	Predicting shape change and optimizing material layout for 4D printing	120
	Acrylate photopolymer resin	DLP	ResNet (CNN-based)	Voxel-level material distribution	Predicting shape deformations and optimizing material distribution	121

Abbreviations: ABS: Acrylonitrile butadiene styrene; AL: Active learning; ANN: Artificial neural network; BO: Bayesian optimization; CART: Classification and regression tree; CGAN: Conditional generative adversarial network; CNN: Convolutional neural network; DANN: Domain adversarial neural networks; DLP: Digital light processing; DT: Decision trees; EA: Evolutionary algorithm; EWMA: Exponentially weighted moving average; FDM: Fused deposition modeling; GelMA: Gelatin methacrylate; GPR: Gaussian process regression; K-NN: k-nearest neighbor; KR: Kernel ridge regression; LSTM: Long short-term memory; ML: Machine learning; MLP: Multi-layer perceptron; PLA: Polylactic acid; RF: Random forest; RNN: Recurrent neural network; RR: Ridge regression; RVFL: Random vector functional link network; SLA: Stereolithography; SVM: Support vector machine; SVR: Support vector regression UV: Ultraviolet; YOLO: You Only Look Once.

YOLOv3-Tiny model accelerated by the Open Neural Network Exchange runtime achieved 70 FPS, underscoring the viability of high-speed *in situ* defect compensation.

In addition to image-based approaches, sensor signals have also been integrated into ML frameworks to predict defects.<sup>75,83</sup> In one study, environmental parameters (temperature, humidity, air pressure, and gas-particle concentration) were monitored in real-time and used with an XceptionTime model to classify FDM process states automatically.<sup>83</sup> Air pressure emerged as the most critical feature, possibly because its relatively stable baseline made small variations highly indicative and also helped prevent

model overfitting. Another work employed a dual approach combining imaging and sensor data.<sup>75</sup> A CNN-based model classified the severity of interlayer delamination from nozzle-near images, while signals from a strain gauge attached to the build platform predicted warping that might develop gradually (Figure 3A). The strain data were interpreted using a physics-based model, which indicated that warping was likely to occur once the strain exceeded a certain threshold.

Compared with FDM, adopting ML for DIW is relatively new, but several studies have explored ML-based optimization of DIW processes.<sup>84-86</sup> A study has reported

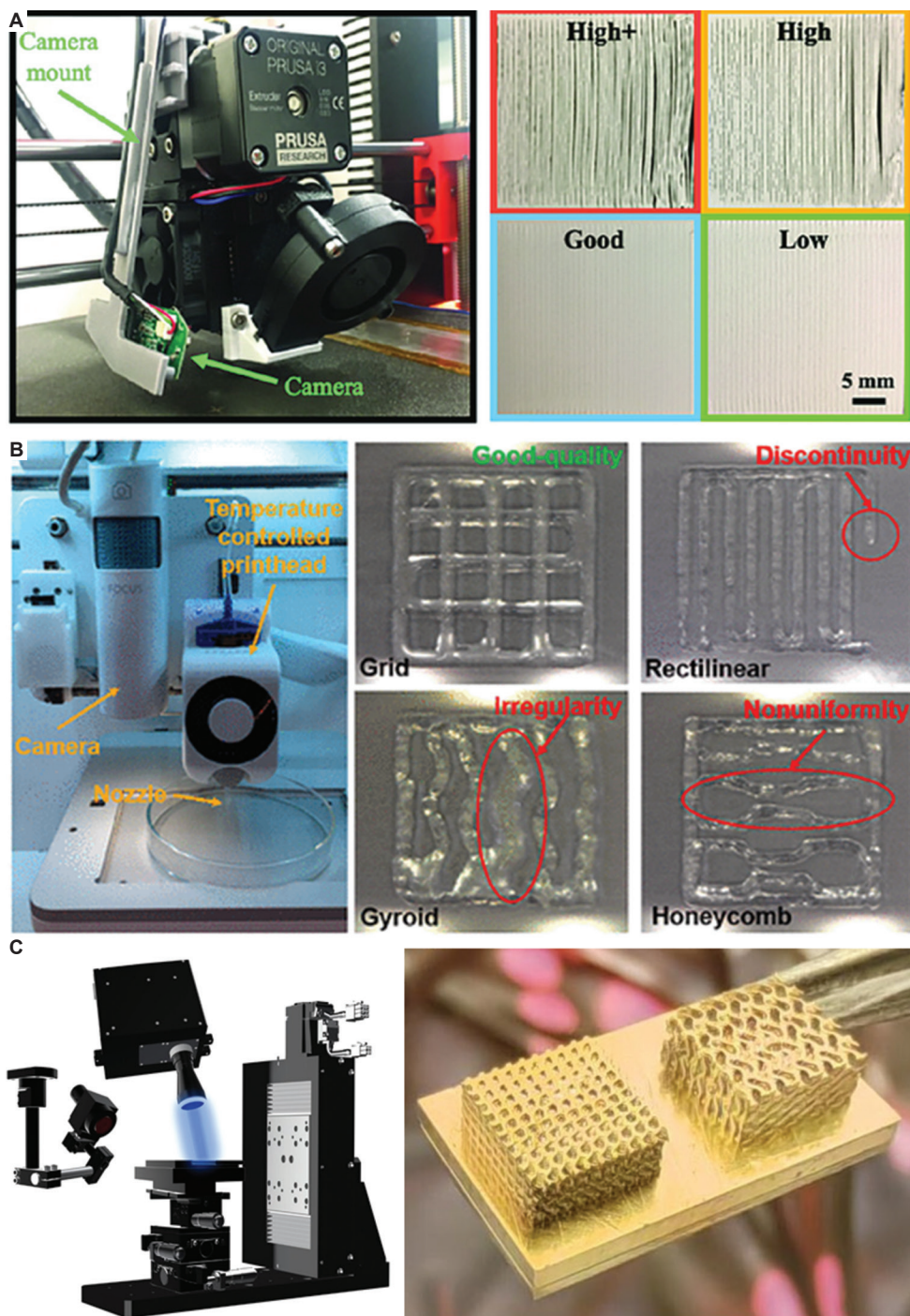


**Figure 3.** Process optimizations for polymer 3D printing. (A) Fused deposition modeling printer nozzle with an integrated monitoring system and corresponding images representing four nozzle height conditions. Reproduced with permission from Jin *et al.*<sup>80</sup> Copyright © 2020 Wiley. (B) Bioprinting platform combined with an anomaly detection system, along with representative images distinguishing normal and anomalous cases. Reproduced with permission from Jin *et al.*<sup>90</sup> Copyright © 2023 American Chemical Society. (C) Digital light processing printer and optimized printed structures. Reproduced with permission from Wang *et al.*<sup>106</sup> Copyright © 2024 Taylor & Francis.

an ML-based approach for real-time anomaly detection in bioprinting processes.<sup>85</sup> By employing the ResNeXt-50 CNN, the model effectively classified irregularities such as

interlayer discontinuities and nonuniformities, while data augmentation techniques were implemented to enhance its generalization performance. Experimental results

demonstrated a 99.03% F1-score, highlighting the high accuracy of the proposed detection method (Figure 3B). Another study leveraged ML to predict the printability of bioink formulations.<sup>86</sup> A total of 210 bioink compositions were experimentally constructed from 16 biomaterials, and decision trees, RF, and ANN were compared. Notably, the RF model achieved the highest precision (90.6%) and accuracy (88.1%), thus providing reliable bioink recommendations, while ANN offered better recall (87.3%) and demonstrated superior extrapolation capability. These findings illustrate how data-driven methods can overcome the limitations of purely experimental approaches, enabling rapid identification of optimal formulations.

In vat photopolymerization, process parameters—such as light intensity, exposure time, print speed, and build orientation—must be considered alongside resin properties (viscosity, photoinitiator concentration, and reactivity).<sup>84,87–90</sup> When printing solid-particle-filled resins in DLP, light scattering may occur as particles interact with the curing beam.<sup>91–93</sup> A similar phenomenon can emerge when cells are included in a hydrogel-based bioink due to refractive index differences between cells and the surrounding gel.<sup>67,91,92</sup> Scattering diverts light away from the intended target region, compromising pattern fidelity. Recent research used a deep learning-based correction method to mitigate cell-induced light scattering and enhance print quality in DLP-based bioprinting.<sup>92</sup> A master-slave neural network based on U-Net was employed to automatically generate optimized correction masks that suppress the scattering effect. This approach can significantly reduce iterative trial-and-error. Another study addressed grayscale DLP printing optimization by building a recurrent neural network (RNN) with LSTM layers to learn the relationship between per-pixel grayscale values and the final deformed structure.<sup>52</sup> Coupling this with finite element modeling (FEM) enabled faster and more accurate deformation prediction, while an evolutionary algorithm (EA) optimized grayscale distribution to achieve target deformation patterns. The proposed ML–EA hybrid approach significantly reduced computational time compared with conventional FEM-centric optimization, maintaining comparable precision. In a separate effort to improve geometric fidelity, boundary distortion in vat photopolymerization was mitigated using an ML-driven model that predicts and compensates for boundary shifts during layer projection.<sup>94</sup> More recently, ML-guided temperature prediction models have been coupled with numerical simulation to develop optimized control schemes for DLP printing, improving thermal uniformity and curing accuracy.<sup>95</sup>

In SLA and DLP, the printing apparatus can be arranged in either top-down or bottom-up configurations.<sup>96–98</sup> The

top-down setup places the laser or projector above the resin, lowering the platform with each layer, which can disturb the resin surface level and expose the newly formed layer to ambient oxygen, thereby inhibiting photopolymerization. It also tends to require larger vats and more resin volume. By contrast, bottom-up printing positions the light source below the vat and raises the platform upward. While this reduces some top-down constraints, separating each cured layer from the transparent vat window can induce mechanical stress. Several ML-driven approaches have been proposed to optimize bottom-up printing.<sup>53,99,100</sup> One group developed a real-time monitoring system to detect part detachment during the upward movement of the build platform in DLP.<sup>99</sup> Using strain gauges to track platform deformation and a photodetector to measure UV exposure; they applied an RF classifier along with an exponentially weighted moving average p-control chart to detect part detachment in real time and halt the process automatically. The system achieved an F1-score of 99.03% and demonstrated robust process stability by stopping printing after repeated detections. Another study proposed an ML-driven predictive model to optimize idle times during the bottom-up approach, where the platform was raised, fresh resin flowed in, and the platform descended again.<sup>100</sup> Introducing the concept of a prediction feature region allowed them to estimate wait time effectively without resorting to complex fluid simulations. A multi-layer perceptron model was trained to identify geometry-specific idle times, yielding a 47% reduction in average waiting time and a 25% overall reduction in total print time compared with conventional methods. Similarly, for bottom-up SLA, a deep learning model has been employed to predict layer-wise stress distributions.<sup>75</sup> Training datasets built from FEA simulations fed into a basic CNN and a 2-Stream CNN architecture achieved up to a 55% reduction in prediction error compared to a conventional neural network (NN) model with high accuracy even in non-uniform geometries.

ML has also been leveraged for high-precision vat photopolymerization (Figure 3C). In one DLP study, an RF model was trained to learn the relationships between UV exposure time, light intensity, layer thickness, and final print error. This approach maintained an average printing error below 2.3  $\mu\text{m}$ .<sup>101</sup> Moreover, it demonstrated a minimum feature size of  $\sim 20 \mu\text{m}$  in complex triply periodic minimal surface structures, highlighting the model's capacity for generalization to intricate geometries. In addition, ML-based surrogate modeling has been applied in projection two-photon lithography to optimize polymerization dynamics and improve printability, further enhancing precision in microscale fabrication.<sup>102</sup>

### 3.1.2. Property optimization

Beyond process optimization, ML has proven valuable for predicting or enhancing the mechanical and physical properties of 3D-printed parts. One study applied ML to optimize the mechanical properties of FDM-fabricated components,<sup>103</sup> focusing on layer height, printing speed, and printing temperature. By comparing RF, SVM, and k-nearest neighbors (K-NN) models for tensile strength prediction, the authors found that K-NN achieved the highest accuracy. They then used a sequential least squares programming-based optimization algorithm to determine optimal printing parameters. This ML-based approach enables the optimization of mechanical performance while reducing reliance on purely experimental approaches. A related study developed an ML model to predict the hardness of additively manufactured ABS, demonstrating the feasibility of using ML for estimating physical properties beyond tensile strength.<sup>104</sup>

A related investigation leveraged ML to predict the mechanical strength of biomedical structures printed through FDM.<sup>105</sup> In this case, polydopamine (PDM)-coated PLA plates were tested for mechanical performance using RF, K-NN, AdaBoost, Decision Tree, and LSTM models. Input variables included infill density, PDM coating parameters (submersion time, shaker speed), and coating solution concentration. Similarly, hierarchical ML techniques have been explored to enhance the fidelity of biopolymer-based 3D prints, addressing challenges in achieving consistent mechanical and structural integrity in biofabrication (Figure 4A).<sup>106</sup> Another study combined ML with sensor data to predict the mechanical properties of FDM products.<sup>107</sup> Employing an LSTM-based deep learning model, the authors accounted for thermal and mechanical fluctuations at the layer level. Real-time data – such as infrared readings, temperature measurements, signals from thermocouples, and accelerometer outputs – were fed into the LSTM network to analyze how nozzle temperature, print speed, and layer height influence tensile strength. Compared with traditional ML models (RF, SVR), the LSTM approach demonstrated up to a 24.3% improvement in the coefficient of determination ( $R^2$ ). Furthermore, layer-wise relevance propagation revealed that layer height was the single most influential factor on tensile strength.

Similarly, ML and sensor data have been applied to predict surface quality in FDM.<sup>108</sup> Traditional process parameters (e.g., printing speed, layer height) alone proved inadequate for capturing variability in surface roughness. To address this limitation, a combination of infrared sensors, thermocouples, and accelerometers was employed to collect real-time data, followed by an ensemble learning model

combining six different ML algorithms to quantitatively forecast surface roughness. This approach underscores how sensor-based ML models can enhance predictive accuracy beyond conventional parameter-driven methods.

ML has been instrumental in optimizing the properties of functional materials such as thermoelectric composites. Recent research has employed ML-assisted 3D printing to fabricate thermoelectric materials with ultrahigh performance at room temperature, enhancing energy conversion efficiency through optimized microstructural control (Figure 4B).<sup>109</sup> In vat photopolymerization, ML has also been used to optimize functional polymer composites, including mechanoluminescent materials. Studies have shown that ML-based optimization in SLA and DLP printing can enhance light-emitting properties by refining resin formulations and curing parameters, contributing to advancements in smart materials for sensing and display applications.<sup>110</sup> Moreover, high-throughput ML approaches have been integrated into the design of photodegradable hydrogels, enabling rapid formulation screening and optimization for biomedical applications (Figure 4C).<sup>111</sup>

### 3.1.3. Design optimization

Functional polymers – often referred to as stimuli-responsive, active, smart, or intelligent polymers – can undergo shape change in response to external stimuli such as heat, electric or magnetic fields, or pH.<sup>57,65,72,112-114</sup> Owing to advances in sophisticated manufacturing methods, these polymers can now be designed with increasing complexity. Nevertheless, achieving specific shape transformations or functionalities often relies on labor-intensive, trial-and-error procedures, incurring substantial time and expense.

To address these challenges, recent work employed an RNN to predict deformation patterns from a given material distribution.<sup>115</sup> Specifically, a bi-layered active composite beam composed of two materials with differing thermal expansion coefficients was optimized by integrating ML and EA. Conventional finite element-based optimization is often prohibitively expensive for complex geometries, whereas the RNN-based approach significantly reduces computational costs. By predicting the deformation behavior of a bilayer active composite beam, the system could leverage EA to propose optimal material layouts that govern shape change via volumetric expansion mismatch. This framework achieved over 99% reduction in computational expenses compared with typical finite element workflows without sacrificing target-shape fidelity. Moreover, by coupling this pipeline with computer vision techniques, the authors demonstrated the ability to convert hand-drawn sketches into automatically generated 4D-printed structures.

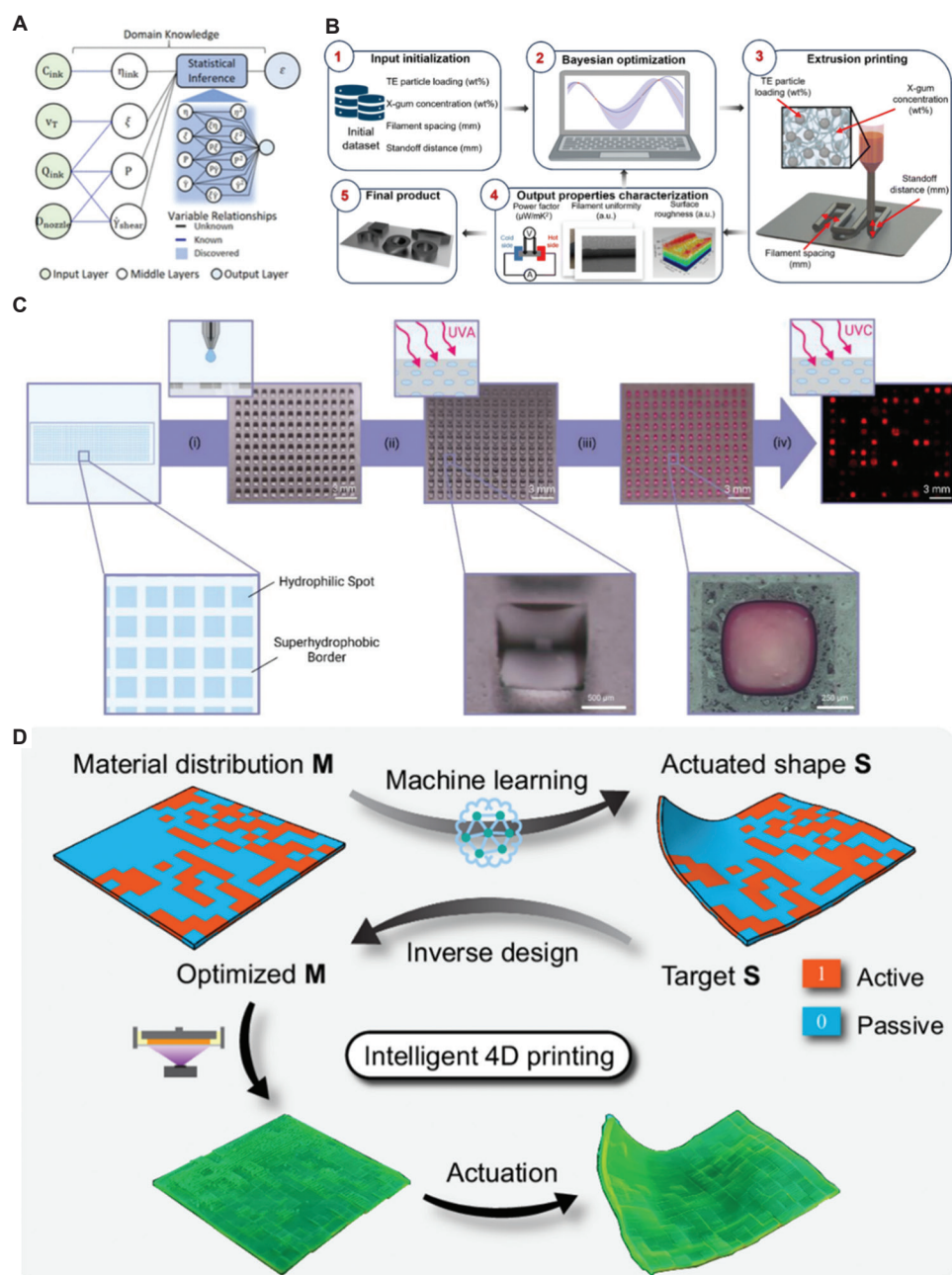


**Figure 4.** Property and design optimizations for polymer 3D printing. (A) Hierarchical machine learning framework integrating experimental knowledge to reduce data-driven discovery efforts. Reproduced with permission from Bone *et al.*<sup>111</sup> Copyright © 2020 American Chemical Society. (B) Machine learning-assisted extrusion printing workflow for thermoelectric inks with four input variables and three output properties. Reproduced with permission from Song *et al.*<sup>114</sup> Copyright © 2024 Royal Society of Chemistry. (C) Experimental workflow for synthesizing and screening sub-microliter-scale photodegradable hydrogels. Reproduced with permission from Seifermann *et al.*<sup>116</sup> Copyright © 2023 Wiley. (D) Overview of voxel-level inverse design of 4D-printed active composite plates enabled by machine learning. Reproduced with permission from Rodriguez and Goodman.<sup>122</sup> Copyright © 2024 Springer Nature.

In their subsequent study, the same authors extended this approach to active composite plates.<sup>116</sup> While plate architectures offer higher design freedom and enable more intricate shape transformations than beam structures, they

also present a combinatorial explosion of possible design variables. To handle this complexity, the authors combined ML with gradient descent (GD) and EA for the inverse design of active plates. A ResNet-based ML model was

developed as a forward prediction tool to precisely forecast shape deformation from a given material distribution; this was then coupled with GD and EA to form an inverse design loop. By optimizing the voxel-level material layout, the proposed method effectively controlled 3D shape transformations in more complex configurations. The results highlight how ML-driven strategies can replace or augment high-cost finite element simulations, significantly accelerating the design of 4D-printable smart polymer structures (Figure 4D).

### 3.2. Metals

Metals exhibit a regular atomic lattice structure held together by robust metallic bonds, which impart notable physical properties such as high density, strength, and electrical/thermal conductivity.<sup>117,118</sup> Moreover, techniques such as heat treatment, alloying, and post-processing enable the tailored adjustment of these physical and chemical properties, facilitating their application as essential materials in aerospace, medical, and automotive industries.<sup>119-123</sup> Recently, to achieve complex geometries and weight reduction, the integration of metal materials with 3D printing technology has garnered significant attention, with two principal AM processes widely employed.

For enhanced geometric complexity and reduced weight, metals are increasingly used in 3D printing technologies.<sup>124-127</sup> A representative metal 3D printing method, PBF, selectively melts and solidifies the powder using a high-energy source.<sup>128-130</sup> Typically, fine metal powders (10–60  $\mu\text{m}$ ) such as aluminum, stainless steel, nickel, or titanium are used, enabling the production of high-precision parts. Another method, DED, deposits metal powder (or wire) by melting it with a high-power laser or a plasma arc.<sup>43,131-133</sup> While the alloys commonly utilized in PBF can also be employed in DED, the powder used in DED is generally larger (around 50 – 150  $\mu\text{m}$ ). Compared to PBF, the DED process may have lower dimensional accuracy but fewer constraints on part size and faster production speeds, making it highly attractive for industrial applications. A summary of representative ML models and their applications in metal-based 3D printing is provided in Table 2.

#### 3.2.1. Process optimization

Various defects can arise in metal AM (both PBF and DED), such as excessive porosity, balling, lack of fusion, spattering, and warping. These defects occur due to the complex interplay among multiple process parameters, including laser power, scanning speed, and powder feed rate.<sup>122,134,135</sup> Conventional optimization typically relies on trial and error, which can be time-intensive, costly,

and potentially misaligned with experimental results. To address these challenges, ML approaches have gained prominence. ML models can learn intricate correlations among variables, predict optimal parameters, minimize defects, and enhance print quality.

An augmented ML framework integrating mechanistic modeling and domain knowledge has also been proposed to mitigate the lack of fusion in laser PBF (LPBF) processes (Figure 5A).<sup>136</sup> By computing five dimensionless variables from process parameters and material properties and applying decision tree and linear regression models, lack of fusion defects were predicted with over 90% accuracy. The resulting index and process maps facilitate quantitative defect prediction and alloy-specific parameter optimization.

While many ML applications focus on real-time monitoring and control during printing, model-driven approaches for pre-print process parameter optimization are also gaining traction. A representative example is the integration of high-throughput LPBF experiments with ensemble ML models to optimize process parameters for 316L stainless steel (Figure 5B).<sup>137</sup> By simultaneously fabricating 54 samples under varied laser power and scanning speed, and training ML models on porosity, hardness, and corrosion data, researchers successfully predicted optimal parameters that significantly reduced porosity (<0.1%) while enhancing tensile strength and corrosion resistance. The trained model also demonstrated transferability to AlSi7Mg, indicating the framework's potential for cross-material optimization and accelerated process design.

Mitigating defects that arise during printing is crucial for ensuring the reliability and performance of the final parts, and research has been actively conducted to address issues related to thermal fluctuations. In particular, deep reinforcement learning has been applied to PBF processes to regulate laser speed and power in real time, thereby maintaining a stable melt pool shape and preventing overheating.<sup>138,139</sup> Such methods effectively reduce defects and improve print quality. Meanwhile, for DED processes, ML-based thermal characteristic prediction has been investigated. Using XGBoost and LSTM algorithms, researchers developed a model that analyzes the relationships between process parameters and temperature, thereby predicting temperature distributions.<sup>140</sup> This strategy effectively controls temperature variations, leading to improved microstructure formation and mechanical properties.

Furthermore, a vision-based real-time defect detection technique was introduced using an autoencoder-based ConvLSTM model.<sup>141</sup> This model autonomously detects

Table 2. Summary of ML models for metal-based 3D printing

Motivation	Material	AM method	ML model	Model inputs	Remarks	References
Process optimization	SS316L, Ti-6Al-4V	PBF	Deep reinforcement learning	Heat distribution, melt pool depth	Control process parameters such as laser velocity and power in real time	138
	Metal powder	PBF	Multi-input neural network	Thermal images, process parameters (scan vector length, heat trace length, heat transfer distance, cumulative scan time)	Feedback control based on multi-input data to achieve the desired thermal history	139
	CarTech® 718 superalloy	DED	XGBoost, LSTM	Laser power, scan speed, layer index, time index, average height, average width	Real-time melt pool temperature prediction	140
	Ti-6Al-4V	DED	ConvLSTM Autoencoder	Video frames of melt pool dynamics	Detect melt pool anomalies (wire dripping, arcing, oscillation, stubbing) for quality control	141
	Inconel 625	PBF	C-RNN	Melt pool video frames	Improve defect detection using spatiotemporal analysis of melt pool videos	142
	SS316L, Ti-6Al-4V, Inconel 718	PBF	Vision transformer	High-speed imaging of melt pool dynamics	Improve process development and defect detection in 3D printing of new metal alloys through <i>in situ</i> process mapping	143
	SS316L	DED	CNN	Coaxial camera images of melt pool	Improve fault detection by monitoring nozzle clogging and abnormalities in the powder stream	144
	Inconel 718	DED	Bayesian LSTM, BOTSP0	Temperature history, laser power profile, spatial location	Develop a digital twin framework for real-time predictive control, enhancing process stability and efficiency	150
Property optimization	SS316L	PBF	DT (CART), RF, XGBoost	Build location, post-chamber pressure drop, powder properties, gas flow characteristics	Quality prediction based on the combination of build location and post-chamber pressure drop	148
	Ti-6Al-4V	PBF	GPR, BO	Laser power, scan speed, hatch spacing, porosity data	Discovered an expanded processing window that optimizes mechanical properties and density	149
	Inconel 625	DED	CNN, YOLOv8	Melt pool video frames, bead geometry data	Predict geometric characteristics and analyze their correlation with process parameters and bead geometry for real-time process control	150
	Ti-6Al-4V	DED	CGAN	Laser power, powder feed rate, scan speed	Predict and optimize surface morphology to improve surface quality and reduce cost	151
Design optimization	ER70S-6 steel	DED	SVR, NSGA-II	Laser power, travel speed, wire feed rate	Optimize process parameters for achieving desired layer geometry	152

Abbreviations: BO: Bayesian optimization; BOTSP0: Bayesian optimization for time series process optimization; C-RNN: Convolutional recurrent neural network; CART: Classification and regression tree; CGAN: Conditional generative adversarial network; CNN: Convolution neural network; ConvLSTM: Convolutional long short-term memory; DED: Directed energy deposition; DT: Decision tree; GPR: Gaussian process regression; LSTM: Long short-term memory; ML: Machine learning; NSGA-II: Non-dominated sorting genetic algorithm-II; PBF: Powder bed fusion; RF: Random forest; SVR: Support vector regression; XGBoost: Extreme gradient boosting; YOLO: You Only Look Once.

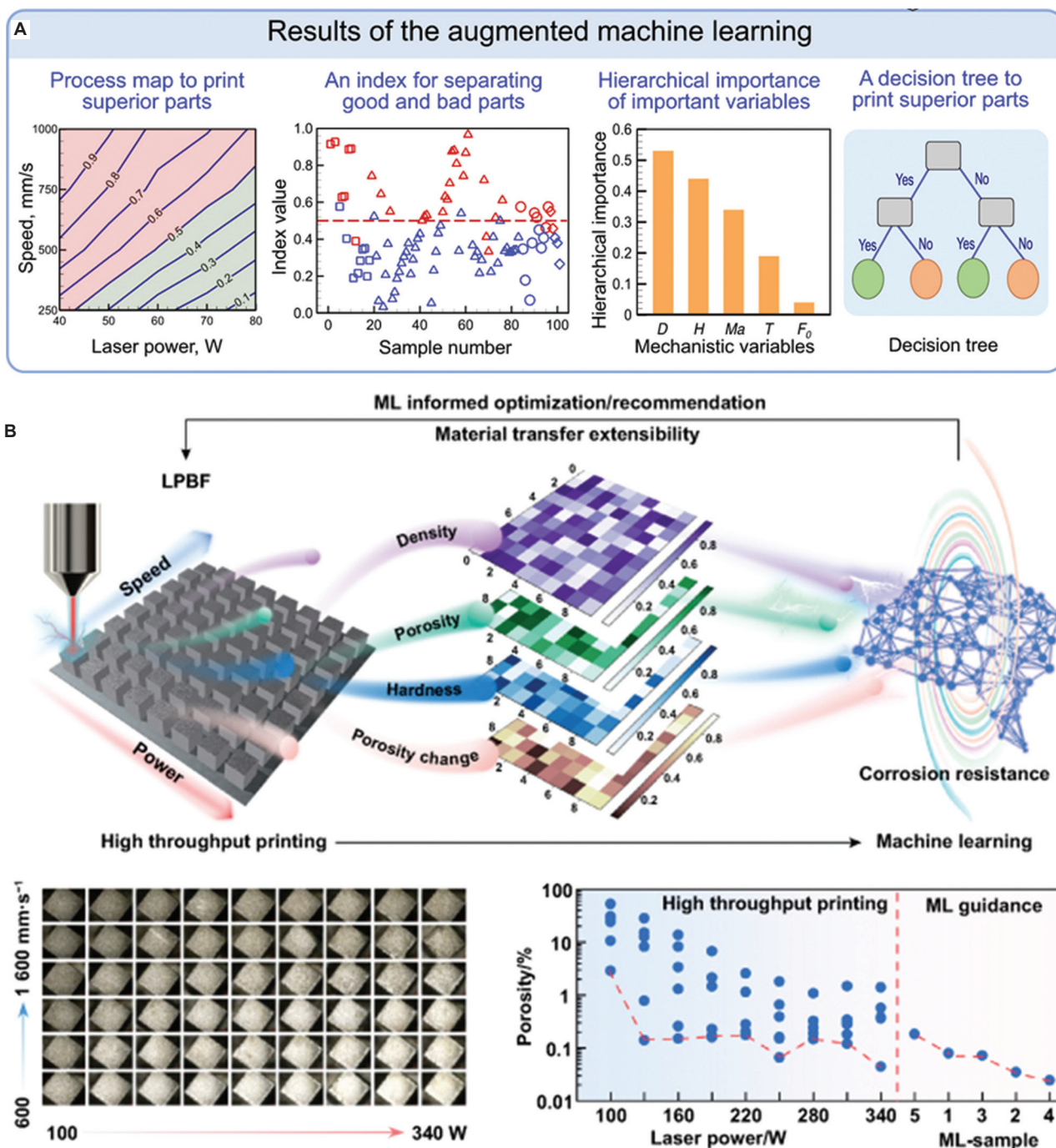


**Figure 5.** Process optimization for metal 3D printing. (A) Outputs of the augmented machine learning framework. Reproduced with permission from Seifermann *et al.*<sup>116</sup> Copyright © 2022 Springer Nature. (B) Schematic of high-throughput experimentation and machine learning-guided process optimization in laser powder bed fusion. Reproduced from Jain *et al.*<sup>117</sup> Copyright © 2025 IOP Publishing. Abbreviations: LPBF: Laser powder bed fusion; ML: Machine learning.

abnormal melt pool fluctuations, effectively identifying critical defects and consequently improving process stability and quality assurance. In addition, ML-based strategies have attracted attention for real-time monitoring

and quality control in metal 3D printing. Existing CNN-based analyses have been limited to spatial features, but combining CNNs with RNNs allows simultaneous analysis of spatial and temporal characteristics.<sup>142</sup> This integrated

approach enables real-time detection of surface quality degradation in PBF and more accurate layer-by-layer surface finish monitoring. Moreover, employing high-speed imaging data to generate process maps and variability maps for various alloys can further improve the reliability and quality stability of metal 3D printing. Notably, the use of vision transformers enables real-time analysis of dynamic melt pool changes, significantly enhancing process control efficiency (Figure 6A).<sup>143</sup> In DED processes, a vision-based real-time powder stream defect detection technique has also been introduced.<sup>144,145</sup> By analyzing melt pool images acquired through a coaxial camera to classify normal versus abnormal states and identifying defective nozzles during deposition, researchers have demonstrated improvements in the precision of in-process quality monitoring. Ultimately, such real-time monitoring and ML-based analytical methods are critical for automating and advancing metal 3D printing processes, and they form indispensable components for establishing stable mass-production systems.

### 3.2.2. Property optimization

Optimizing the mechanical, thermal, and functional properties in metal AM is paramount for simultaneously ensuring the performance of the final product and the stability of the manufacturing process. In particular, combining microstructure analyses (e.g., electron backscatter diffraction, X-ray CT) with deep learning is an active area of research aimed at quantifying correlations among material properties.<sup>146,147</sup>

For PBF processes, ML techniques have been used to improve repeatable quality by analyzing how part location and chamber pressure variations impact mechanical properties, and by optimizing process control strategies accordingly.<sup>148</sup> Furthermore, by employing Bayesian optimization and GP regression, researchers have explored expanded process windows to optimize the mechanical properties and density of Ti-6Al-4V alloys.<sup>149</sup> This approach has demonstrated the effective mitigation of balling instabilities in newly discovered high-density process regions.

In DED processes, a CNN-based real-time monitoring and melt pool segmentation approach has been introduced for process stability and optimization.<sup>150</sup> A YOLO-based model was employed to predict geometric features of the melt pool, such as area, height, and width, and to analyze the correlations between process parameters and bead geometry, thereby facilitating real-time process control (Figure 6B). An artificial intelligence (AI)-based method using conditional GAN was also proposed to generate virtual surface morphologies of Ti-6Al-4V parts.<sup>151</sup> When

provided with process parameters, this model offers a visual prediction of the expected surface roughness, showing high alignment with experimental observations and underscoring its utility for improving mechanical properties.

In addition, ultrasound-assisted DED (UADED) has been explored as a method to improve melt pool stability and reduce process defects. An unsupervised learning model has been applied for *in situ* monitoring of melt pool dynamics, spatters, and plume formation in UADED.<sup>152</sup> The model effectively classifies process variations by extracting and reconstructing features from high-speed imaging data, enabling real-time detection of anomalies and enhancing the overall stability of the deposition process.

### 3.2.3. Design optimization

To meet the dual demands of complex geometries and requisite performance in metal components, effective approaches must be adopted at the design stage, in addition to process optimization. Traditional simulation-based optimizations can require prohibitively large amounts of iterative computation. However, ML, particularly reinforcement learning, allows for the rapid and accurate exploration of additively manufactured shapes and structures. Combining reinforcement learning with multi-objective optimization algorithms can effectively address diverse objectives, such as topology optimization, weight reduction, and structural integrity. For instance, a study integrating support vector regression with non-dominated sorting genetic algorithm-II (NSGA-II) demonstrated the precise prediction of a component's final height and width, which was then leveraged to refine process control strategies.<sup>153</sup> By enhancing geometric accuracy and optimizing the interplay between design and manufacturing processes, metal 3D printing can be extended to a far broader range of applications.

### 3.3. Ceramic

Ceramic AM has gained significant attention due to its ability to fabricate complex geometries with high thermal, chemical, and mechanical stability. Unlike traditional ceramic manufacturing methods that require extensive post-processing, such as sintering and machining, AM techniques such as DIW, SLA, and powder-based extrusion offer a more flexible and efficient approach to producing ceramic components. However, challenges such as viscosity control, printability optimization, defect detection, and microstructural consistency remain critical obstacles in achieving high-quality ceramic prints. To address these issues, ML has been integrated into various stages of the ceramic AM process, including material formulation, process parameter optimization, defect detection, and quality assurance.

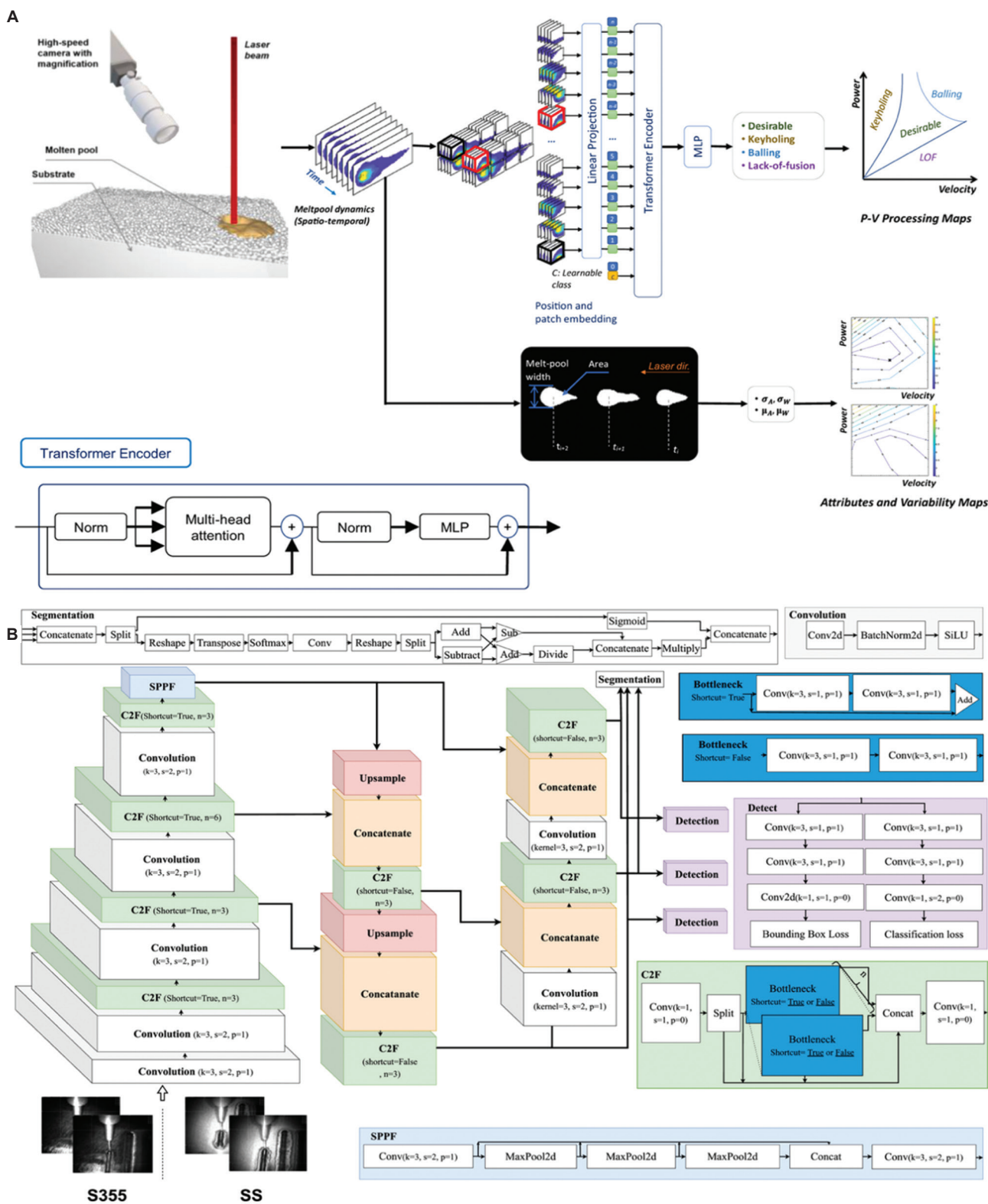


**Figure 6.** Process monitoring for melt pool detection. (A) *In situ* process development pipeline using high-speed imaging to capture molten pool dynamics, classify defects, and generate variability maps for process stability assessment. Reproduced with permission from Guirguis *et al.*<sup>148</sup> Copyright © 2024 Springer Nature. (B) You Only Look Once (YOLO) architecture integrating an additional segmentation branch for simultaneous object detection and segmentation. Reproduced with permission from Asadi *et al.*<sup>155</sup> Copyright © 2024 Elsevier.

One of the key applications of ML in ceramic AM is the prediction of viscoelastic and printability properties of ceramic pastes, particularly in binder-free DIW systems. Since the rheological behavior of ceramic pastes strongly influences their printability and structural integrity, researchers have utilized ML models to correlate formulation parameters with viscoelastic properties. Recent studies have demonstrated that ML-driven predictive models can effectively optimize ceramic ink compositions, ensuring improved extrusion stability and defect-free printing.<sup>154</sup>

Beyond material formulation, ML has played a crucial role in enhancing defect detection and surface quality evaluation in 3D-printed ceramic components. Due to the inherent brittleness of ceramics, even minor surface imperfections can lead to mechanical failure, making precise defect detection essential. Deep learning-based image processing techniques have been employed to identify surface defects in ceramic AM, mitigating interference from background noise and improving detection accuracy.<sup>155</sup> Furthermore, low-contrast defects, particularly in curved ceramic surfaces, pose significant challenges for conventional inspection methods. Deep learning models trained on high-resolution imaging datasets have demonstrated superior performance in identifying and classifying such defects, improving the reliability of ceramic AM processes.<sup>156</sup>

Another major challenge in ceramic AM is process stability and consistency across deposition lines in extrusion-based printing techniques. Variability in extrusion pressure, layer adhesion, and drying-induced deformations can compromise final part quality. To address these issues, ML-based quality optimization frameworks have been developed to analyze real-time process data and adjust deposition parameters dynamically. These models enable adaptive control of layer deposition, reducing print failures and enhancing mechanical uniformity in ceramic structures.<sup>157</sup>

In addition to process control, ML has facilitated the material development and optimization of lithography-based ceramic AM, particularly for porous alumina ceramics. The microstructure of porous ceramics is highly dependent on photopolymerization kinetics, resin composition, and post-processing conditions. By leveraging ML algorithms to predict porosity, shrinkage behavior, and mechanical performance, researchers have improved the material design process for high-performance ceramic components.<sup>158</sup>

Beyond material design and process monitoring, another critical application of ML in ceramic AM is the prediction of microstructural evolution during post-processing

steps such as sintering. Supervised learning models have been trained to correlate process parameters and binder content with sintering outcomes—including shrinkage, densification, and grain coarsening—enabling optimization of thermal profiles to minimize residual stress and improve final part integrity.<sup>159</sup> Other studies have applied ML techniques to tailor ceramic microstructures by predicting grain growth and porosity as functions of printing conditions and sintering temperature profiles.<sup>160</sup> However, modeling ceramic microstructures remains particularly challenging due to the complex multiscale phenomena involved, including powder packing, binder removal, and thermally driven phase transitions.<sup>157</sup> Progress in ML for ceramic AM is further constrained by the scarcity of high-quality datasets, as experimental studies are limited and involve high variability across materials and processes.<sup>154</sup> Moreover, the brittle nature of ceramics demands extremely high prediction accuracy since minor defects or heterogeneities can lead to catastrophic failure.<sup>160</sup> These factors highlight the need for specialized ML strategies and interdisciplinary domain knowledge tailored to the unique challenges of ceramic AM.<sup>161</sup>

Overall, the integration of ML into ceramic AM has significantly enhanced material formulation, process optimization, defect detection, and quality control. By leveraging advanced ML models, researchers and manufacturers can overcome the limitations of conventional ceramic printing techniques, paving the way for improved mechanical performance, reduced production costs, and increased industrial adoption. However, challenges such as data scarcity, model generalization across different ceramic materials, and real-time implementation of ML algorithms in AM workflows remain key areas for future research. Continued advancements in ML-driven ceramic AM optimization will further strengthen the role of AI in next-generation AM.

### **3.4. Carbon-based materials**

Carbon-based materials have garnered significant interest in AM due to their exceptional mechanical, electrical, and thermal properties. Carbon fiber-reinforced polymers, carbon nanotube composites, and graphene-based materials exhibit high strength-to-weight ratios, electrical conductivity, and flexibility, making them ideal for applications in aerospace, energy storage, structural reinforcements, and wearable electronics.

One of the most critical applications of ML in carbon AM is the optimization of mechanical properties in continuous carbon fiber-reinforced composites. The mechanical behavior of these materials is influenced by fiber alignment, resin infiltration, and interfacial bonding.<sup>162</sup> Deep learning models

such as CNNs and multi-objective optimization techniques like NSGA-II have been employed to fine-tune printing parameters, ensuring improved tensile strength, flexural performance, and reduced void formation.<sup>163</sup> In addition, ML-based predictive modeling has been applied to estimate the flexural strength of additively manufactured carbon fiber composites, aiding in material selection and process design.<sup>164</sup>

In this review, continuous fiber-reinforced composites and nano-carbon composites—including those utilizing carbon nanotubes and graphene—are collectively discussed under the category of carbon-based materials, as they share common goals such as enhancing mechanical strength, electrical conductivity, and structural performance through carbon-based reinforcements. Despite this shared objective, these materials differ significantly in terms of scale, structure, and manufacturing challenges. Continuous carbon fibers provide macroscopic reinforcement and often induce anisotropic mechanical behavior in printed parts, requiring ML models that can account for fiber orientation, continuity, and alignment during process monitoring or property prediction. In contrast, nano-carbon composites employ dispersed carbon nanotubes or graphene as nanoscale fillers that influence rheological behavior, filler dispersion, and electrical percolation networks. Accordingly, ML approaches in nano-carbon systems tend to focus on optimizing material formulations and predicting bulk properties – such as strength, elasticity, or conductivity – based on composition and processing conditions.

While both material systems rely on carbon reinforcements, their distinct physical characteristics demand tailored ML strategies. Continuous fiber-based composites benefit from spatially aware models capable of capturing fiber trajectories and interfacial features, whereas nano-carbon systems often utilize ML to uncover correlations between nano-filler morphology, distribution uniformity, and macroscopic functional properties. This distinction highlights the necessity of material-specific ML pipelines, even within a unified classification of carbon-based materials in AM.

Beyond mechanical optimization, ML has been leveraged to enhance the dimensional accuracy of 3D-printed carbon-based structures. Variability in the curing process, thermal expansion, and shrinkage can lead to deviations from intended geometries, particularly in polydimethylsiloxane-carbon nanotube (PDMS-CNT) composites. ML-driven models have been used to predict and correct dimensional inaccuracies, improving precision in printed components.<sup>165</sup>

In energy storage applications, ML-guided optimization has played a crucial role in tuning the architecture and performance of carbon microlattices for supercapacitors.

The intricate microstructure of these lattices directly affects their electrochemical properties, including charge storage capacity and ion transport efficiency. ML models have enabled the design of 3D-printed carbon microlattices with tailored properties, enhancing supercapacitor performance for next-generation energy storage solutions.<sup>166</sup>

Strain sensing and structural health monitoring represent another important area where ML has advanced carbon-based AM. 3D-printed carbon nanotube/polypyrrole/UV-curable composites have been studied for their strain-sensing capabilities, with ML models facilitating accurate prediction of electromechanical responses and real-time sensor calibration.<sup>167</sup> Similarly, graphene-based self-powered strain sensors for smart tires in autonomous vehicles have been developed, utilizing ML for real-time performance optimization and fault detection.<sup>168</sup>

Graphene-based materials have also found applications in gas sensing, Internet of Things (IoT)-enabled energy harvesting, and biocompatible electronic interfaces. ML has been employed to enhance the sensitivity and selectivity of textile-based graphene gas sensors, improving their performance in energy harvesting-assisted IoT applications.<sup>169</sup> In addition, graphene-based nanomembrane bioelectronics have been optimized using ML to achieve multimodal human-machine interfaces with improved flexibility and durability (Figure 7A).<sup>170</sup>

Furthermore, ML has contributed to the development of conformal, wearable carbon-based sensors for health monitoring. 3D-printed graphene-based humidity and strain sensors have been designed for human motion prediction, leveraging ML to refine sensor calibration and response accuracy (Figure 7B).<sup>171</sup>

In summary, the integration of ML into carbon-based AM has significantly advanced the fabrication, optimization, and application of these materials. By harnessing ML-driven insights, researchers have improved mechanical properties, enhanced structural accuracy, optimized energy storage devices, and enabled next-generation sensor technologies. However, challenges such as real-time ML implementation, multi-material process optimization, and the generalization of predictive models across different carbon-based materials remain key areas for further investigation. Continued advancements in ML-driven optimization will expand the capabilities of carbon-based AM, driving innovations in high-performance materials for industrial and biomedical applications.

## 4. Conclusions and future perspectives

The integration of ML with AM has demonstrated significant potential in optimizing 3D printing processes, improving

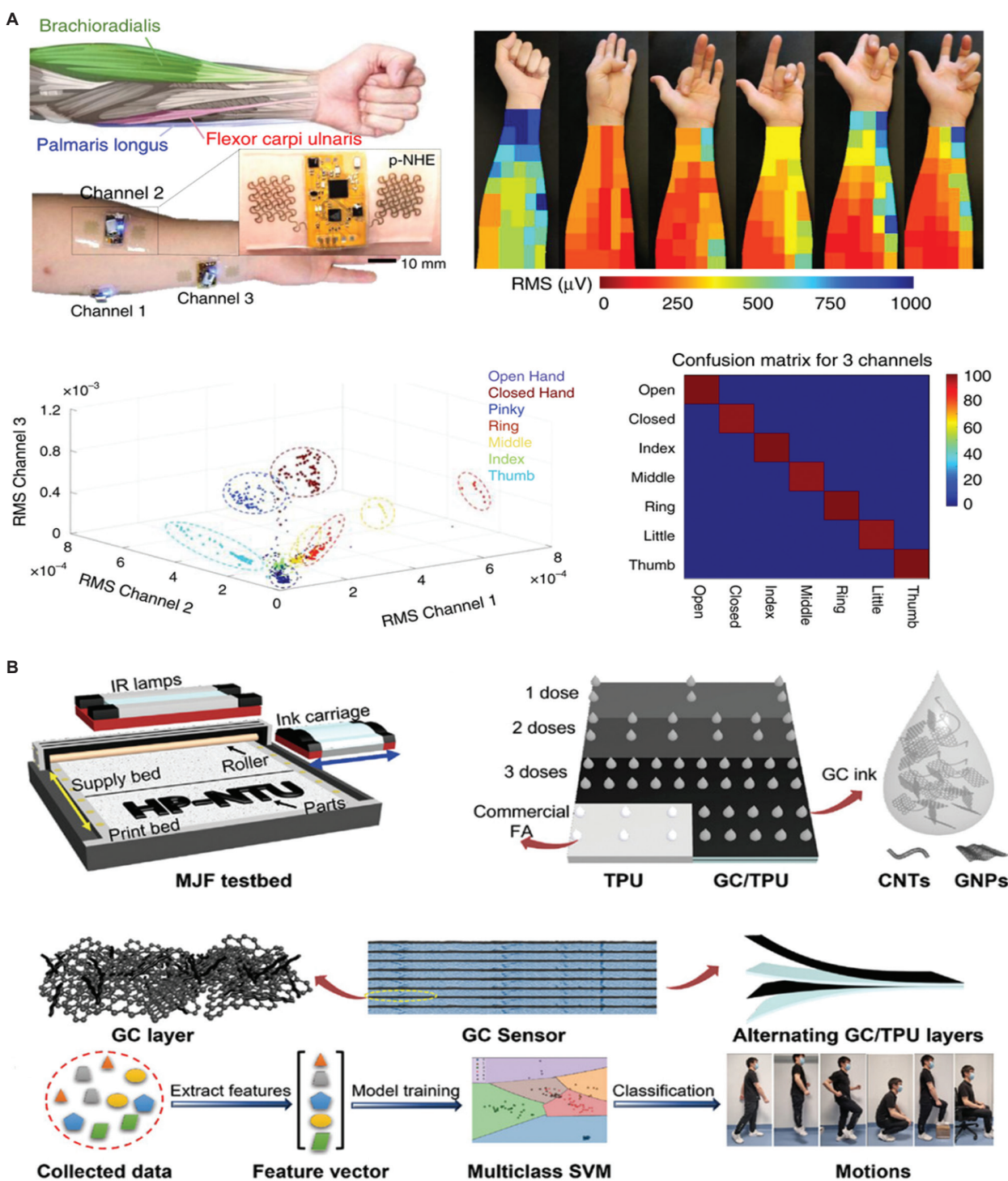


**Figure 7.** Machine learning applications for materials processing and biomechanical sensing. (A) Deep learning-based selection of three channels for classifying seven finger movement classes. Reproduced with permission from Kwon *et al.*<sup>170</sup> Copyright © 2020 Springer Nature. (B) Human motion prediction using a support vector machine model trained on variation data from graphene nanoplate-carbon nanotube sensors. Reproduced with permission from Hou *et al.*<sup>171</sup> Copyright © 2023 Wiley. Abbreviations: CNT: Carbon nanotube; GC: Graphene nanoplate-carbon nanotube; GNP: Graphene nanoplate; IR: Infrared; MJJF: Multi jet fusion; RMS: Root mean square; SVM: Support vector machine; TPU: Thermoplastic polyurethane.

quality control, and enabling real-time monitoring. As AM continues to evolve into a key technology for next-generation manufacturing, the demand for higher precision, material efficiency, and scalable production methods has intensified. The application of ML in AM has addressed many of these challenges by providing data-driven solutions for process parameter optimization, defect detection, and mechanical property prediction, thereby reducing reliance on empirical trial-and-error methods.

This review explores the role of ML in optimizing 3D printing, highlighting advancements in process monitoring, defect mitigation, material property prediction, and design optimization. In polymer-based AM, ML techniques have significantly enhanced printability assessment, process stability, and surface quality prediction. Studies on FDM, DIW, and vat photopolymerization (SLA/DLP) have demonstrated how ML models, particularly CNNs, GANs, and time-series models, can improve printing accuracy by compensating for environmental variations, detecting defects in real time, and optimizing material formulations. Similarly, in metal-based AM, ML applications in PBF and DED have contributed to thermal control, melt pool monitoring, and mechanical property enhancement. Reinforcement learning and hybrid physics-informed ML models have facilitated adaptive process control, leading to improved consistency in microstructural integrity and mechanical performance.

Despite these advancements, persistent technical challenges remain in realizing the full potential of ML in AM. Data scarcity and variability continue to impede model training, as high-quality labeled datasets are often limited in AM contexts. Models also struggle to generalize across different machines, materials, and process settings, meaning an ML model tuned for one scenario may perform poorly when applied elsewhere. Moreover, many advanced ML models function as “black boxes,” raising interpretability concerns and limiting user trust in critical manufacturing decisions. Achieving real-time, closed-loop process control via ML is another hurdle due to computational constraints, and current implementations still face latency and integration issues. Finally, there is a need to better integrate fundamental physics with data-driven approaches to generate emerging physics-informed ML techniques that aim to improve prediction accuracy and reliability while reducing reliance on massive training data. Addressing these unresolved issues will be crucial for transitioning from promising prototypes to robust, industrial-grade intelligent AM systems.

In the future, the convergence of ML with advanced sensing technologies, *in situ* monitoring systems, and cloud-based manufacturing platforms will drive further

innovation in AM. Multi-modal data fusion techniques, incorporating thermal imaging, X-ray CT, and acoustic sensors, will refine defect detection accuracy and improve process stability. Moreover, the development of self-learning AI-driven AM systems, capable of autonomously optimizing print parameters and material compositions, will enable fully automated, intelligent manufacturing workflows.

Ultimately, the synergy between ML and AM is poised to revolutionize manufacturing by enabling higher precision, faster production cycles, and more sustainable fabrication processes. As interdisciplinary collaborations between materials science, computational modeling, and AI engineering continue to grow, the vision of fully functional, AI-optimized 3D printing for industrial-scale applications is becoming increasingly tangible. Continued research efforts in scalable ML architectures, real-time adaptive control, and robust AM process simulations will be essential for advancing next-generation intelligent manufacturing ecosystems.

## Acknowledgments

None.

## Funding

This work was supported by the Technology Development Program (Grant No. S3248116) funded by the Ministry of SMEs and Startups (MSS, Korea), and by the National Research Foundation of Korea (NRF) grant, funded by the Korean government (MSIT; Grant No. RS-2023-00211636).

## Conflict of interest

Im Doo Jung is an Editorial Board Member of this journal, but was not in any way involved in the editorial and peer-review process conducted for this paper, directly or indirectly. Separately, other authors declared that they have no known competing financial interests or personal relationships that could have influenced the work reported in this paper.

## Author contributions

*Conceptualization:* Im Doo Jung, Hayeol Kim

*Visualization:* Im Doo Jung, Hayeol Kim, Kyung-Hwan Kim

*Writing – original draft:* All authors

*Writing – review & editing:* Im Doo Jung, Hayeol Kim

## Ethics approval and consent to participate

Not applicable.

## Consent for publication

Not applicable.

## Availability of data

Not applicable.

## References

- Wong KV, Hernandez A. A review of additive manufacturing. *Int Sch Res Notices*. 2012;2012(1):208760.  
doi: 10.5402/2012/208760
- Rajaguru K, Karthikeyan T, Vijayan V. Additive manufacturing- State of art. *Mater Today Proc*. 2020;21:628-633.  
doi: 10.1016/j.matpr.2019.06.728
- Abdulhameed O, Al-Ahmari A, Ameen W, Mian SH. Additive manufacturing: Challenges, trends, and applications. *Adv Mech Eng*. 2019;11(2):1-27.  
doi: 10.1177/1687814018822880
- Srivastava M, Rathee S. Additive manufacturing: Recent trends, applications and future outlooks. *Prog Addit Manuf*. 2022;7(2):261-287.  
doi: 10.1007/s40964-021-00229-8
- Dilberoglu UM, Gharehpapagh B, Yaman U, Dolen M. The role of additive manufacturing in the era of industry 4.0. *Procedia Manuf*. 2017;11:545-554.  
doi: 10.1016/j.promfg.2017.07.148
- Kantaros A, Bimis A, Karalekas D. *In situ* Characterization of Residual Strains in Layered Manufacturing. In: *Presented at: 5<sup>th</sup> International Conference on Materials Integrated Non Destructive Testing (IC-MINDT-2013)*. Athens, Greece; 2013. Available from: <https://ssrn.com/abstract=5143213> [Last accessed on 2025 May 14].  
doi: 10.2139/ssrn.5143213
- Jung ID, Lee MS, Lee J, et al. Embedding sensors using selective laser melting for self-cognitive metal parts. *Addit Manuf*. 2020;33:101151.  
doi: 10.1016/j.addma.2020.101151
- Guo SZ, Qiu K, Meng F, Park SH, McAlpine MC. 3D printed stretchable tactile sensors. *Adv Mater*. 2017;29(27):1701218.  
doi: 10.1002/adma.201701218
- Yang J, Li B, Liu J, Tu Z, Wu X. Application of additive manufacturing in the automobile industry: A mini review. *Processes*. 2024;12(6):1101.  
doi: 10.3390/pr12061101
- Alami AH, Olabi AG, Alashkar A, et al. Additive manufacturing in the aerospace and automotive industries: Recent trends and role in achieving sustainable development goals. *Ain Shams Eng J*. 2023;14(11):102516.  
doi: 10.1016/j.asej.2023.102516
- Ramola M, Yadav V, Jain R. On the adoption of additive manufacturing in healthcare: A literature review. *J Manuf Technol Manag*. 2019;30(1):48-69.  
doi: 10.1108/JMTM-03-2018-0094
- Park JW, Shin YC, Kang H G, et al. *In vivo* analysis of post-joint-preserving surgery fracture of 3D-printed Ti-6Al-4V implant to treat bone cancer. *Bio Des Manuf*. 2021;4:879-888.  
doi: 10.1007/s42242-021-00147-2
- Sanaei N, Fatemi A, Phan N. Defect characteristics and analysis of their variability in metal L-PBF additive manufacturing. *Mater Des*. 2019;182:108091.  
doi: 10.1016/j.matdes.2019.108091
- De Pastre MA, Quinsat Y, Lartigue C. Effects of additive manufacturing processes on part defects and properties: A classification review. *Int J Interact Des Manuf*. 2022;16(4):1471-1496.  
doi: 10.1007/s12008-022-00839-8
- Peng X, Kong L, Fuh JYH, Wang H. A review of post-processing technologies in additive manufacturing. *J Manuf Mater Process*. 2021;5(2):38.  
doi: 10.3390/jmmp5020038
- Dharmadhikari S, Menon N, Basak A. A reinforcement learning approach for process parameter optimization in additive manufacturing. *Addit Manuf*. 2023;71:103556.  
doi: 10.1016/j.addma.2023.103556
- Sawant DA, Shinde BM, Raykar SJ. Post processing techniques used to improve the quality of 3D printed parts using FDM: State of art review and experimental work. *Mater Today Proc*. 2023.  
doi: 10.1016/j.matpr.2023.09.202
- Wajahat M, Kim JH, Kim JH, Jung ID, Pyo J, Seol SK. 4D printing of ultrastretchable magnetoactive soft material architectures for soft actuators. *ACS Appl Mater Interfaces*. 2023;15(51):59582-59591.  
doi: 10.1021/acsami.3c12173
- Jeon H, Wajahat M, Park S, et al. 3D printing of luminescent perovskite quantum dot-polymer architectures. *Adv Funct Mater*. 2024;34(29):2400594.  
doi: 10.1002/adfm.202400594
- Tapia G, Elwany AH, Sang H. Prediction of porosity in metal-based additive manufacturing using spatial Gaussian process models. *Addit Manuf*. 2016;12:282-290.  
doi: 10.1016/j.addma.2016.05.009
- Khanzadeh M, Chowdhury S, Marufuzzaman M, Tschopp MA, Bian L. Porosity prediction: Supervised-learning of thermal history for direct laser deposition. *J Manuf Syst*. 2018;47:69-82.

- doi: 10.1016/j.jmsy.2018.04.001
22. Garg A, Lam JSL, Savalani MM. A new computational intelligence approach in formulation of functional relationship of open porosity of the additive manufacturing process. *Int J Adv Manuf Technol.* 2015;80:555-565.  
doi: 10.1007/s00170-015-6989-2
  23. Qin J, Hu F, Liu Y, *et al.* Research and application of machine learning for additive manufacturing. *Addit Manuf.* 2022;52:102691.  
doi: 10.1016/j.addma.2022.102691
  24. Wang C, Tan XP, Tor SB, Lim CS. Machine learning in additive manufacturing: State-of-the-art and perspectives. *Addit Manuf.* 2020;36:101538.  
doi: 10.1016/j.addma.2020.101538
  25. Chen L, Moon SK. *In-situ* defect detection in laser-directed energy deposition with machine learning and multi-sensor fusion. *J Mech Sci Technol.* 2024;38(9):4477-4484.  
doi: 10.1007/s12206-024-2401-1
  26. Scime L, Beuth J. Using machine learning to identify in-situ melt pool signatures indicative of flaw formation in a laser powder bed fusion additive manufacturing process. *Addit Manuf.* 2019;25:151-165.  
doi: 10.1016/j.addma.2018.11.010
  27. Chen L, Yao X, Xu P, Moon SK, Bi G. Rapid surface defect identification for additive manufacturing with *in-situ* point cloud processing and machine learning. *Virtual Phys Prototyp.* 2021;16(1):50-67.  
doi: 10.1080/17452759.2020.1832695
  28. Qi X, Chen G, Li Y, Cheng X, Li C. Applying neural-network-based machine learning to additive manufacturing: Current applications, challenges, and future perspectives. *Engineering.* 2019;5(4):721-729.  
doi: 10.1016/j.eng.2019.04.012
  29. Trovato M, Belluomo L, Bici M, Prist M, Campana F, Cicconi P. Machine learning in design for additive manufacturing: A state-of-the-art discussion for a support tool in product design lifecycle. *Int J Adv Manuf Technol.* 2025;137:2157-2180.  
doi: 10.1007/s00170-025-15273-9
  30. Rojek I, Mikołajewski D, Kempniński M, Galas K, Piszcz A. Emerging applications of machine learning in 3D printing. *Appl Sci.* 2025;15(4):1781.  
doi: 10.3390/app15041781
  31. Kumar S, Gopi T, Harikeerthana N, *et al.* Machine learning techniques in additive manufacturing: A state of the art review on design, processes and production control. *J Intell Manuf.* 2023;34(1):21-55.  
doi: 10.1007/s10845-022-02029-5
  32. Oleff A, Küster B, Stonis M, Overmeyer L. Process monitoring for material extrusion additive manufacturing: A state-of-the-art review. *Prog Addit Manuf.* 2021;6(4):705-730.  
doi: 10.1007/s40964-021-00192-4
  33. Mahmoud D, Magolon M, Boer J, Elbestawi MA, Mohammadi MG. Applications of machine learning in process monitoring and controls of L-PBF additive manufacturing: A review. *Appl Sci.* 2021;11(24):11910.  
doi: 10.3390/app112411910
  34. Zhou L Y, Fu J, He Y. A review of 3D printing technologies for soft polymer materials. *Adv Funct Mater.* 2020;30(28):2000187.  
doi: 10.1002/adfm.202000187
  35. Zhang Y, Jarosinski W, Jung YG, Zhang J. Additive manufacturing processes and equipment. In: *Additive Manufacturing: Materials, Processes, Quantifications and Applications.* Oxford, UK: Butterworth-Heinemann; 2018. p. 39-51.  
doi: 10.1016/B978-0-12-812155-9.00002-5
  36. Tan LJ, Zhu W, Zhou K. Recent progress on polymer materials for additive manufacturing. *Adv Funct Mater.* 2020;30(43):2003062.  
doi: 10.1002/adfm.202003062
  37. Saadi MASR, Maguire A, Pottackal NT, *et al.* Direct ink writing: A 3D printing technology for diverse materials. *Adv Mater.* 2022;34(28):2108855.  
doi: 10.1002/adma.202108855
  38. Nohut S, Schwentenwein M. Vat photopolymerization additive manufacturing of functionally graded materials: A review. *J Manuf Mater Process.* 2022;6(1):17.  
doi: 10.3390/jmmp6010017
  39. Lewandowski JJ, Seifi M. Metal additive manufacturing: A review of mechanical properties. *Ann Rev Mater Res.* 2016;46(1):151-186.  
doi: 10.1146/annurev-matsci-070115-032024
  40. Frazier WE. Metal additive manufacturing: A review. *J Mater Eng Perform.* 2014;23:1917-1928.  
doi: 10.1007/s11665-014-0958-z
  41. Du W, Ren X, Pei Z, Ma C. Ceramic binder jetting additive manufacturing: A literature review on density. *J Manuf Sci Eng.* 2020;142(4):040801.  
doi: 10.1115/1.4046248
  42. Mirzababaei S, Pasebani S. A review on binder jet additive manufacturing of 316L stainless steel. *J Manuf Mater Process.* 2019;3(3):82.  
doi: 10.3390/jmmp3030082
  43. Svetlizky D, Das M, Zheng B, *et al.* Directed energy deposition (DED) additive manufacturing: Physical

- characteristics, defects, challenges and applications. *Mater Today*. 2021;49:271-295.  
doi: 10.1016/j.mattod.2021.03.020
44. Petrich J, Snow Z, Corbin D, Reutzel EW. Multi-modal sensor fusion with machine learning for data-driven process monitoring for additive manufacturing. *Addit Manuf*. 2021;48:102364.  
doi: 10.1016/j.addma.2021.102364
  45. Ren W, Wen G, Zhang Z, Mazumder J. Quality monitoring in additive manufacturing using emission spectroscopy and unsupervised deep learning. *Mater Manuf Process*. 2022;37(11):1339-1346.  
doi: 10.1080/10426914.2021.1906891
  46. Kapusuzoglu B, Mahadevan S. Physics-informed and hybrid machine learning in additive manufacturing: Application to fused filament fabrication. *JOM*. 2020;72(12):4695-4705.  
doi: 10.1007/s11837-020-04438-4
  47. Acharya R, Sharon JA, Staroselsky A. Prediction of microstructure in laser powder bed fusion process. *Acta Mater*. 2017;124:360-371.  
doi: 10.1016/j.actamat.2016.11.018
  48. Fergani O, Berto F, Welo T, Liang SY. Analytical modelling of residual stress in additive manufacturing. *Fatigue Fract Eng Mater Struct*. 2017;40(6):971-978.  
doi: 10.1111/ffe.12560
  49. Chen Q, Guillemot G, Gandin CA, Bellet M. Three-dimensional finite element thermomechanical modeling of additive manufacturing by selective laser melting for ceramic materials. *Addit Manuf*. 2017;16:124-137.  
doi: 10.1016/j.addma.2017.02.005
  50. Davoudinejad A. Vat photopolymerization methods in additive manufacturing. In: *Additive Manufacturing: Handbooks in Advanced Manufacturing*. Amsterdam, The Netherlands: Elsevier. p. 159-181; 2021.  
doi: 10.1016/B978-0-12-818411-0.00007-0
  51. Goh GD, Hamzah NMB, Yeong WY. Anomaly detection in fused filament fabrication using machine learning. *3D Print Addit Manuf*. 2023;10(3):428-437.  
doi: 10.1089/3dp.2021.0231
  52. Zhao B, Zhang M, Dong L, Wang D. Design of grayscale digital light processing 3D printing block by machine learning and evolutionary algorithm. *Compos Commun*. 2022;36:101395.  
doi: 10.1016/j.coco.2022.101395
  53. Khadilkar A, Wang J, Rai R. Deep learning-based stress prediction for bottom-up SLA 3D printing process. *Int J Adv Manuf Technol*. 2019;102:2555-2569.  
doi: 10.1007/s00170-019-03363-4
  54. Chung J, Shen B, Law ACC, Kong ZJ. Reinforcement learning-based defect mitigation for quality assurance of additive manufacturing. *J Manuf Syst*. 2022;65:822-835.  
doi: 10.1016/j.jmsy.2022.11.008
  55. Wu S, Hamel CM, Ze Q, Yang F, Qi HJ, Zhao R. Evolutionary algorithm-guided voxel-encoding printing of functional hard-magnetic soft active materials. *Adv Intell Syst*. 2020;2(8):2000060.  
doi: 10.1002/aisy.202000060
  56. Miriyev A, Stack K, Lipson H. Soft material for soft actuators. *Nat Commun*. 2017;8(1):596.  
doi: 10.1038/s41467-017-00685-3
  57. Kim Y, Parada GA, Liu S, Zhao XF. Ferromagnetic soft continuum robots. *Sci Robot*. 2019;4(33):eaax7329.  
doi: 10.1126/scirobotics.aax7329
  58. Jang EJ, Lee SY, Kim KH, Lee GY. Design and fabrication of a millimeter-scale rotary actuator based on the twisted shape memory alloy (SMA) wires. *J Korean Soc Precis Eng*. 2022;39(6):403-410.  
doi: 10.7736/jkspe.022.034
  59. Seong M, Sun K, Kim S, et al. Multifunctional magnetic muscles for soft robotics. *Nat Commun*. 2024;15(1):7929.  
doi: 10.1038/s41467-024-52347-w
  60. Jo H, Park JS, Lim HY, Lee GY. Laser sintered silver nanoparticles on the PDMS for a wearable strain sensor capable of detecting finger motion. *ACS Appl Nano Mater*. 2023;6(24):22998-23011.  
doi: 10.1021/acsanm.3c04386
  61. Kim JH, Park S, Ahn J, et al. Meniscus-guided micro-printing of prussian blue for smart electrochromic display. *Adv Sci*. 2023;10(3):2205588.  
doi: 10.1002/advs.202205588
  62. Kim H, Kim KH, Jeong J, Lee Y, Jung ID. Recent progress on materials for functional additive manufacturing. *Mat Sci Add Manuf*. 2024;3(2):3323.  
doi: 10.36922/msam.3323
  63. Wickramasinghe S, Do T, Tran P. FDM-based 3D printing of polymer and associated composite: A review on mechanical properties, defects and treatments. *Polymers*. 2020;12(7):1529.  
doi: 10.3390/polym12071529
  64. Fu Z, Angeline V, Sun W. Evaluation of printing parameters on 3D extrusion printing of pluronic hydrogels and machine learning guided parameter recommendation. *Int J Bioprinting*. 2021;7(4):434.  
doi: 10.18063/ijb.v7i4.434
  65. Kim Y, Yuk H, Zhao R, Chester SA, Zhao X. Printing

- ferromagnetic domains for untethered fast-transforming soft materials. *Nature*. 2018;558(7709):274-279.  
doi: 10.1038/s41586-018-0185-0
66. Kim SH, Yeon YK, Lee JM, *et al.* Precisely printable and biocompatible silk fibroin bioink for digital light processing 3D printing. *Nat Commun*. 2018;9(1):1620.  
doi: 10.1038/s41467-018-03759-y
67. Madrid-Wolff J, Boniface A, Loterie D, Delrot P, Moser C. Controlling light in scattering materials for volumetric additive manufacturing. *Adv Sci*. 2022;9(22):2105144.  
doi: 10.1002/advs.202105144
68. Mu Q, Wang L, Dunn CK, *et al.* Digital light processing 3D printing of conductive complex structures. *Addit Manuf*. 2017;18:74-83.  
doi: 10.1016/j.addma.2017.08.011
69. Peng X, Kuang X, Roach DJ, *et al.* Integrating digital light processing with direct ink writing for hybrid 3D printing of functional structures and devices. *Addit Manuf*. 2021;40:101911.  
doi: 10.1016/j.addma.2021.101911
70. Patel DK, Sakhaei AH, Layani M, Zhang B, Ge Q, Magdassi S. Highly stretchable and UV curable elastomers for digital light processing based 3D printing. *Adv Mater*. 2017;29(15):1606000.  
doi: 10.1002/adma.201606000
71. Kelly BE, Bhattacharya I, Heidari H, Shusteff M, Spadaccini CM, Taylor HK. Volumetric additive manufacturing via tomographic reconstruction. *Science*. 2019;363(6431):1075-1079.  
doi: 10.1126/science.aau7114
72. Han D, Farino C, Yang C, *et al.* Soft robotic manipulation and locomotion with a 3D printed electroactive hydrogel. *ACS Appl Mater Interfaces*. 2018;10(21):17512-17518.  
doi: 10.1021/acsami.8b04250
73. Sapkota A, Ghimire SK, Adanur S. A review on fused deposition modeling (FDM)-based additive manufacturing (AM) methods, materials and applications for flexible fabric structures. *J Ind Text*. 2024;54:1-51.  
doi: 10.1177/15280837241282110
74. Garg A, Bhattacharya A. An insight to the failure of FDM parts under tensile loading: Finite element analysis and experimental study. *Int J Mech Sci*. 2017;120:225-236.  
doi: 10.1016/j.ijmecsci.2016.11.032
75. Jin Z, Zhang Z, Gu GX. Automated real-time detection and prediction of interlayer imperfections in additive manufacturing processes using artificial intelligence. *Adv Intell Syst*. 2020;2(1):1900130.  
doi: 10.1002/aisy.201900130
76. Tan L, Huang T, Liu J, Li Q, Wu X. Deep adversarial learning system for fault diagnosis in fused deposition modeling with imbalanced data. *Comput Ind Eng*. 2023;176:108887.  
doi: 10.1016/j.cie.2022.108887
77. Zhai C, Wang J, Tu YP, Chang G, Ren X, Ding C. Robust optimization of 3D printing process parameters considering process stability and production efficiency. *Addit Manuf*. 2023;71:103588.  
doi: 10.1016/j.addma.2023.103588
78. Kantaros A, Karalekas D. Fiber Bragg grating based investigation of residual strains in ABS parts fabricated by fused deposition modeling process. *Mater Des*. 2013;50:44-50.  
doi: 10.1016/j.matdes.2013.02.067
79. Delli U, Chang S. Automated process monitoring in 3D printing using supervised machine learning. *Procedia Manuf*. 2018;26:865-870.  
doi: 10.1016/j.promfg.2018.07.111
80. Khan MF, Alam A, Siddiqui MA, *et al.* Real-time defect detection in 3D printing using machine learning. *Mater Today Proc*. 2021;42:521-528.  
doi: 10.1016/j.matpr.2020.10.482
81. Fu Y, Downey A, Yuan L, Pratt A, Balogun Y. *In situ* monitoring for fused filament fabrication process: A review. *Addit Manuf*. 2021;38:101749.  
doi: 10.1016/j.addma.2020.101749
82. Jin Z, Zhang Z, Gu GX. Autonomous in-situ correction of fused deposition modeling printers using computer vision and deep learning. *Manuf Lett*. 2019;22:11-15.  
doi: 10.1016/j.mfglet.2019.09.005
83. Westphal E, Seitz H. Machine learning for the intelligent analysis of 3D printing conditions using environmental sensor data to support quality assurance. *Addit Manuf*. 2022;50:102535.  
doi: 10.1016/j.addma.2021.102535
84. Nasrin T, Pourkamali-Anaraki F, Peterson AM. Application of machine learning in polymer additive manufacturing: A review. *J Polym Sci*. 2024;62(12):2639-2669.  
doi: 10.1002/pol.20230649
85. Jin Z, Zhang Z, Shao X, Gu GX. Monitoring anomalies in 3D bioprinting with deep neural networks. *ACS Biomater Sci Eng*. 2021;9(7):3945-3952.  
doi: 10.1021/acsbiomaterials.0c01761
86. Chen H, Liu Y, Balabani S, Hirayama R, Huang J. Machine learning in predicting printable biomaterial formulations for direct ink writing. *Research (Wash D C)*. 2023;6:0197.  
doi: 10.34133/research.0197
87. Valizadeh I, Tayyarian T, Weeger O. Influence of process

- parameters on geometric and elasto-visco-plastic material properties in vat photopolymerization. *Addit Manuf.* 2023;72:103641.  
doi: 10.1016/j.addma.2023.103641
88. Andreu A, Su PC, Kim JH, *et al.* 4D printing materials for vat photopolymerization. *Addit Manuf.* 2021;44:102024.  
doi: 10.1016/j.addma.2021.102024
89. Pazhamannil RV, Hadidi HM, Puthumana G. Development of a low-cost volumetric additive manufacturing printer using less viscous commercial resins. *Polym Eng Sci.* 2023;63(1):65-77.  
doi: 10.1002/pen.26186
90. Wu H, Chen P, Yan C, Cai C, Shi Y. Four-dimensional printing of a novel acrylate-based shape memory polymer using digital light processing. *Mater Des.* 2019;171:107704.  
doi: 10.1016/j.matdes.2019.107704
91. Hosseinabadi HG, Nieto D, Yousefinejad A, *et al.* Ink material selection and optical design considerations in DLP 3D printing. *Appl Mater Today.* 2023;30:101721.  
doi: 10.1016/j.apmt.2022.101721
92. Guan J, You S, Xiang Y, *et al.* Compensating the cell-induced light scattering effect in light-based bioprinting using deep learning. *Biofabrication.* 2021;14(1):015011.  
doi: 10.1088/1758-5090/ac3b92
93. You S, Guan J, Alido J, *et al.* Mitigating scattering effects in light-based three-dimensional printing using machine learning. *J Manuf Sci Eng.* 2020;142(8):081002.  
doi: 10.1115/1.4046986
94. Zhao L, Zhao Z, Ma L, Li S, Men Z, Wu L. Developing the optimized control scheme for digital light processing 3D printing by combining numerical simulation and machine learning-guided temperature prediction. *J Manuf Process.* 2024;132:363-374.  
doi: 10.1016/j.jmapro.2024.10.049
95. Ma Y, Tian Z, Wang B, *et al.* Enhancing the 3D printing fidelity of vat photopolymerization with machine learning-driven boundary prediction. *Mater Des.* 2024;241:112978.  
doi: 10.1016/j.matdes.2024.112978
96. Chaudhary R, Fabbri P, Leoni E, Mazzanti F, Akbari R, Antonini C. Additive manufacturing by digital light processing: A review. *Prog Addit Manuf.* 2023; 8(2):331-351.  
doi: 10.1007/s40964-022-00336-0
97. Zakeri S, Vippola M, Levänen E. A comprehensive review of the photopolymerization of ceramic resins used in stereolithography. *Addit Manuf.* 2020;35:101177.  
doi: 10.1016/j.addma.2020.101177
98. Wang X, Liu J, Zhang Y, *et al.* Advances in precision microfabrication through digital light processing: System development, material and applications. *Virtual Phys Prototyp.* 2023;18(1):e2248101.  
doi: 10.1080/17452759.2023.2248101
99. Frumosu FD, Méndez Ribó M, Shan S, Zhang Y, Kulahci M. Online monitoring for error detection in vat photopolymerization. *Int J Comput Integr Manuf.* 2023;36(9):1313-1330.  
doi: 10.1080/0951192X.2022.2162600
100. Cao L, Lu L, Liu X. Waiting time prediction for bottom-up vat photopolymerization. *Addit Manuf.* 2023;74:103693.  
doi: 10.1016/j.addma.2023.103693
101. Wang X, Liu J, Dong R, Gilchrist MD, Zhang N. High-precision digital light processing (DLP) printing of microstructures for microfluidics applications based on a machine learning approach. *Virtual Phys Prototyp.* 2024;19(1):e2318774.  
doi: 10.1080/17452759.2024.2318774
102. Pingali R, Saha SK. Printability prediction in projection two-photon lithography via machine learning based surrogate modeling of photopolymerization. *J Micro Nano-Manuf.* 2022;10(3):031005.  
doi: 10.1115/1.4063021
103. Charalampous P, Kladovasilakis N, Kostavelis I, Tsongas K, Tzetzis D, Tzovaras D. Machine learning-based mechanical behavior optimization of 3D print constructs manufactured via the FFF process. *J Mater Eng Perform.* 2022;31(6):4697-4706.  
doi: 10.1007/s11665-021-06535-0
104. Veeman D, Sudharsan S, Surendhar GJ, Shanmugam R, Guo L. Machine learning model for predicting the hardness of additively manufactured acrylonitrile butadiene styrene. *Mater Today Commun.* 2023;35:106147.  
doi: 10.1016/j.mtcomm.2023.106147
105. Sharma S, Gupta V, Mudgal D, Srivastava V. Predicting biomechanical properties of additively manufactured polydopamine coated poly lactic acid bone plates using deep learning. *Eng Appl Artif Intell.* 2023;124:106587.  
doi: 10.1016/j.engappai.2023.106587
106. Bone JM, Childs C M, Menon A *et al.* Hierarchical machine learning for high-fidelity 3D printed biopolymers. *ACS Biomater Sci Eng.* 2020;6(12):7021-7031.  
doi: 10.1021/acsbmaterials.0c00755
107. Zhang J, Wang P, Gao RX. Deep learning-based tensile strength prediction in fused deposition modeling. *Comput Ind.* 2019;107:11-21.  
doi: 10.1016/j.compind.2019.01.011
108. Li Z, Zhang Z, Shi J, Wu D. Prediction of surface roughness in extrusion-based additive manufacturing with machine

- learning. *Robot Comp Integr Manuf.* 2019;57:488-495.  
doi: 10.1016/j.rcim.2019.01.004
109. Song K, Xu G, Tanvir ANM, *et al.* Machine learning-assisted 3D printing of thermoelectric materials of ultrahigh performances at room temperature. *J Mater Chem A.* 2024;12(32):21243-21251.  
doi: 10.1039/D4TA03062A
110. Jo J, Park K, Song H, Lee H, Ryu S. Innovative 3D printing of mechanoluminescent composites: Vat photopolymerization meets machine learning. *Addit Manuf.* 2024;90:104324.  
doi: 10.1016/j.addma.2024.104324
111. Seifermann M, Reiser P, Friederich P, Levkin PA. High-throughput synthesis and machine learning assisted design of photodegradable hydrogels. *Small Methods.* 2023;7(9):2300553.  
doi: 10.1002/smtd.202300553
112. Jain A, Armstrong CD, Joseph VR, Ramprasad R, Qi HJ. Machine-guided discovery of acrylate photopolymer compositions. *ACS Appl Mater Interfaces.* 2024;16(14):17992-18000.  
doi: 10.1021/acsami.4c00759
113. Gao W, Wang H, Xu Y, *et al.* Accurately predicting multiple performance of 3D printing photopolymers using ensemble learning. *ACS Appl Polym Mater.* 2024;6(8):4501-4508.  
doi: 10.1021/acsapm.3c03102
114. Yang GZ, Fischer P, Nelson B. New materials for next-generation robots. *Sci Robot.* 2017;2(10):eaap9294.  
doi: 10.1126/scirobotics.aap9294
115. Sun X, Yue L, Yu L, *et al.* Machine learning-evolutionary algorithm enabled design for 4D-printed active composite structures. *Adv Funct Mater.* 2022;32(10):2109805.  
doi: 10.1002/adfm.202109805
116. Sun X, Yue L, Yu L, *et al.* Machine learning-enabled forward prediction and inverse design of 4D-printed active plates. *Nat Commun.* 2024;15(1):5509.  
doi: 10.1038/s41467-024-49775-z
117. Rodriguez JA, Goodman DW. The nature of the metal-metal bond in bimetallic surfaces. *Science.* 1992;257(5072):897-903.  
doi: 10.1126/science.257.5072.897
118. Berry JF, Lu CC. Metal-metal bonds: From fundamentals to applications. *Inorg Chem.* 2017;56(14):7577-7581.  
doi: 10.1021/acs.inorgchem.7b01330
119. Laleh M, Sadeghi E, Revilla RI, *et al.* Heat treatment for metal additive manufacturing. *Prog Mater Sci.* 2023;133:101051.  
doi: 10.1016/j.pmatsci.2022.101051
120. Rajan TV, Sharma CP, Sharma A. *Heat Treatment, Principles and Techniques.* New Delhi, India: Prentice-Hall of India; 2006.
121. De Boer FR, Mattens W, Boom R, Miedema AR, Niessen AK. *Cohesion in Metals: Transition Metal Alloys.* Amsterdam, The Netherlands: Elsevier; 1988.
122. Khan HM, Karabulut Y, Kitay O, Kaynak Y, Jawahir IS. Influence of the post-processing operations on surface integrity of metal components produced by laser powder bed fusion additive manufacturing: A review. *Mach Sci Technol.* 2020;25(1):118-176.  
doi: 10.1080/10910344.2020.1855649
123. Vafadar A, Guzzomi F, Rassau A, Hayward K. Advances in metal additive manufacturing: A review of common processes, industrial applications, and current challenges. *Appl Sci.* 2021;11(3):1213.  
doi: 10.3390/app11031213
124. Buchanan C, Gardner L. Metal 3D printing in construction: A review of methods, research, applications, opportunities and challenges. *Eng Struct.* 2019;180:332-348.  
doi: 10.1016/j.engstruct.2018.11.045
125. Das S, Bourell DL, Babu SS. Metallic materials for 3D printing. *MRS Bull.* 2016;41(10):729-741.  
doi: 10.1557/mrs.2016.217
126. Herzog D, Seyda V, Wycisk E, Emmelmann C. Additive manufacturing of metals. *Acta Mater.* 2016;117:371-392.  
doi: 10.1016/j.actamat.2016.07.019
127. Park JW, Seo E, Park H, *et al.* Hybrid solid mesh structure for electron beam melting customized implant to treat bone cancer. *Int J Bioprinting.* 2023;9(4):716.  
doi: 10.18063/ijb.716
128. King WE, Anderson AT, Ferencz RM, *et al.* Laser powder bed fusion additive manufacturing of metals: Physics, computational, and materials challenges. *Appl Phys Rev.* 2015;2(4):041304.  
doi: 10.1063/1.4937809
129. Ladani L, Sadeghilaridjani M. Review of powder bed fusion additive manufacturing for metals. *Metals.* 2021;11(9):1391.  
doi: 10.3390/met11091391
130. Seo E, Sung H, Jeon H, *et al.* Laser powder bed fusion for AI assisted digital metal components. *Virtual Phys Prototyp.* 2022;17(4):806-820.  
doi: 10.1080/17452759.2022.2068804
131. Saboori A, Gallo D, Biamino S, Fino P, Lombardi M. An overview of additive manufacturing of titanium components by directed energy deposition: Microstructure and mechanical properties. *Appl Sci.* 2017;7(9):883.  
doi: 10.3390/app7090883
132. Ansari M, Jabari E, Toyserkani E. Opportunities and

- challenges in additive manufacturing of functionally graded metallic materials via powder-fed laser directed energy deposition: A review. *J Mater Process Technol.* 2021;294:117117.  
doi: 10.1016/j.jmatprotec.2021.117117
133. Kim H, Seo J, Chung Baek AM, *et al.* Direct energy deposition for smart micro reactor. *Virtual Phys Prototyp.* 2024;19(1):e2411024.  
doi: 10.1080/17452759.2024.2411024
134. Brennan MC, Keist JS, Palmer TA. Defects in metal additive manufacturing processes. *J Mater Eng Perform.* 2021;30:4808-4818.  
doi: 10.1007/s11665-021-05919-6
135. Du Plessis A, Yadroitsava I, Yadroitsev I. Effects of defects on mechanical properties in metal additive manufacturing: A review focusing on X-ray tomography insights. *Mater Des.* 2020;187:108385.  
doi: 10.1016/j.matdes.2019.108385
136. Jiang M, Mukherjee T, Du Y, DebRoy T. Superior printed parts using history and augmented machine learning. *NPJ Comput Mater.* 2022;8(1):184.  
doi: 10.1038/s41524-022-00866-9
137. Zhang Y, Lin C, Tian Y, *et al.* Machine learning enhanced metal 3D printing: High throughput optimization and material transfer extensibility. *Int J Extrem Manuf.* 2025;7:045004.  
doi: 10.1088/2631-7990/adbb96
138. Ogoke F, Farimani AB. Thermal control of laser powder bed fusion using deep reinforcement learning. *Addit Manuf.* 2021;46:102033.  
doi: 10.1016/j.addma.2021.102033
139. Zhong Q, Tian X, Huang X, Huo C, Li D. Using feedback control of thermal history to improve quality consistency of parts fabricated via large-scale powder bed fusion. *Addit Manuf.* 2021;42:101986.  
doi: 10.1016/j.addma.2021.101986
140. Zhang Z, Liu Z, Wu D. Prediction of melt pool temperature in directed energy deposition using machine learning. *Addit Manuf.* 2021;37:101692.  
doi: 10.1016/j.addma.2020.101692
141. Abranovic B, Sarkar S, Chang-Davidson E, Beuth J. Melt pool level flaw detection in laser hot wire directed energy deposition using a convolutional long short-term memory autoencoder. *Addit Manuf.* 2024;79:103843.  
doi: 10.1016/j.addma.2023.103843
142. Williams RJ, Sing SL. Spatiotemporal analysis of powder bed fusion melt pool monitoring videos using deep learning. *J Intell Manuf.* 2024;36:2409-2422.  
doi: 10.1007/s10845-024-02355-w
143. Guirguis D, Tucker C, Beuth J. Accelerating process development for 3D printing of new metal alloys. *Nat Commun.* 2024;15(1):582.  
doi: 10.1038/s41467-024-44783-5
144. Lee H, Heogh W, Yang J, *et al.* Deep learning for in-situ powder stream fault detection in directed energy deposition process. *J Manuf Syst.* 2022;62:575-587.  
doi: 10.1016/j.jmsy.2022.01.013
145. Karkaria V, Goeckner A, Zha R, *et al.* Towards a digital twin framework in additive manufacturing: Machine learning and bayesian optimization for time series process optimization. *J Manuf Syst.* 2024;75:322-332.  
doi: 10.1016/j.jmsy.2024.04.023
146. Tan XP, Tan YJ, Chow CSL, Tor SB, Yeong WY. Metallic powder-bed based 3D printing of cellular scaffolds for orthopaedic implants: A state-of-the-art review on manufacturing, topological design, mechanical properties and biocompatibility. *Mater Sci Eng C.* 2017;76:1328-1343.  
doi: 10.1016/j.msec.2017.02.094
147. Ladd C, So JH, Muth J, Dickey MD. 3D printing of free standing liquid metal microstructures. *Adv Mater.* 2013;25(36):5081-5085.  
doi: 10.1002/adma.201301400
148. Huang DJ, Li H. A machine learning guided investigation of quality repeatability in metal laser powder bed fusion additive manufacturing. *Mater Des.* 2021;203:109606.  
doi: 10.1016/j.matdes.2021.109606
149. Montalbano T, Nimer S, Daffron M, Croom B, Ghosh S, Storck S. Machine learning enabled discovery of new L-PBF processing domains for Ti-6Al-4V. *Addit Manuf.* 2025;98:104632.  
doi: 10.1016/j.addma.2024.104632
150. Asadi R, Queguineur A, Wiikinkoski O, *et al.* Process monitoring by deep neural networks in directed energy deposition: CNN-based detection, segmentation, and statistical analysis of melt pools. *Robot Comput Integr Manuf.* 2024;87:102710.  
doi: 10.1016/j.rcim.2023.102710
151. Kim T, Kim JG, Park S, *et al.* Virtual surface morphology generation of Ti-6Al-4V directed energy deposition via conditional generative adversarial network. *Virtual Phys Prototyp.* 2023;18(1):e2124921.  
doi: 10.1080/17452759.2022.2124921
152. Yang Z, Zhu L, Dun Y, *et al.* In-situ monitoring of the melt pool dynamics in ultrasound-assisted metal 3D printing using machine learning. *Virtual Phys Prototyp.* 2023;18(1):e2251453.

- doi: 10.1080/17452759.2023.2251453
153. Cai Y, Wang Y, Chen H, Xiong J. Searching optimal process parameters for desired layer geometry in wire-laser directed energy deposition based on machine learning. *Virtual Phys Prototyp.* 2024;19(1):e2352066.  
doi: 10.1080/17452759.2024.2352066
154. Pulido-Victoria LA, Flores-Tlacuahuac A, Panales-Pérez A., Lara-Ceniceros TE, Ávila-López MA, Bonilla-Cruz J. Prediction of viscoelastic and printability properties on binder-free TiO<sub>2</sub>-based ceramic pastes by DIW through a machine learning approach. *Comput Chem Eng.* 2025;193:108920.  
doi: 10.1016/j.compchemeng.2024.108920
155. Chen W, Zou B, Zheng Q, Huang C, Li L, Liu J. Research on anti-interference detection of 3D-printed ceramics surface defects based on deep learning. *Ceram Int.* 2023;49(13):22479-22491.  
doi: 10.1016/j.ceramint.2023.04.081
156. Chen W, Zou B, Huang C, *et al.* The defect detection of 3D-printed ceramic curved surface parts with low contrast based on deep learning. *Ceram Int.* 2023;49(2):2881-2893.  
doi: 10.1016/j.ceramint.2022.09.272
157. Zhou J, Li L, Lu L, Cheng Y. Machine learning-based quality optimisation of ceramic extrusion 3D printing deposition lines. *Mater Today Commun.* 2024;41:110841.  
doi: 10.1016/j.mtcomm.2024.110841
158. Nohut S, Schwentenwein M. Machine learning assisted material development for lithography-based additive manufacturing of porous alumina ceramics. *Open Ceram.* 2024;18:100573.  
doi: 10.1016/j.oceram.2024.100573
159. Tang J, Geng X, Li D, *et al.* Machine learning-based microstructure prediction during laser sintering of alumina. *Sci Rep.* 2021;11(1):10724.  
doi: 10.1038/s41598-021-89816-x
160. Saimon AI, Yangué E, Yue X, Kong Z, Liu C. Advancing additive manufacturing through deep learning: A comprehensive review of current progress and future challenges. *IISE Trans.* 2025:1-24.  
doi: 10.1080/24725854.2024.2443592
161. Chen Q, Zhang W, Liang X, *et al.* Machine learning-assisted multi-property prediction and sintering mechanism exploration of mullite-corundum ceramics. *Materials.* 2025;18(6):1384.  
doi: 10.3390/ma18061384
162. Raj T, Tiwary A, Jain A, *et al.* Machine learning-assisted prediction modeling for anisotropic flexural strength variations in fused filament fabrication of graphene reinforced poly-lactic acid composites. *Prog Addit Manuf.* 2024;10:2585-2599.  
doi: 10.1007/s40964-024-00768-w
163. Yi J, Deng B, Peng F, *et al.* Study on the parameters optimization of 3D printing continuous carbon fiber-reinforced composites based on CNN and NSGA-II. *Compos Part A Appl Sci Manuf.* 2025;190:108657.  
doi: 10.1016/j.compositesa.2024.108657
164. Zhang Z, Shi J, Yu T, *et al.* Predicting flexural strength of additively manufactured continuous carbon fiber-reinforced polymer composites using machine learning. *J Comput Inf Sci Eng.* 2020;20(6):061015.  
doi: 10.1115/1.4047477
165. Raj R, Mahato S, Moharana AP, Dixit AR. Predicting dimensional accuracy in 3D printed polydimethylsiloxane-carbon nanotubes composites via machine learning. *Polym Compos.* 2024;45(4):2965-2980.  
doi: 10.1002/pc.27963
166. Yang H, Fang L, Yuan Z, *et al.* Machine learning guided 3D printing of carbon microlattices with customized performance for supercapacitive energy storage. *Carbon.* 2023;201:408-414.  
doi: 10.1016/j.carbon.2022.08.083
167. Poompiw N, Sukmas W, Aumnate C, *et al.* Strain sensing characteristics of 3D-printed carbon nanotubes/polypyrrole/UV-curable composites: Experimental validation and machine learning predictions. *Prog Addit Manuf.* 2025;10(1):581-591.  
doi: 10.1007/s40964-024-00642-9
168. Maurya D, Khaleghian S, Sriramdas R, *et al.* 3D printed graphene-based self-powered strain sensors for smart tires in autonomous vehicles. *Nat Commun.* 2020;11(1):5392.  
doi: 10.1038/s41467-020-19088-y
169. Zhu J, Cho M, Li Y, *et al.* Machine learning-enabled textile-based graphene gas sensing with energy harvesting-assisted IoT application. *Nano Energy.* 2021;86:106035.  
doi: 10.1016/j.nanoen.2021.106035
170. Kwon YT, Kim YS, Kwon S, *et al.* All-printed nanomembrane wireless bioelectronics using a biocompatible solderable graphene for multimodal human-machine interfaces. *Nat Commun.* 2020;11(1):3450.  
doi: 10.1038/s41467-020-17288-0
171. Hou Y, Gao M, Gao J, *et al.* 3D printed conformal strain and humidity sensors for human motion prediction and health monitoring via machine learning. *Adv Sci.* 2023;10(36):2304132.  
doi: 10.1002/advs.202304132

## PERSPECTIVE ARTICLE

# Rethinking industrial artificial intelligence: A unified foundation framework

 Jay Lee  and Hanqi Su\* 

Center for Industrial Artificial Intelligence, Department of Mechanical Engineering, A. James Clark School of Engineering, University of Maryland, College Park, Maryland, United States of America

## Abstract

Recent advancements in industrial artificial intelligence (AI) are reshaping the industry by driving smarter manufacturing, predictive maintenance, and intelligent decision-making. However, existing approaches often focus primarily on algorithms and models while overlooking the importance of systematically integrating domain knowledge, data, and models to develop more comprehensive and effective AI solutions. Therefore, the effective development and deployment of industrial AI require a more comprehensive and systematic approach. To address this gap, this paper reviews previous research, rethinks the role of industrial AI, and proposes a unified industrial AI foundation framework comprising three core modules: the knowledge module, data module, and model module. These modules help to extend and enhance the industrial AI methodology platform, supporting various industrial applications. In addition, a case study on rotating machinery diagnosis is presented to demonstrate the effectiveness of the proposed framework, and several future directions are highlighted for the development of the industrial AI foundation framework.

### \*Corresponding author:

 Hanqi Su  
 (hanqisu@umd.edu)

**Citation:** Lee J, Su H. Rethinking industrial artificial intelligence: A unified foundation framework. *Int J AI Mater Design*. 2025;2(2):56-68. doi: 10.36922/IJAMD025080006

**Received:** February 21, 2025

**1st revised:** March 23, 2025

**2nd revised:** March 28, 2025

**Accepted:** April 2, 2025

**Published Online:** April 15, 2025

**Copyright:** © 2025 Author(s). This is an Open-Access article distributed under the terms of the Creative Commons Attribution License, permitting distribution, and reproduction in any medium, provided the original work is properly cited.

**Publisher's Note:** AccScience Publishing remains neutral with regard to jurisdictional claims in published maps and institutional affiliations.

**Keywords:** Industrial artificial intelligence; Industry 4.0; Machine learning; Deep learning; Large language model; Domain knowledge

## 1. Introduction

The rapid advancement of industrial artificial intelligence (AI) is reshaping industries worldwide.<sup>1-4</sup> Recent breakthroughs in technologies such as deep learning,<sup>1,2</sup> industrial internet of things (IIoT),<sup>5,6</sup> large language models (LLMs),<sup>7,8</sup> prognostics and health management,<sup>9,10</sup> big data analytics,<sup>11,12</sup> and cyber-physical systems (CPS)<sup>13,14</sup> have accelerated the adoption of industrial AI, enabling industrial systems to extract actionable insights from vast amounts of industrial data and support intelligent decision-making. However, current approaches often overemphasize algorithms and models while lacking a unified framework that systematically integrates domain knowledge, data, and models. To unlock the full potential of industrial AI, a structured framework is needed – one that integrates domain knowledge, high-quality data, and intelligent AI models to address complex challenges in real-world industrial settings.

Recognizing this gap, this paper proposes a unified industrial AI foundation framework composed of knowledge, data, and model modules to enhance the industrial AI methodology platform. The remainder of the paper is structured as follows:

Section 2 reviews related work; Section 3 redefines the role of industrial AI; Section 4 introduces the proposed foundation framework; Section 5 provides a case study on rotating machinery diagnosis; Section 6 discusses future directions; and Section 7 concludes the paper.

## 2. Related work

This section reviews existing studies and frameworks focusing on the integration of AI within various industrial applications. Several research works have proposed frameworks aimed at enhancing industrial productivity, decision-making, and operations by leveraging AI capabilities. Table 1 provides a clear summary of these previous industrial AI frameworks, highlighting their primary contributions. For instance, Lee *et al.*<sup>4</sup> introduced an industrial AI ecosystem framework that integrates enabling technologies, such as data technology, analytic technology, platform technology, and operation technology, within the established CPS (5C) architecture, guided by key ABCDE elements. Building on this foundation, Peres *et al.*<sup>2</sup> expanded the framework into a more comprehensive conceptual framework, emphasizing challenges, design principles, essential technologies, capabilities, attributes,

and industrial application areas. On the other hand, Zhang *et al.*<sup>15</sup> developed a comprehensive reference framework structured around seven critical dimensions (object, domain, stage, requirement, technology, function, and solutions). In addition, Yang *et al.*<sup>16</sup> proposed an intelligent manufacturing framework combining human-machine cooperation with autonomous intelligent control systems specifically tailored to the process industry. Ahmed *et al.*<sup>17</sup> highlighted AI and explainable AI (XAI) methodologies, categorizing various XAI methods and their applicability in Industry 4.0 contexts, while Jan *et al.*<sup>1</sup> structured a four-stage AI data pipeline, outlining data acquisition/validation, data processing/fusion, model training/testing, and model interpretation. Furthermore, Leng *et al.*<sup>3</sup> introduced a four-layer technical reference framework encompassing layers from hardware to industrial applications. Most recently, Lee and Su<sup>7</sup> proposed a unified industrial large knowledge model (ILKM) framework emphasizing domain-specific knowledge integration through LLMs and machine learning (ML) approaches.

Although these frameworks have successfully identified important aspects of AI integration across different industrial applications, several limitations remain.

**Table 1. Summary of existing frameworks for industrial artificial intelligence applications**

Authors	Year	Proposed industrial artificial intelligence (AI) frameworks
Lee <i>et al.</i> <sup>4</sup>	2018	Proposed an industrial AI ecosystem framework to integrate enabling technologies – data technology, analytic technology, platform technology, and operation technology – within the Cyber-Physical System (5C) architecture. The framework systematically guides AI implementation in smart manufacturing under the guidance of five key ABCDE elements: analytics technology, big data technology, cloud or cyber technology, domain know-how, and evidence.
Zhang <i>et al.</i> <sup>15</sup>	2019	Presented a comprehensive industrial AI reference framework consisting of seven key dimensions: Object (who), domain (where), application stage (when), application requirement (why), intelligent technology (which), intelligent function (what), and solutions (how); and offers a detailed overall planning for systematically integrating AI across diverse industrial scenarios.
Peres <i>et al.</i> <sup>2</sup>	2020	Proposed a conceptual industrial AI framework highlighting essential enabling technologies (data, analytics, platforms, operations, and human-machine interaction) while systematically identifying critical challenges, attributes, capabilities, design principles, and common application domains in Industry 4.0.
Yang <i>et al.</i> <sup>16</sup>	2021	Presented a two-tier intelligent manufacturing framework designed for the process industry, integrating human-machine cooperation, and intelligent autonomous control systems to achieve intelligent optimal decision-making.
Ahmed <i>et al.</i> <sup>17</sup>	2022	Conducted a comprehensive survey on AI and explainable AI (XAI) methodologies within Industry 4.0, categorizing various XAI approaches (model-specific, model-agnostic, local/global, visualization-based methods, and surrogate models), highlighting their applicability, benefits, and challenges in industrial contexts.
Jan <i>et al.</i> <sup>1</sup>	2023	Proposed a structured, four-stage industrial AI data pipeline (data acquisition/validation, data processing/fusion, model training/testing, and model interpretation). They identified common themes, issues, and industry-specific solutions related to AI integration in various sectors, providing insights into practical challenges and opportunities within Industry 4.0.
Leng <i>et al.</i> <sup>3</sup>	2024	Presented a technical reference framework structured in four layers (hardware infrastructure, computing engine, AI algorithms, and industrial application layer together with related empowering technologies across layers), identifying three core opportunities (collaborative intelligence, self-learning intelligence, and crowd intelligence) crucial for realizing Industry 5.0's vision of human-centric, resilient, and sustainable manufacturing.
Lee and Su <sup>7</sup>	2024	Proposed a unified industrial large knowledge model framework consisting of four systematic steps: (i) construction of a large knowledge library; (ii) preparation of domain-specific instruction data; (iii) development of domain-specific knowledge large language models; and (iv) establishment of intelligent domain expert machine learning systems; guided by the “6S Principle” (specialized knowledge, scrutability, safety, scalability, sustainability, and systematization).

These include the lack of systematic domain-specific knowledge integration, a tendency to focus on theoretical conceptualization without clear and objective guidelines, and an overemphasis on data and models without sufficient attention to systematic thinking that connects knowledge, data, and models. Motivated by these gaps, the following two sections revisit the role of industrial AI and present a unified industrial AI foundation framework aimed at addressing these critical shortcomings.

### 3. Rethinking the role of industrial AI

The role of industrial AI can be best understood through a two-layer perspective, as shown in Figure 1, where the physical layer consists of humans, things, and systems, while the digital layer consists of knowledge, data, and models. Based on recent emerging technologies such as IIoT,<sup>5,6</sup> digital twin,<sup>18,19</sup> CPS,<sup>13,14</sup> industrial big data analytics,<sup>11,12</sup> deep learning,<sup>1,2</sup> and LLMs,<sup>7,8</sup> industrial AI acts as a dynamic bridge between the physical and digital layers, continuously refining and applying AI-driven insights to improve and optimize the real-world industrial systems. More specifically, human expertise forms the

basis of domain knowledge, which contains accumulated experience, research insights, and best practices from AI-driven approaches. With the rise of IoT technology, things, including machines, sensors, and other devices, generate vast amounts of data, which is an essential prerequisite for conducting industrial AI analytics, modeling, and decision-making in modern industry. Moreover, systems such as CPS, IIoT systems, and other intelligent industrial systems use AI models to automate operations, enable intelligent decision-making, and improve real-time control.

While the two-layer perspective provides a conceptual understanding of how industrial AI bridges the physical and digital domains, real-world industrial settings present several challenges. In practice, developers and engineers face persistent difficulties in transforming heterogeneous data from IIoT devices into reliable, AI-ready formats due to inconsistent data quality, lack of standard preprocessing pipelines, and fragmented metadata management.<sup>5</sup> CPS, although widely discussed, often remains difficult to operationalize, as maintaining consistency between real-world operations and virtual models requires continuous data synchronization and robust model updating.<sup>13</sup> Despite its promise, digital twin development is challenged by the complexity of integrating multi-source data streams, real-time analytics, and simulation modeling requirements.<sup>18</sup> Furthermore, the increasing availability of LLMs introduces new opportunities but also pose practical challenges in domain knowledge understanding, extraction, and interpretability for industrial use cases.<sup>7</sup> Based on our observations from industry collaborations and project experiences, these complexities frequently result in ad-hoc solutions, isolated development efforts, and inefficiencies in scaling AI-driven applications. Therefore, these observations and challenges motivate the need for a structured foundation framework that systematically connects knowledge, data, and models, as presented in the following section.

### 4. Industrial AI foundation framework

In this section, we propose a unified industrial AI foundation framework designed to systematically guide the development and deployment of industrial AI solutions, as illustrated in Figure 2. The framework consists of three core modules: (i) knowledge module; (ii) data module; and (iii) model module. Within each module, we identify four key components, resulting in 12 important aspects that collectively provide structured direction for industrial AI developers and practitioners. These modules enhance and extend the industrial AI methodology platform by providing a structured, modular foundation for existing and emerging industrial AI methodologies. Figure 2

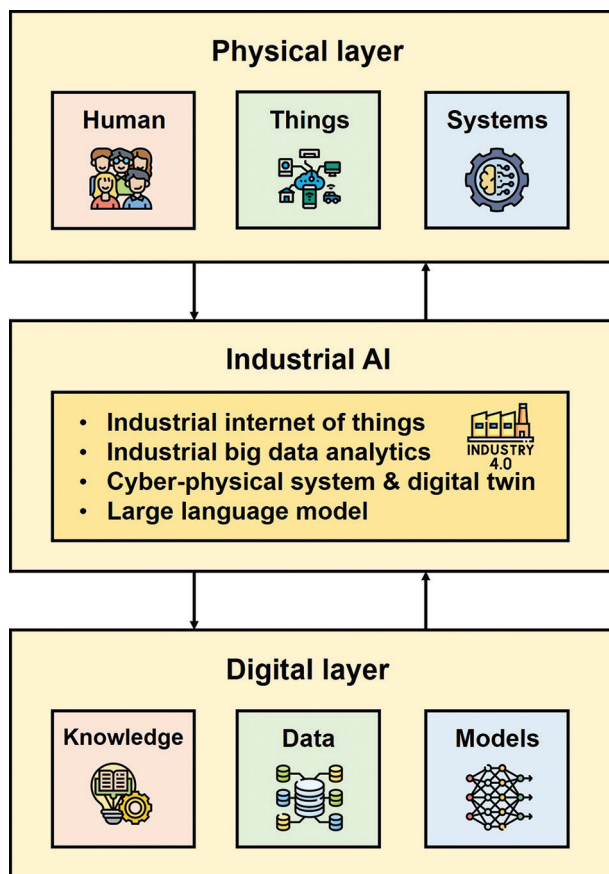
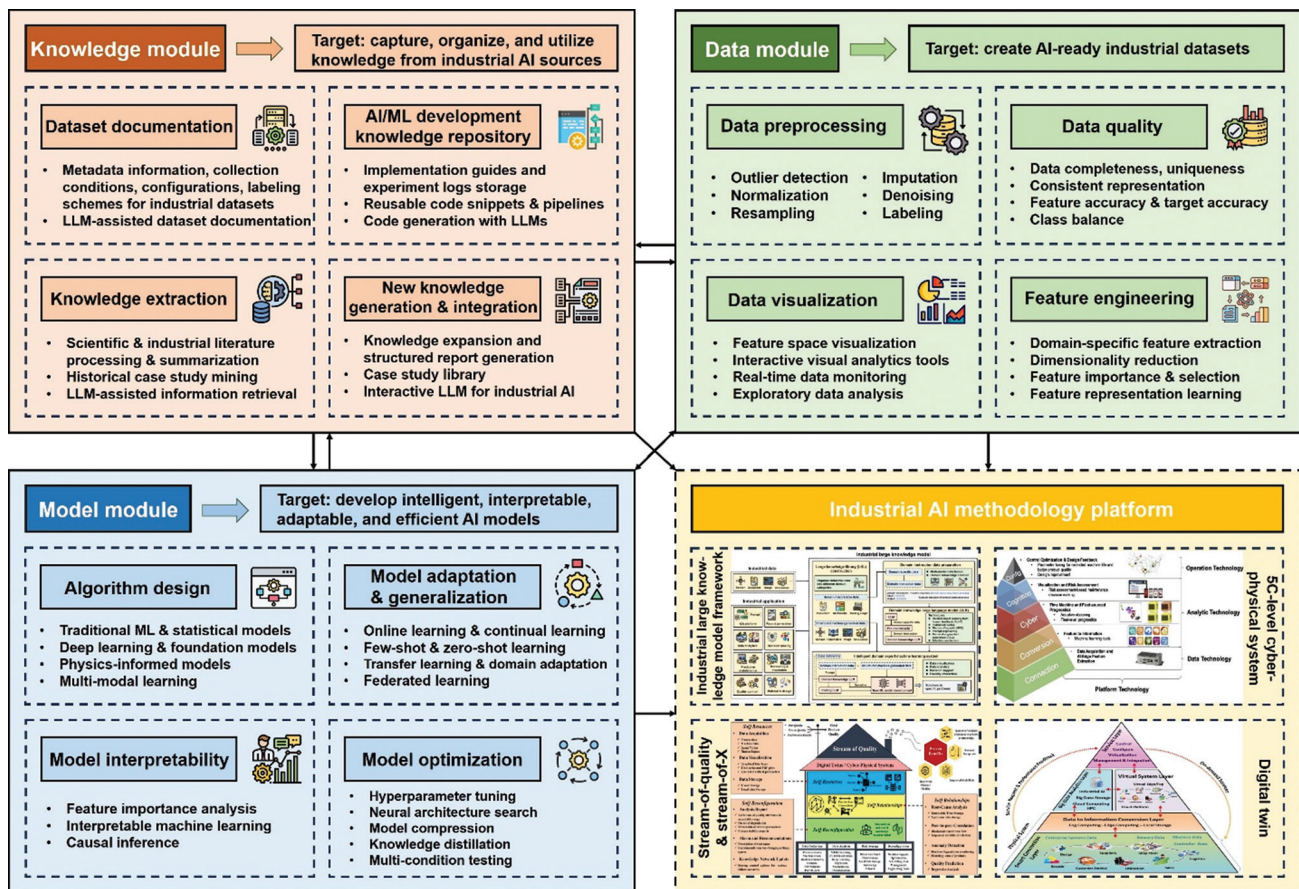


Figure 1. The role of industrial artificial intelligence in bridging the physical and digital layers. Image created by the authors.



**Figure 2.** A unified industrial artificial intelligence (AI) foundation framework. The industrial large knowledge model framework image is reprinted with permission from Lee and Su.<sup>7</sup> The stream of quality image is reprinted with permission from Lee *et al.*<sup>20</sup> Copyright © 2022 Society of Manufacturing Engineers (SME). The 5C-cyber-physical system figure is reprinted with permission from Lee *et al.*<sup>4</sup> Copyright © 2018 SME. The digital twin image is reprinted with permission from Lee *et al.*<sup>19</sup> Copyright © 2020 The Institution of Engineering and Technology. Abbreviations: LLM: Large language model; ML: Machine learning.

illustrates the overall structure of the proposed framework, highlighting the interconnections and dynamic feedback between knowledge, data, and model modules. Each pair of modules is connected by forward and backward arrows, highlighting that these modules continuously inform and refine one another, rather than existing in a linear sequence. In addition, forward arrows from all three modules point toward the industrial AI methodology platform, indicating that the platform is strengthened by these three modules. In Sections 4.1-4.4, the details of the knowledge, data, and model modules are outlined, followed by an explanation of how they enhance and extend the capabilities of the industrial AI methodology platform.

#### 4.1. Knowledge module

The knowledge module focuses on capturing, organizing, and utilizing domain knowledge to support the entire industrial AI development cycle. In complex industrial settings, domain expertise often exists in unstructured

forms, such as reports, manuals, research papers, and maintenance logs. Rather than reflecting an anthropocentric design philosophy in the traditional sense, the knowledge module aims to transform these scattered resources into structured, accessible, and reusable formats that guide data analytics and model development – serving as a foundation that enables scalable, automated, and context-aware AI system development. It focuses on the following four aspects.

##### 4.1.1. Knowledge extraction

Knowledge extraction refers to the systematic process of converting unstructured information into structured, searchable knowledge representations. This is essential for enabling automated reasoning and guiding data preprocessing and model design. Techniques such as knowledge graph construction<sup>21-23</sup> and LLM-assisted information extraction<sup>24</sup> are commonly used. For instance, tools such as OpenKE,<sup>25</sup> TransOMCS,<sup>26</sup> and gBuilder<sup>27</sup> can

help with knowledge graph construction, while LLMs, such as GPT-3/4,<sup>28,29</sup> Llama1/2,<sup>30,31</sup> PaLM,<sup>32</sup> and DeepSeek,<sup>33</sup> can automate the summarization and extraction of key technical information from technical reports and research articles.

#### **4.1.2. Dataset documentation as industrial knowledge**

Dataset documentation is a critical part of building structured industrial knowledge. It involves systematically recording dataset metadata, collection conditions, sensor configurations, labeling schemes, and linking datasets with domain knowledge. This ensures that datasets evolve from isolated assets into long-term, reusable knowledge resources that can be properly understood, reused, and referenced in future work. Platforms such as GitHub and Hugging Face demonstrate best practices in dataset documentation, providing clear descriptions, structured metadata fields, and version histories. In addition, LLMs could enrich dataset documentation.<sup>34</sup>

#### **4.1.3. AI/ML development knowledge repository**

An AI/ML development knowledge repository provides a centralized space to store reusable code templates, implementation guides, hyperparameter tuning records, and experiment logs. This repository accelerates development by allowing engineers to reuse proven techniques and implementation methods. Examples include maintaining shared code repositories on GitHub combined with experiment documentation platforms and using platforms such as MLflow or Weights and Biases for tracking experiments, packaging code, managing models, and sharing results. Moreover, LLMs also enhance multiple aspects, including code generation, information retrieval, and interactive AI-assisted exploration.<sup>35-38</sup>

#### **4.1.4. New knowledge generation and integration**

As models are developed and validated, they produce new insights and interpretations that should be continuously integrated into the existing knowledge base. This process involves capturing lessons learned, model interpretation outputs, model results, and deployment feedback, feeding them back into structured documentation and knowledge graphs. This iterative process ensures that the knowledge module remains dynamic and evolves alongside technological progress and deployment experiences.

### **4.2. Data module**

The data module focuses on transforming raw industrial data into AI-ready datasets to improve data usability and reliability, enhanced by the domain knowledge from the knowledge module. In processing data, this module

focuses on four key aspects: data preprocessing, data quality, feature engineering, and data visualization.

#### **4.2.1. Data preprocessing**

This is a fundamental prerequisite for successful industrial AI applications, as raw data often contains issues such as noise, missing values, anomalies, class imbalances, and labeling inconsistencies. A well-structured data preprocessing pipeline typically involves several key techniques, including outlier detection methods (such as isolation forests, local outlier factor, and statistical thresholding), data imputation methods (including mean, median, multiple imputation, k-nearest neighbors, and regression-based approaches), signal denoising methods (such as wavelet transforms and filtering), and resampling methods (including synthetic minority over-sampling technique, random over-sampling, and under-sampling).<sup>39</sup> In addition, researchers are encouraged to adopt, design, and document reusable preprocessing pipelines using standardized tools such as Pandas, scikit-learn, PyTorch, and TensorFlow to ensure reproducibility and scalability.

#### **4.2.2. Data quality**

Data quality directly impacts the reliability of AI models, as poor-quality data can degrade model performance and lead to poor decision-making. Key dimensions of data quality include consistent representation, completeness, uniqueness, feature accuracy, target accuracy, and target class balance.<sup>40</sup> Therefore, developers should adopt systematic data quality checks as part of their pipelines. For instance, CleanML demonstrates how various data quality issues can significantly affect the performance of common ML models.<sup>41</sup> Furthermore, Foroni *et al.*<sup>42</sup> extended conventional data quality definitions by evaluating not only how data deviate from an ideal clean dataset but also how these deviations influence task outcomes.

#### **4.2.3. Feature engineering**

Feature engineering focuses on extracting meaningful representations from raw data, improving model performance, interpretability, and efficiency.<sup>43</sup> In industrial applications, well-designed features can greatly improve model accuracy. Common techniques include domain-specific feature extraction, such as time-domain statistical measures, frequency-domain features derived from Fourier transforms, and time-frequency domain features. Dimensionality reduction methods, including principal component analysis (PCA), t-distributed stochastic neighbor embedding (t-SNE), and linear discriminant analysis, help reduce complexity while maintaining important information. Feature importance ranking methods are used to identify key variables that most

influence model predictions, guiding feature selection. In addition, deep learning-based feature representation learning can discover complex patterns in datasets. Tools such as tsfresh, PyCaret, and Shapley Additive Explanations (SHAP) provide automated pipelines for feature extraction, feature importance, and feature selection. Therefore, effective feature engineering ensures that AI models focus on the most informative inputs while minimizing redundancy and noise.

#### **4.2.4. Data visualization**

Data visualization plays an important role in making complex datasets interpretable for both humans and AI systems.<sup>44</sup> Visualization supports tasks such as exploratory data analysis, feature space visualization, anomaly detection, and real-time monitoring. For instance, feature space visualization using t-SNE or PCA projections can help detect outliers or clusters in high-dimensional sensor data. Real-time dashboards that visualize data streams from machines and production lines help operational teams identify issues early and improve system reliability. Moreover, industrial practitioners are encouraged to utilize interactive visualization tools, such as Plotly, Tableau, and D3, to enable dynamic data exploration.

### **4.3. Model module**

With structured knowledge and AI-ready data in place, the model module is responsible for developing intelligent, adaptable, interpretable, and efficient AI models to drive industrial AI applications in Industry 4.0. This module provides four key aspects to help developers systematically design, adapt, and refine models that meet complex industrial requirements.

#### **4.3.1. Algorithm design**

Algorithm design serves as the foundation for developing AI models. Developers should select or design models that align with data characteristics, domain constraints, and application requirements. Typical options range from traditional ML and statistical methods – such as decision tree, random forest, support vector machine, gradient boosting, k-nearest neighbors, Gaussian mixture model, and various clustering algorithms – to deep learning architectures, including convolutional neural networks (CNNs), recurrent neural networks, graph neural networks, transformers, and their variants.<sup>45,46</sup> These algorithms are applicable to problems involving both continuous variables (e.g., vibration signals, temperature, and pressure) and discrete variables (e.g., operational states, fault modes, and control events). Beyond traditional ML and deep learning architectures, physics-informed neural networks (PINNs) have emerged as valuable tools in industrial AI.<sup>47,48</sup>

PINNs incorporate physical laws and equations into the learning process, improving model reliability in scenarios where data are sparse but prior knowledge is available. In addition, multi-modal learning approaches, which combine information from multiple modalities – such as images, text, audio, tabular data, and sensor measurements – enable the development of more comprehensive models suitable for complex industrial scenarios.<sup>49,50</sup> Furthermore, foundation models, which are pre-trained on large-scale diverse datasets, offer a promising approach for transferable and adaptable AI across different industrial domains. These models can be fine-tuned for specific tasks, allowing for efficient deployment with reduced training time and improved generalization.<sup>51</sup> In the process of algorithm design, developers may utilize prior knowledge and experience to create new model architectures or iteratively refine existing models through systematic experimentation and testing. When open-source implementations are available, they can be reproduced and further extended based on established methods.

#### **4.3.2. Model interpretability**

Model interpretability is crucial for ensuring that AI models are transparent and explainable. One important direction is interpretable ML, which focuses on developing models that are transparent by design, such as regression models, decision trees, and generalized additive models. These models, along with techniques such as rule-based learning and sparse linear models, can provide clear and consistent explanations, making them suitable for industrial applications.<sup>52,53</sup> However, with the increasing use of deep learning models, which are often treated as black boxes, it has become challenging to understand and explain how such models make predictions. To address this, developers are encouraged to use *post hoc* explanation methods, such as the SHAP values,<sup>54</sup> Local Interpretable Model-agnostic Explanations,<sup>55</sup> and integrated gradients. These methods enable feature importance analysis and provide explanations of model predictions in both global and local contexts. In addition, causal inference techniques can enhance model interpretability by identifying cause-and-effect relationships between input variables and model outcomes. Approaches such as structural causal models, counterfactual analysis, and invariant causal prediction can be used to provide more robust and stable explanations, particularly in dynamic industrial settings.<sup>56</sup>

#### **4.3.3. Model adaptation and generalization**

Model adaptation refers to the ability of an AI model to adjust its parameters or structure to accommodate new data distributions, domains, or operational scenarios without requiring complete retraining. Meanwhile, model

generalization refers to the model's ability to maintain accurate predictions when exposed to previously unseen data or tasks. They are essential to ensure that models remain robust, reliable, and effective in real-world industrial settings. Several key techniques support model adaptation and generalization. Transfer learning and domain adaptation allow models trained in one context or domain to be fine-tuned or adjusted for use in another, reducing the need for large amounts of newly labeled data.<sup>57,58</sup> Federated learning enables decentralized model training across multiple industrial sites, allowing collaborative improvement of models while preserving data privacy and security.<sup>59</sup> In addition, few-shot and zero-shot learning techniques allow models to make accurate predictions in new domains with limited (few-shot) or no (zero-shot) task-specific training data.<sup>60,61</sup> These are especially valuable when collecting and labeling new industrial data is time-consuming or expensive. Online learning allows models to continuously update as new data streams become available, maintaining relevance and accuracy in real-time applications.<sup>62</sup> Likewise, continual learning techniques enable models to incrementally incorporate knowledge from new data without catastrophic forgetting of previously learned information, supporting long-term model evolution in dynamic environments.<sup>63</sup>

#### **4.3.4 Model optimization and deployment readiness**

Model optimization is essential for improving the performance, efficiency, and reliability of AI models in industrial applications. It involves tuning model parameters, selecting appropriate architectures, and improving computational efficiency. Common techniques include hyperparameter optimization methods, such as grid search, random search, and Bayesian optimization, which systematically explore the parameter space to find optimal configurations.<sup>64</sup> In addition to hyperparameter tuning, model optimization also addresses structural design and computational efficiency to meet industrial requirements. Neural architecture search (NAS) methods, including differentiable NAS and evolutionary algorithms, can automate the discovery of architectures that achieve optimal trade-offs between accuracy, latency, and memory consumption.<sup>65</sup> Model compression techniques, such as pruning (magnitude-based or structured pruning), weight quantization, and low-rank factorization, are commonly used to reduce inference time and deployment costs without significant loss of performance.<sup>66</sup> Knowledge distillation further enhances deployment readiness by transferring knowledge from large teacher models to smaller student models.<sup>67</sup> Furthermore, multi-condition testing could be performed to ensure that models perform reliably across different operating scenarios.<sup>68</sup>

#### **4.4. Industrial AI methodology platform**

The industrial AI methodology platform provides structured approaches, architectures, and guiding principles to ensure AI applications are systematically integrated into industrial systems. This platform includes multiple well-established methodologies that shape AI integration in industrial settings. Examples include: (i) ILKM: ILKM bridges LLMs with domain-specific industrial knowledge to support reasoning, explanation, and contextual decision-making in industrial AI;<sup>7</sup> (ii) 5C CPS: CPS provides a structured approach for integrating AI with industrial systems through five levels (connection, conversion, cyber, cognition, and configuration), enabled by operation technology, analytic technology, data technology, and platform technology;<sup>4,14</sup> (iii) stream-of-quality and stream-of-X: This shows a paradigm that defines a structured methodology for continuous monitoring, optimization, and decision-making in industrial systems, particularly for multi-stage manufacturing processes;<sup>20</sup> and (iv) digital twin: It integrates data, simulation, and services to create a virtual representation of physical entities, achieving industrial intelligence by utilizing AI, IoT, and ML techniques.<sup>19</sup>

While existing methodologies have played an important role in advancing industrial AI, their implementation can be further enhanced by the proposed industrial AI foundation framework. Rather than redefining the core methodologies, the knowledge, data, and model modules offer comprehensive and systematic views that support both existing and emerging industrial AI approaches. By promoting more structured development processes, they ensure that the design, implementation, and deployment of industrial AI solutions are more effective, reliable, and scalable. A concrete example is using ILKM to enable intelligent question-answering (QA) systems for maintenance personnel, who frequently need to query complex maintenance manuals and troubleshooting guides during equipment servicing. The knowledge module enables the structured extraction of key procedures, fault descriptions, and parameter settings from maintenance manuals and technical documentation. This content is organized into knowledge graphs and indexed repositories that can be efficiently queried by LLMs. The data module ensures that domain-specific datasets – including historical maintenance logs and annotated QA pairs – are properly documented, versioned, and linked to the knowledge base. Standardized metadata (e.g., machine type, operating conditions, and fault categories) allows the LLM to retrieve relevant answers aligned with specific equipment and scenarios. The model module guides the fine-tuning of LLMs on domain-specific QA datasets. It also defines best



AI foundation framework, guiding knowledge extraction, data preparation, model development, and evaluation in a structured and systematic manner.

The process began with the knowledge module. Under its guidance, domain knowledge was extracted from existing publications related to the dataset by leveraging the latest LLMs, GPT-4o, through OpenAI's application programming interface. Researchers interacted with the LLM using targeted research questions such as: "Can you provide the background information about this dataset?;" "In [target] paper, how did the authors perform data processing?;" and "How can one develop specific ML models such as 1D-CNN, LSTM, or Transformer for this task?" GPT-4o provided structured responses, summaries, and code generation examples, helping researchers quickly understand the dataset's background, signal characteristics, data preparation requirements, feature extraction strategies, and model development practices.

The data module was applied to ensure systematic preprocessing. A structured pipeline was designed under the guidance of domain knowledge from prior studies. The process began with data cleaning to improve data quality, followed by data segmentation to increase the number of usable samples for model training. Next, feature engineering was performed using the fast Fourier transform to convert raw time-series signals into frequency domain features. The dataset was then split into training, validation, and test sets in a 3:1:1 ratio to ensure robust model evaluation. Throughout this stage, researchers continued to interact with LLMs to validate the soundness of their preprocessing strategies or to quickly obtain code examples for implementing new ideas.

After ensuring that the data were AI-ready, in the model module, researchers developed and evaluated eight different AI models based on previous methodologies and their expertise. These included: (i) tree-based model (decision tree and random forest); (ii) CNN-based model (naive 1D-CNN, residual 1D-CNN); (iii) long short-term memory (LSTM)-based model (naive LSTM, bi-LSTM, hybrid-LSTM); and (iv) transformer-based model (vanilla transformer). Deep learning models were selected for their ability to automatically extract complex patterns from large-scale, frequency-domain features and for their proven robustness in handling variations in operating conditions without the need for extensive manual feature engineering. Hyperparameter tuning and performance evaluation were performed following the experience indicated in the previous research and researchers' development experience.

The classification accuracy and confusion matrix are presented in [Figure 3](#), demonstrating high performance

across various architectures, with the transformer model achieving the highest accuracy of 99.47%. These results highlight the potential of advanced deep learning architectures in industrial fault diagnosis. Compared with previous studies on similar gearbox fault classification tasks, the proposed approach demonstrates clear improvement. For instance, Su and Lee<sup>69</sup> developed a residual CNN that achieved 96.99% accuracy, Vaerenberg *et al.*<sup>70</sup> used power spectral density preprocessing, log normalization, and a 3-layer CNN to reach 96.9% accuracy, and Gauriat *et al.*<sup>71</sup> proposed multi-class neural additive models with 92.03% accuracy. The higher performance achieved in this study is attributed to not only the model design but also the systematic application of the industrial AI foundation framework. The structured guidance from the knowledge, data, and model modules ensured consistent data preprocessing, appropriate model selection, and effective hyperparameter tuning, ultimately enhancing reliability, scalability, and real-world applicability.

## 6. Future direction

To further strengthen the industrial AI foundation framework, several key directions require further exploration. One critical aspect is talent development. Incorporating 4P-based learning (principle, practice, problem-solving, and professional) and interdisciplinary training in AI/ML, engineering, and industrial applications could benefit the next generation of industrial AI practitioners. Another promising direction is data foundry, which aims to establish a standardized framework for industrial dataset collection, annotation, benchmarking, and management. A well-structured data foundry would enhance collaborative AI research, reproducibility, and cross-industry data sharing while also facilitating the hosting of the Industrial AI Data Challenge Competitions to promote innovation and benchmark AI model performance on industrial datasets. Meanwhile, the foundation framework can be extended toward discrete event dynamic systems and hybrid control systems. This would involve adapting the knowledge, data, and model modules to better handle event-based transitions, symbolic representations, and hierarchical system logic. Furthermore, future research should explore the development of an LLM-assisted intelligent knowledge management system to better make use of historical case studies, domain expertise, and best practices. Such a system could autonomously acquire, structure, and retrieve relevant information, providing researchers and engineers with contextualized and actionable insights to improve AI model development and decision-making in industrial applications.

## 7. Conclusion

This paper proposes a unified industrial AI foundation framework, structured into three core modules – the knowledge module, data module, and model module – which collectively support and enhance the industrial AI methodology platform. The role of industrial AI is explored in detail, and a case study on intelligent rotating machinery diagnosis demonstrates the framework's potential. Furthermore, several future directions are discussed. Overall, our unified industrial AI foundation framework provides a systematic approach to developing, validating, and deploying industrial AI solutions for future industries. Despite these contributions, we acknowledge that acquiring and labeling industrial data remains a significant challenge. Furthermore, while the framework leverages LLMs for knowledge extraction, human guidance is still required, and computational costs may limit its deployment in certain industrial settings. Moving forward, we encourage further research and collaboration between academia, industry, and AI practitioners to refine and expand this framework, fostering the next generation of intelligent, knowledge-data-driven industrial AI ecosystems.

## Acknowledgments

None.

## Funding

None.

## Conflict of interest

Jay Lee is an Editorial Board Member of this journal but was not in any way involved in the editorial and peer-review process conducted for this paper, directly or indirectly. Separately, other authors declared that they have no known competing financial interests or personal relationships that could have influenced the work reported in this paper.

## Author contributions

*Conceptualization:* All authors

*Writing–original draft:* Hanqi Su

*Writing–review & editing:* All authors

## Ethics approval and consent to participate

Not applicable.

## Consent for publication

Not applicable.

## Availability of data

The dataset used in the case study is available for download from <https://data.phmsociety.org/phm2023-conference-data-challenge/>.

## References

1. Jan Z, Ahamed F, Mayer W, *et al.* Artificial intelligence for industry 4.0: Systematic review of applications, challenges, and opportunities. *Expert Syst Appl.* 2022;216:119456. doi: 10.1016/j.eswa.2022.119456
2. Peres RS, Jia X, Lee J, Sun K, Colombo AW, Barata J. Industrial artificial intelligence in industry 4.0 - systematic review, challenges and outlook. *IEEE Access.* 2020;8:220121-220139. doi: 10.1109/access.2020.3042874
3. Leng J, Zhu X, Huang Z, *et al.* Unlocking the power of industrial artificial intelligence towards Industry 5.0: Insights, pathways, and challenges. *J Manuf Syst.* 2024;73:349-363. doi: 10.1016/j.jmsy.2024.02.010
4. Lee J, Davari H, Singh J, Pandhare V. Industrial artificial intelligence for industry 4.0-based manufacturing systems. *Manuf Lett.* 2018;18:20-23. doi: 10.1016/j.mfglet.2018.09.002
5. Sisinni E, Saifullah A, Han S, Jennehag U, Gidlund M. Industrial internet of things: Challenges, opportunities, and directions. *IEEE Trans Industr Inform.* 2018;14(11):4724-4734. doi: 10.1109/tii.2018.2852491
6. Khalil RA, Saeed N, Masood M, Fard YM, Alouini MS, Al-Naffouri TY. Deep learning in the industrial internet of Things: Potentials, challenges, and emerging applications. *IEEE Internet Things J.* 2021;8(14):11016-11040. doi: 10.1109/jiot.2021.3051414
7. Lee J, Su H. A unified industrial large knowledge model framework in Industry 4.0 and smart manufacturing. *Int J AI Mater Des.* 2024;1(2):41-47. doi: 10.36922/ijamd.3681
8. Chang Y, Wang X, Wang J, *et al.* A survey on evaluation of large language models. *ACM Trans Intell Syst Technol.* 2024;15(3):1-45. doi: 10.1145/3641289
9. Zio E. Prognostics and Health Management (PHM): Where are we and where do we (need to) go in theory and practice. *Reliab Eng Syst Saf.* 2021;218:108119. doi: 10.1016/j.res.2021.108119

10. Su H, Lee J. Machine learning approaches for diagnostics and prognostics of industrial systems using open source data from PHM data challenges: A review. *Int J Progn Health Manag.* 2024;15(2):1-26.  
doi: 10.36001/ijphm.2024.v15i2.3993
11. Yan J, Meng Y, Lu L, Li L. Industrial big data in an industry 4.0 environment: Challenges, schemes, and applications for predictive maintenance. *IEEE Access.* 2017;5:23484-23491.  
doi: 10.1109/access.2017.2765544
12. Wang J, Xu C, Zhang J, Zhong R. Big data analytics for intelligent manufacturing systems: A review. *J Manuf Syst.* 2021;62:738-752.  
doi: 10.1016/j.jmsy.2021.03.005
13. Pivoto DGS, de Almeida LFF, da Rosa Righi R, Rodrigues JJPC, Lugli AB, Alberti AM. Cyber-physical systems architectures for industrial internet of things applications in Industry 4.0: A literature review. *J Manuf Syst.* 2021;58:176-192.  
doi: 10.1016/j.jmsy.2020.11.017
14. Lee J, Bagheri B, Kao HA. A cyber-physical systems architecture for industry 4.0-based manufacturing systems. *Manuf Lett.* 2014;3:18-23.  
doi: 10.1016/j.mfglet.2014.12.001
15. Zhang X, Ming X, Liu Z, Yin D, Chen Z, Chang Y. A reference framework and overall planning of industrial artificial intelligence (I-AI) for new application scenarios. *Int J Adv Manuf Technol.* 2018;101(9-12):2367-2389.  
doi: 10.1007/s00170-018-3106-3
16. Yang T, Yi X, Lu S, Johansson KH, Chai T. Intelligent manufacturing for the process industry driven by industrial artificial intelligence. *Engineering.* 2021;7(9):1224-1230.  
doi: 10.1016/j.eng.2021.04.023
17. Ahmed I, Jeon G, Piccialli F. From artificial intelligence to explainable artificial intelligence in industry 4.0: A survey on what, how, and where. *IEEE Trans Industr Inform.* 2022;18(8):5031-5042.  
doi: 10.1109/tii.2022.3146552
18. Tao F, Zhang H, Liu A, Nee AYC. Digital twin in industry: State-of-the-art. *IEEE Trans Industr Inform.* 2019;15(4):2405-2415.  
doi: 10.1109/tii.2018.2873186
19. Lee J, Azamfar M, Singh J, Siahpour S. Integration of digital twin and deep learning in cyber-physical systems: Towards smart manufacturing. *IET Collab Intell Manuf.* 2020;2:34-36.  
doi: 10.1049/iet-cim.2020.0009
20. Lee J, Gore P, Jia X, Siahpour S, Kundu P, Sun K. Stream-of-quality methodology for industrial internet-based manufacturing system. *Manuf Lett.* 2022;34:58-61.  
doi: 10.1016/j.mfglet.2022.09.004
21. Buchgeher G, Gabauer D, Martinez-Gil J, Ehrlinger L. Knowledge graphs in manufacturing and production: A systematic literature review. *IEEE Access.* 2021;9:55537-55554.  
doi: 10.1109/access.2021.3070395
22. Zhong L, Wu J, Li Q, Peng H, Wu X. A comprehensive survey on automatic knowledge graph construction. *ACM Comput Surv.* 2023;56(4):1-62.  
doi: 10.1145/3618295
23. Pan S, Luo L, Wang Y, Chen C, Wang J, Wu X. Unifying large language models and knowledge graphs: A roadmap. *IEEE Trans Knowl Data Eng.* 2024;36(7):3580-3599.  
doi: 10.1109/tkde.2024.3352100
24. Kirk JR, Wray RE, Lindes P, Laird JE. Improving knowledge extraction from LLMs for task learning through agent analysis. *Proc AAAI Conf Artif Intell.* 2024;38(16):18390-18398.  
doi: 10.1609/aaai.v38i16.29799
25. Han X, Cao S, Lv X, et al. OpenKE: An Open Toolkit for Knowledge Embedding. In: *Proceedings of the 2018 Conference on Empirical Methods in Natural Language Processing: System Demonstrations.* Association for Computational Linguistics; 2018.  
doi: 10.18653/v1/D18-2024
26. Zhang H, Khashabi D, Song Y, Roth D. TransOMCS: From Linguistic Graphs to Commonsense Knowledge. In: *Proceedings of the Twenty-Ninth International Joint Conference on Artificial Intelligence (IJCAI-20).* 2020.  
doi: 10.24963/ijcai.2020/554
27. Li Y, Zou L. gBuilder: A Scalable knowledge graph construction system for unstructured corpus. *arXiv.* 2023.  
doi: 10.48550/arXiv.2208.09705
28. Brown T, Mann B, Ryder N, et al. Language models are few-shot learners. *arXiv.* 2020.  
doi: 10.48550/arXiv.2005.14165
29. Achiam J, Adler S, Agarwal S, et al. GPT-4 technical report. *arXiv.* 2024.  
doi: 10.48550/arXiv.2303.08774
30. Touvron H, Lavril T, Izacard G, et al. LLaMA: Open and efficient foundation language models. *arXiv.* 2023.  
doi: 10.48550/arXiv.2302.13971
31. Touvron H, Martin L, Stone K, et al. LLaMA 2: Open foundation and fine-tuned chat models. *arXiv.* 2023.  
doi: 10.48550/arXiv.2307.09288
32. Chowdhery A, Narang S, Devlin J, et al. PaLM: Scaling language modeling with pathways. *arXiv.* 2022.

- doi: 10.48550/arXiv.2204.02311
33. Liu A, Feng B, Wang B, *et al.* DeepSeek-V2: A strong, economical, and efficient mixture-of-experts language model. *arXiv*. 2024.  
doi: 10.48550/arXiv.2405.04434
  34. Giner-Miguel J, Gómez A, Cabot J. Using large language models to enrich the documentation of datasets for machine learning. *arXiv*. 2024.  
doi: 10.48550/arXiv.2404.15320
  35. Vaithilingam P, Zhang T, Glassman EL. Expectation vs. Experience: Evaluating the Usability of Code Generation Tools Powered by Large Language Models. In: *CHI Conference on Human Factors in Computing Systems Extended Abstracts (CHI '22 Extended Abstracts)*. 2022.  
doi: 10.1145/3491101.3519665
  36. Fan W, Ding Y, Ning L, *et al.* A survey on RAG Meeting LLMs: Towards Retrieval-Augmented Large Language Models. In: *Proceedings of the 28<sup>th</sup> ACM SIGKDD Conference on Knowledge Discovery and Data Mining*. 2024. p. 6491-6501.  
doi: 10.1145/3637528.3671470
  37. Strobelt H, Webson A, Sanh V, *et al.* Interactive and visual prompt engineering for ad-hoc task adaptation with large language models. *IEEE Trans Vis Comput Graph*. 2022;29:1146-1156.  
doi: 10.1109/tvcg.2022.3209479
  38. He Q, Zeng J, Huang W, *et al.* Can large language models understand real-world complex instructions? *Proc AAAI Conf Artif Intell*. 2024;38(16):18188-18196.  
doi: 10.1609/aaai.v38i16.29777
  39. Cofre-Martel S, Lopez Droguett E, Modarres M. Big machinery data preprocessing methodology for data-driven models in prognostics and health management. *Sensors (Basel)*. 2021;21(20):6841.  
doi: 10.3390/s21206841
  40. Mohammed S, Budach L, Feuerpfeil M, *et al.* The effects of data quality on machine learning performance. *arXiv*. 2024.  
doi: 10.48550/arXiv.2207.14529
  41. Li P, Rao X, Blase J, Zhang Y, Chu X, Zhang C. CleanML: A Study for Evaluating the Impact of Data Cleaning on ML Classification Tasks. In: *2021 IEEE 37<sup>th</sup> International Conference on Data Engineering (ICDE)*. 2021.  
doi: 10.1109/icde51399.2021.00009
  42. Foroni D, Lissandrini M, Velegrakis Y. Estimating the Extent of the Effects of Data Quality through Observations. In: *2021 IEEE 37<sup>th</sup> International Conference on Data Engineering (ICDE)*. 2021.  
doi: 10.1109/icde51399.2021.00176
  43. Zheng A, Casari A. *Feature Engineering for Machine Learning Principles and Techniques for Data Scientists*. Beijing, Boston, Farnham: O'Reilly; 2018.
  44. Allen L, Atkinson J, Jayasundara D, Cordiner J, Moghadam PZ. Data visualization for Industry 4.0: A stepping-stone toward a digital future, bridging the gap between academia and industry. *Patterns (N Y)*. 2021;2(5):100266.  
doi: 10.1016/j.patter.2021.100266
  45. Bertolini M, Mezzogori D, Neroni M, Zammori F. Machine learning for industrial applications: A comprehensive literature review. *Expert Syst Appl*. 2021;175:114820.  
doi: 10.1016/j.eswa.2021.114820
  46. Sarker IH. Deep learning: A comprehensive overview on techniques, taxonomy, applications and research directions. *SN Comput Sci*. 2021;2(6):420.  
doi: 10.1007/s42979-021-00815-1
  47. Xu Y, Kohtz S, Boakye J, Gardoni P, Wang P. Physics-informed machine learning for reliability and systems safety applications: State of the art and challenges. *Reliab Eng Syst Saf*. 2022;230:108900.  
doi: 10.1016/j.res.2022.108900
  48. Li H, Zhang Z, Li T, Si X. A review on physics-informed data-driven remaining useful life prediction: Challenges and opportunities. *Mech Syst Signal Process*. 2024;209:111120-111120.  
doi: 10.1016/j.ymsp.2024.111120
  49. Ektefaie Y, Dasoulas G, Noori A, Farhat M, Zitnik M. Multimodal learning with graphs. *Nat Mach Intell*. 2023;5(4):340-350.  
doi: 10.1038/s42256-023-00624-6
  50. Su H, Song B, Ahmed F. Multi-modal Machine Learning for Vehicle Rating Predictions Using Image, Text, and Parametric Data. In: *International Design Engineering Technical Conferences and Computers and Information in Engineering Conference*. Vol. 87295. American Society of Mechanical Engineers; 2023.  
doi: 10.1115/DETC2023-115076
  51. Zhang H, Semujju SD, Wang Z, *et al.* Large scale foundation models for intelligent manufacturing applications: A survey. *J Intell Manuf*. 2025:1-52.  
doi: 10.1007/s10845-024-02536-7
  52. Linardatos P, Papastefanopoulos V, Kotsiantis S. Explainable AI: A review of machine learning interpretability methods. *Entropy (Basel)*. 2020;23(1):18.  
doi: 10.3390/e23010018
  53. Li X, Xiong H, Li X., Interpretable deep learning: Interpretation, interpretability, trustworthiness, and beyond.

- Knowl Inf Syst.* 2022;64(12):3197-3234.  
doi: 10.1007/s10115-022-01756-8
54. Lundberg SM, Lee SI. A Unified Approach to Interpreting Model Predictions. In: *Advances in Neural Information Processing Systems 30 (NIPS 2017)*. Vol. 30. Curran Associates, Inc.; 2017.
55. Ribeiro MT, Singh S, Guestrin C. "Why Should I Trust You?": Explaining the Predictions of Any Classifier. In: *Proceedings of the 22<sup>nd</sup> ACM SIGKDD International Conference on Knowledge Discovery and Data Mining - KDD '16*. 2016. p. 1135-1144.  
doi: 10.1145/2939672.2939778
56. Li Z, Guo X, Qiang S. A survey of deep causal models and their industrial applications. *ArtifIntell Rev.* 2024;57(11):298.  
doi: 10.1007/s10462-024-10886-0
57. Singhal P, Walambe R, Ramanna S, Kotecha K. Domain adaptation: Challenges, methods, datasets, and applications. *IEEE Access.* 2023;11:6973-7020.  
doi: 10.1109/access.2023.3237025
58. Li W, Huang R, Li J, *et al.* A perspective survey on deep transfer learning for fault diagnosis in industrial scenarios: Theories, applications and challenges. *Mech Syst Signal Process.* 2022;167:108487.  
doi: 10.1016/j.ymsp.2021.108487
59. Banabilah S, Aloqaily M, Alsayed E, Malik N, Jararweh Y. Federated learning review: Fundamentals, enabling technologies, and future applications. *Inf Process Manag.* 2022;59(6):103061.  
doi: 10.1016/j.ipm.2022.103061
60. Song Y, Wang T, Cai P, Mondal SK, Sahoo JP. A comprehensive survey of few-shot learning: Evolution, applications, challenges, and opportunities. *ACM Comput Surv.* 2023;55:1-40.  
doi: 10.1145/3582688
61. Wang W, Zheng VW, Yu H, Miao C. A survey of zero-shot learning: Settings, methods, and applications. *ACM Trans Intell Syst Technol.* 2019;10(2):1-37.  
doi: 10.1145/3293318
62. Hoi SCH, Sahoo D, Lu J, Zhao P. Online learning: A comprehensive survey. *Neurocomputing.* 2021;459(1):249-289.  
doi: 10.1016/j.neucom.2021.04.112
63. Wang L, Zhang X, Su H, Zhu J. A comprehensive survey of continual learning: Theory, method and application. *IEEE Trans Pattern Anal Mach Intell.* 2024;46(8):5362-5383.  
doi: 10.1109/tpami.2024.3367329
64. Yang L, Shami A. On hyperparameter optimization of machine learning algorithms: Theory and practice. *Neurocomputing.* 2020;415:295-316.  
doi: 10.1016/j.neucom.2020.07.061
65. Elsken T, Metzen JH, Hutter F. Neural architecture search: A survey. *J Mach Learn Res.* 2019;20(55):1-21.  
doi: 10.48550/arXiv.1808.05377
66. Deng BL, Li G, Han S, Shi L, Xie Y. Model compression and hardware acceleration for neural networks: A comprehensive survey. *Proc IEEE.* 2020;108(4):485-532.  
doi: 10.1109/jproc.2020.2976475
67. Gou J, Gou J, Yu B, Maybank SJ, Tao D. Knowledge distillation: A survey. *Int J Comput Vis.* 2021;129(6):1789-1819.  
doi: 10.1007/S11263-021-01453-Z
68. Kim S, Kim I, You D. Multi-condition multi-objective optimization using deep reinforcement learning. *J Comput Phys.* 2022;462:111263.  
doi: 10.1016/j.jcp.2022.111263
69. Su H, Lee J. An advanced diagnostic model for gearbox degradation prediction under various operating conditions and degradation levels. *Annu Conf PHM Soc.* 2024;16(1).  
doi: 10.36001/phmconf.2024.v16i1.3869
70. Vaerenberg R, Marx D, Hosseinli SA, *et al.* Preprocessing and modeling approach for gearbox pitting severity prediction under unseen operating conditions and fault severities. *Int J Progn Health Manag.* 2024;15(1):1-12.  
doi: 10.36001/ijphm.2024.v15i1.3808
71. Gauriat CM, Pencolé Y, Ribot P, Brouillet G. Multi-class Neural Additive Models: An Interpretable Supervised Learning Method for Gearbox Degradation Detection. In: *2024 IEEE International Conference on Prognostics and Health Management (ICPHM)*. 2024. p. 41-48.  
doi: 10.1109/icphm61352.2024.10627522

## ORIGINAL RESEARCH ARTICLE

# Prediction of the lack-of-fusion defect of laser powder bed fusion based on deep learning

**Lidong Wang\*** 

Institute for Systems Engineering Research, Mississippi State University, Mississippi, United States of America

 (This article belongs to the *Special Issue: Applications of Deep Learning in Advanced Materials Processing*)

## Abstract

Laser powder bed fusion (LPBF) is one of the additive manufacturing (AM) techniques and the most studied laser-based AM process for metals and alloys. The optimization of the laser process parameters of LPBF and the prediction of defects, for example, keyholes, cracks, and lack of fusion (LOF), are important for improving the quality of products made with LPBF. Deep learning (DL) is powerful in analyzing complex processes and predicting anomalies; however, much data is generally required for training a DL model. Experimental studies on AM (e.g., LPBF) habitually employ the design of experiments to decrease the number of experiments and save time and costs. Hence, the experimental data are not prepared for DL model creation in most situations. This paper studies the creation of a DL model on a small experimental dataset with unbalanced data and the prediction of the LOF defect of LPBF utilizing the created DL model. Data analytics is mainly conducted based on four DL methods, including Elman neural networks, Jordan neural networks, deep neural networks (DNN) with weights initialized by the deep belief network, and the regular DNN based on four algorithms: "rprop+", "rprop-", "sag," and "slr." It is shown that the regular DNN after the z-score standardization of the small dataset helps create a more accurate DL model and achieve better analytics and prediction results than the three other DL methods in this paper. The three other DL methods do not work well in the prediction of LOF based on the small dataset (with unbalanced data).

**Keywords:** Additive manufacturing; Laser powder bed fusion; Deep learning; Deep neural network; Defect prediction

---

**\*Corresponding author:**

 Lidong Wang  
 (lidong@iser.msstate.edu)

**Citation:** Wang L. Prediction of the lack-of-fusion defect of laser powder bed fusion based on deep learning. *Int J AI Mater Design*. 2025;2(2):69-78.  
 doi: 10.36922/IJAMD025060005

**Received:** February 5, 2025

**1st revised:** March 27, 2025

**2nd revised:** May 15, 2025

**3rd revised:** May 29, 2025

**Accepted:** June 3, 2025

**Published online:** June 16, 2025

**Copyright:** © 2025 Author(s). This is an Open-Access article distributed under the terms of the Creative Commons Attribution License, permitting distribution, and reproduction in any medium, provided the original work is properly cited.

**Publisher's Note:** AccScience Publishing remains neutral with regard to jurisdictional claims in published maps and institutional affiliations.

## 1. Introduction

Additive manufacturing (AM) is one of the key elements in Industry 4.0. The reliability and quality of metal AM parts or components are critical, especially for a laser powder bed fusion (LPBF) process. Melt pool defects of LPBF, for example, balling, keyholes, and lack of fusion (LOF) can compromise structural integrity.<sup>1</sup> LPBF has advantages, such as complex and precise parts, excellent material densification, *etc.* The laser scanning strategy is one of the significant factors affecting the quality of LPBF parts, where printing defects often occur at the path's endpoints and between the paths. The optimization of process parameters and the improvement of forming environment are

essential approaches to improving the comprehensive performance of LPBF parts.<sup>2</sup>

Defect modeling in an LPBF process is important. Modeling involves simulating and predicting the formation of defects and guiding the process of optimization. It helps achieve better control over LPBF parameters, including the laser power, the scanning speed, *etc.*, to reduce defects and improve the final part quality. Due to inadequate melting and bonding occurring between adjacent layers, LOF is a serious defect that compromises the overall strength and cohesion of the printed structure of LPBF.<sup>3</sup>

Sequentially learned random forest with enhanced sampling was presented for robust and efficient defect classification in an LPBF process.<sup>1</sup> A machine learning (ML) framework that combines a fuzzy logic scheme, a self-organizing map, and a tailored U-Net architecture was presented to improve the defect prediction capability of an LPBF process. The framework and methodology were employed to predict general defects, for example, keyholes and LOF, by analyzing *in situ* optical tomography data. Furthermore, a quality assurance professional was permitted to use the expert knowledge through customizable fuzzy rules.<sup>4</sup>

A deep learning (DL)-based approach to defect detection was proposed that uses various convolutional neural networks and transfer learning techniques to automatically segment and detect the melt pools of LPBF and porosity from microstructure images. The research demonstrated the ability to detect and segment melt pools and porosity accurately, even with a limited set of training data. It also paves the way for effective quality monitoring and quantitative evaluation of defects in LPBF.<sup>5</sup>

LPBF has been a widely utilized AM method for metals. *In situ*, sensing and monitoring have been an effective approach to detecting LPBF defects. A real-time defect detection system with feedback control was proposed based on the integration of 3D point cloud data processing with DL. This research demonstrated that there would be great potential for 3D point cloud-based DL in improving defect detection and quality control in LPBF.<sup>6</sup>

There are more hidden layers in a DL network than in a traditional artificial neural network (ANN). DL can automatically learn and discover relevant features from data or examples; therefore, it can detect patterns and trends and make predictions. Generally, much data is needed for training a DL model. A DL model can improve its performance if more data is used for model training. Overfitting and data availability are two major challenges in DL.<sup>7</sup> Generally, it is necessary to collect a lot of quality data (such as balanced data, not biased data, *etc.*) for DL model

training; however, large amounts of data in engineering are often not available. For example, experimental studies on LPBF often use the design of experiments to reduce the number of experiments to save costs and time. Therefore, much of the experimental data of LPBF is for specific tasks; it is not prepared for ML/DL and the ML/DL model creation. The work in this paper is part of the author's effort to explore a DL model on a small experimental dataset with unbalanced data.

The main objective of this research paper is to establish DL models on a small dataset (with unbalanced data) and predict the LOF defect of LPBF based on the established DL models. The remainder of this paper is organized as follows: the second section introduces LPBF; the third section introduces data (the dataset used in this paper), data pre-processing techniques (min-max normalization and z-score standardization), and evaluation metrics for DL; the fourth section presents four DL methods utilized in this paper, including the Elman neural network, the Jordan neural network, the DNN with weights initialized by the deep belief network (DBN), and the regular DNN based on the four algorithms (rprop+, rprop-, smallest absolute gradient [sag], and smallest learning rate [slr]); the fifth section gives results and discussion; and the sixth section presents the conclusion and future research.

## 2. LPBF

Among the most studied laser-based AM process for metals and alloys is LPBF or selective laser melting. It is suggested that the term "LPBF" should be used according to ASTM standards. LPBF utilizes a high-power laser beam to melt the pre-defined contours selectively in subsequent layers of powder. The molten metal pool solidifies rapidly by cooling. The underlying build platform is lowered, followed by another layer of powder deposition. This cycle is repeated successively till a 3D solid object is constructed. The process is finished inside a chamber full of atmospheric gas (argon, nitrogen) to avoid oxidation.<sup>8</sup> Figure 1 illustrates the LPBF process. A nickel-based alloy is used in this research.

Although there is great potential for LPBF, surface and subsurface defects such as LOF and internal porosities affect the application of internal LPBF, especially where fatigue life is a major concern. The optimization of the fatigue performance of LPBF parts is substantially dependent on the manufacturing process parameters and post-processing of LPBF. It is significant to eradicate the formation of surface and subsurface critical defects (e.g., LOF) by optimizing the melting parameters to obtain materials with good fatigue performance.<sup>9</sup> Figure 2 shows

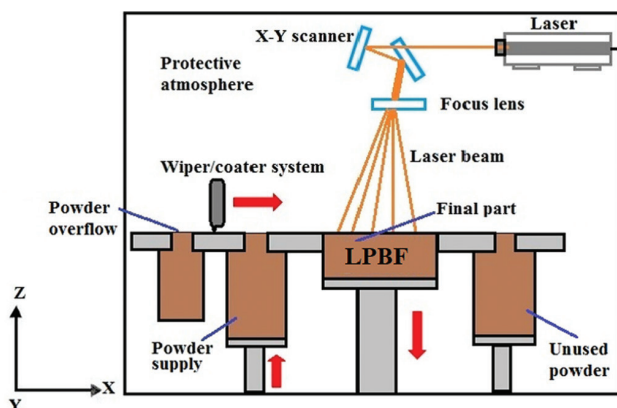


Figure 1. The laser powder bed fusion process<sup>8</sup>

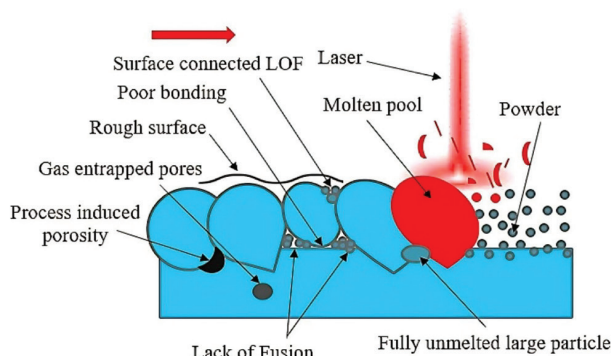


Figure 2. Possible defects and surface imperfections in the laser powder bed fusion (LPBF) process<sup>9</sup>  
Abbreviation: LOF: Lack of fusion.

possible defects and surface imperfections in the LPBF process.

### 3. Data, data pre-processing techniques, and evaluation metrics for DL

The Nickel-based powder superalloy Ni-13Cr-4Al-5Ti has exceptional performance at high temperatures. The LPBF of the superalloy and associated defects were studied, and important results were obtained. The main defects include keyholes, cracks, and LOF. The process parameters include the laser power (W), the scanning speed (mm/s), the hatch space (mm), and the scanning rotation (°).<sup>10</sup> The dataset that was used for DL in this research was part of the experimental data regarding the main defects.<sup>10</sup> This paper focuses on the LOF defect. The experimental data of the LPBF of the superalloy (Ni-13Cr-4Al-5Ti) comprises 52 rows and 5 columns. LOF was utilized for DL in this research. The original experimental data were unbalanced. For example, in the column of the scanning rotation, there were five “0” values, five “45” values, thirty-two “67” values, five “90” values, and five “180” values. In

the column of the scanning speed, there were 14 “1800” values; nine “1700” values and “1900” values, respectively; and five “600” values, “1000” values, “1400” values, and “2200” values, respectively. From an AM perspective, the scanning rotation degree has little effect on the LOF defect formation, as it does not significantly influence energy input. Therefore, the parameter of scanning rotation was not considered in the DL analysis in this research. Because there was unbalanced data in columns (with only 52 rows), the dataset used in this paper was small and unbalanced. In the column of LOF, “yes” was set to 1, and “no” was set to 0 for DL. There were thirty “1” values and twenty-two “0” values. The experimental data were not originally prepared for DL, though it was not necessary for DL training and testing. Table 1 shows partial experimental data of the LPBF of the superalloy.

Two common techniques for normalizing (or scaling) variables are:

- Min-max normalization:  $(X - \min(X))/(\max(X) - \min(X))$
- Z-score standardization:  $(X - \mu)/\sigma$

where  $X$  is the data value,  $\mu$  is the mean, and  $\sigma$  is the standard deviation.

A random sampling with an 80–20 split or a 70–30 split on a big and quality dataset is frequently employed for DL model training and testing. A random sampling with a 60–40 split on the small dataset was conducted in this research because there were only twenty-two “0” values in total in the dataset. This means that the data for training was chosen through a random sampling of 60% of cases or examples in the dataset, and the remaining cases or examples (40%) after the sampling were used for the test. Choosing an 80–20 split or a 70–30 split on the small dataset will lead to a small number of test data and a poor performance evaluation (e.g., an unideal accuracy (ACC) value).

There were only two classes (“Yes” and “No,” or “1” and “0”) in Table 1. One class can be treated as “positive” (its value = 1) while the other can be treated as ‘negative’ (its value = 0). True positive (TP), false positive (FP), true negative (TN), and false negative (FN) can be expressed as follows:<sup>11</sup>

TP: The number of positive instances that are correctly classified as positive.

FP: The number of negative instances that are incorrectly classified as positive.

TN: The number of negative instances that are correctly classified as negative.

FN: The number of positive instances that are incorrectly classified as negative.

**Table 1. Partial experimental data of laser powder bed fusion (selective laser melting)<sup>10</sup>**

No.	Power (W)	Speed (mm/s)	Hatch space (mm)	Lack of fusion
1	200	1000	0.06	Yes (1)
2	200	1800	0.12	Yes (1)
3	240	2200	0.03	Yes (1)
4	240	1800	0.15	Yes (1)
5	270	1700	0.05	Yes (1)
6	270	1800	0.07	Yes (1)
7	280	2200	0.06	Yes (1)
8	280	600	0.09	Yes (1)
9	280	1000	0.12	Yes (1)
10	290	1800	0.05	Yes (1)
11	290	1900	0.06	Yes (1)
12	320	1400	0.03	Yes (1)
13	320	1800	0.06	Yes (1)
14	360	1000	0.03	Yes (1)
15	360	2200	0.12	Yes (1)
16	200	600	0.03	No (0)
17	240	1000	0.09	No (0)
18	270	1900	0.06	No (0)
19	270	1700	0.07	No (0)
20	280	1900	0.05	No (0)
21	280	1800	0.07	No (0)
22	290	1900	0.05	No (0)
23	290	1700	0.06	No (0)
24	290	1700	0.07	No (0)
25	320	600	0.12	No (0)
26	320	1000	0.15	No (0)

The ACC, false positive rate (FPR), and false negative rate (FNR) are utilized as measures for the classification and the performance of DL models in this paper. They can be calculated as follows.<sup>12-14</sup>

$$ACC = (TP + TN)/(TP + FP + TN + FN) \quad (I)$$

$$FPR = (FP)/(FP + TN) \quad (II)$$

$$FNR = (FN)/(FN + TP) \quad (III)$$

The value of  $(TP + FP + TN + FN)$  is equal to the total number of instances in the testing data of the dataset.

Traditional ML methods (e.g., traditional ANN) have been used to predict the LOF defect. The results were not satisfying, which is the expected situation due to the dataset characteristics (small and unbalanced, see Table 1). Generally, this kind of data is also inappropriate for DL and the DL model creation. However, DL is generally more

powerful (e.g., in handling complex data) than traditional ML methods. The objective of this research is to explore DL models on a small experimental dataset with unbalanced data, predict the LOF defect using the created DL models, and improve the modeling and prediction performance (according to the ACC, FPR, and FNR).

## 4. DL methods

### 4.1. The Elman neural network and the Jordan neural network

Both the Elman neural network and the Jordan neural network are recurrent neural networks (RNNs). There are one or more context layers in the Elman neural network, and the number of neurons in the context layer is the same as the number of neurons in the hidden layer. In addition, the context layer neurons are completely connected to all the neurons in the hidden layer. The Jordan neural network is similar to the Elman neural network. The only difference is that the context neurons in the Jordan neural network are fed from the output layer instead of the hidden layer.<sup>15</sup> The Elman neural network and the Jordan neural network are expressed as follows:<sup>16,17</sup>

$$h_t = \sigma_h(W_h x_t + U_h h_{t-1} + b_h) \quad \text{for the Elman neural network} \quad (IV)$$

$$h_t = \sigma_h(W_h x_t + U_h y_{t-1} + b_h) \quad \text{for the Jordan neural network} \quad (V)$$

$$y_t = \sigma_y(W_y h_t + b_y) \quad (VI)$$

where  $x_t$  is the input vector, and the input vector  $V = (V_1, V_2, \dots, V_p)$  in this paper;  $h_t$  is the hidden layer vector; and  $y_t$  is the output vector.  $W$ ,  $U$ , and  $b$  are the parameter matrices and vectors.  $\sigma_h$  and  $\sigma_y$  are the activation functions.

### 4.2. The deep neural network (DNN) with weights initialized by the DBN

The DNN with weights initialized by the DBN means the DNN with the initial values of its weights that are set employing learned features from a pre-trained DBN. This technique is called DNN-DBN in this paper. DBN is a composition of restricted Boltzmann machines (RBMs). The procedures of the DNN with weights initialized by the DBN are: (1) training a DBN, (2) extracting the learned weights after the training of the DBN is completed, (3) initializing the DNN, and (4) performing “fine-tune” with supervised learning.<sup>18</sup>

DBN is employed to determine the weights, biases, and other parameters of the initial DNN. This technique does better than the only DNN-used technique in most situations.<sup>19</sup> The training technique for the RBMs is named

contrastive divergence.<sup>20</sup> Pre-training and fine-tuning are implemented while training a DBN. The following is specific information regarding the methodology and related algorithms.<sup>21,22</sup> The network energy is expressed as  $E(v, h)$ .

Let  $p(v)$  be the probability of a visible vector, and it is described as follows:

$$p(v) = \frac{1}{Z} \sum_h e^{-E(v, h)} \quad (\text{VII})$$

where  $Z = \sum \exp(-E(v, h))$  is the partition function.

To train an RBM, weights are updated as follows:

$$w_{ij}(t+1) = w_{ij}(t) + \eta \cdot \frac{\partial \log(p(v))}{\partial w_{ij}} \quad (\text{VIII})$$

### 4.3. Regular DNNs

In the DNN learning,<sup>23,24</sup> each training tuple can be handled in two steps:<sup>23</sup> Propagating inputs forward and backpropagating the error. For an input vector  $V = (V_1, V_2, \dots, V_p)$ , each hidden layer transforms its inputs from the layer to the next layer by applying an affine transform and a nonlinear mapping as follows:

$$z^{(1)} = V \quad (\text{IX})$$

$$y_j^{(l)} = \sum_{i=1}^{N^{(l)}} w_{ij}^{(l)} z_i^{(l-1)} + \theta_j^{(l)} \quad (l = 2, 3, \dots, L) \quad (\text{X})$$

$$z_j^{(l)} = f(y_j^{(l)}) \quad (\text{XI})$$

where  $L$  is the number of layers;  $N^{(l)}$ ,  $\theta_j^{(l)}$ , and  $w_{ij}^{(l)}$  are the number of nodes in the  $l^{\text{th}}$  layer, the bias of the node  $j$  in the  $l^{\text{th}}$  layer, and the weight of the connection from node  $i$  in the previous layer to node  $j$  of the  $l^{\text{th}}$  layer, respectively; and  $f$  is the activation function (nonlinear).

In this paper, the Elman neural network, the Jordan neural networks, the DNN with weights initialized by the DBN, and regular DNN based on various algorithms were employed to establish DL models and implement the prediction of the LOF of LPBF because all of the DL methods achieved good *ACC*, *FNR*, and *FPR* when large and quality databases such as “spambase” (<https://archive.ics.uci.edu/ml/datasets/Spambase>) were employed in the author’s past research work.

Four algorithms, “rprop+”, “rprop-”, “sag,” and “slr,” were used in this paper. “rprop+” and “rprop-” refer to the resilient back-propagation with and without weight backtracking, respectively. “sag” and “slr” induce the usage of the modified globally convergent algorithm globally

resilient backpropagation (grprop), adjusting the learning rate associated with the sag or the slr.

The calculation of *ACC*, *FPR*, and *FNR* (Equations I, II, and III) in this paper is based on the confusion matrix and the components in the matrix. The confusion matrix (*CM*) is given as follows:

$$CM = \begin{pmatrix} TN & FP \\ FN & TP \end{pmatrix} \quad (\text{XII})$$

## 5. Results and discussion

### 5.1. Results of the Elman neural network and the Jordan neural network

Both the Elman neural network and the Jordan neural network are RNNs. An Elman neural network can be thought of as a model that is constantly unfolding as a sequence of predictors. A Jordan neural network uses a context layer to process sequential data.<sup>15</sup> The dataset (Table 1) used in this paper is experimental data that can be regarded as a sequential dataset over time.

Tables 2 and 3 show part of the results of the Elman neural network and the Jordan neural network after min-max normalization and z-score standardization on the dataset, respectively. It was shown that both the Elman and Jordan neural networks did not work well in establishing DL models on a small dataset (with unbalanced data) and predicting the LOF of the LPBF. Most of the *ACC* values were low, and most of the *FPR* values, as well as most of the *FNR* values, were high or somewhat high. The reason is the small dataset and the unbalanced data in the dataset. The structures of context layers show the number of nodes in the context layers. For instance, c(8) indicates that eight nodes are in the context layer.

### 5.2. Results of the DNN with weights initialized by the DBN

Tables 4 and 5 list part of the results of the DNN with weights initialized by the DBN after min-max normalization and z-score standardization are employed, respectively. It was shown that DNN-DBN did not work well in establishing DL models on a small dataset (with unbalanced data) and predicting the LOF of LPBF. There are the input layer, the output layer, and two or three hidden layers in this technique. The performance (according to the *ACC*, *FPR*, and *FNR*) of the established DL models was not good due to the small dataset and the unbalanced data in the dataset. The structures of hidden layers indicate the number of nodes in the hidden layers. For instance, c(8, 6, 4) indicates that there are three hidden layers, and the number of nodes

**Table 2. Data analytics based on the Elman neural network and the Jordan neural network after data normalization (min-max normalization)**

Algorithms or methods	Structures (context layers)	FPR (%)	FNR (%)	ACC (%)
Elman	c(3)	25.00	38.46	66.67
	c(8)	100.00	15.38	52.38
Jordan	c(3)	37.50	46.15	57.14
	c(8)	37.50	30.77	66.67
	c(12)	62.50	30.77	57.14

Abbreviations: ACC: Accuracy; FNR: False negative rate; FPR: False positive rate.

**Table 3. Data analytics based on the Elman neural network and the Jordan neural network after z-score standardization**

Algorithms or methods	Structures (context layers)	FPR (%)	FNR (%)	ACC (%)
Elman	c(3)	25.00	38.46	66.67
	c(8)	87.50	15.38	57.14
Jordan	c(3)	37.50	46.15	57.14
	c(8)	87.50	15.38	57.14
	c(12)	50.00	23.08	66.67

Abbreviations: ACC: Accuracy; FNR: False negative rate; FPR: False positive rate.

**Table 4. Data analytics based on the DNN-DBN after data normalization (min-max normalization)**

Algorithms or methods	Structures (hidden layers)	FPR (%)	FNR (%)	ACC (%)
DNN-DBN	c(10, 4)	n/a	n/a	n/a
	c(12, 6)	n/a	n/a	n/a
	c(8, 6, 4)	n/a	n/a	n/a

Abbreviations: ACC: Accuracy; DBN: Deep belief network; DNN: Deep neural network; FNR: False negative rate; FPR: False positive rate.

**Table 5. Data analytics based on the DNN-DBN after z-score standardization**

Algorithms or methods	Structures (hidden layers)	FPR (%)	FNR (%)	ACC (%)
DNN-DBN	c(10, 4)	62.50	38.46	52.38
	c(12, 6)	62.50	38.46	52.38
	c(8, 6, 4)	50.00	46.15	52.38

Abbreviations: ACC: Accuracy; DBN: Deep belief network; DNN: Deep neural network; FNR: False negative rate; FPR: False positive rate.

in the three hidden layers is 8, 6, and 4, respectively. In [Table 4](#), n/a means that no normal result is obtained after the min-max normalization is applied, and structure c(10, 4), c(12, 6), or c(8, 6, 4) is utilized.

### 5.3. Results of the regular DNN

Part of the results of the regular DNN established on the small dataset with unbalanced data of the LPBF are listed in [Table 6](#) (after min-max normalization) and [Table 7](#) (after z-score standardization). [Table 6](#) shows that the regular DNN after min-max normalization can obtain better results than the DNN-DBN. After z-score standardization

was employed, the regular DNN could achieve the best results among the DL methods if a suitable algorithm was used. Most of the relevant *FPR* and *FNR* values are much lower than those of the three DL methods (Elman, Jordan, and DNN-DBN). Data analytics based on traditional ANN was also conducted, and the results are shown in [Table 8](#) for comparison with the results of various DL methods. It was demonstrated that some DL methods, such as Elman, Jordan, and DNN-DBN, might obtain worse results than traditional ANN due to insufficient training and test data if a small dataset was used.

**Table 6. Data analytics based on the regular DNN after data normalization (min-max normalization)**

Structures (hidden layers)	Algorithms	FPR (%)	FNR (%)	ACC (%)
c(8, 4)	rprop-	25.00	46.15	61.90
c(8, 5)	rprop-	12.50	53.85	61.90
c(8, 6, 3)	rprop+ or sag	12.50	53.85	61.90

Abbreviations: ACC: Accuracy; DNN: Deep neural network; FNR: False negative rate; FPR: False positive rate

**Table 7. Data analytics based on the regular DNN after z-score standardization**

Structures (hidden layers)	Algorithms	FPR (%)	FNR (%)	ACC (%)
c(7, 4)	slr	25.00	15.38	80.95
c(8, 4)	slr	37.50	7.69	80.95
c(8, 5)	rprop+	12.50	23.08	80.95
c(8, 6)	rprop-	25.00	23.08	76.19
c(8, 6, 3)	rprop- or sag	0.00	61.54	61.90

Abbreviations: ACC: Accuracy; DNN: Deep neural network; FNR: False negative rate; FPR: False positive rate; slr: Smallest learning rate.

**Table 8. Data analytics based on traditional ANN**

Data pre-processing	Structures (number of nodes in the hidden layer)	FPR (%)	FNR (%)	ACC (%)
Min-max normalization	c(6)	0.00	53.85	66.67
	c(10)	12.50	53.85	61.90
	c(14)	0.00	53.85	66.67
z-score standardization	c(6)	75.00	69.23	28.57
	c(10)	12.50	38.46	71.43
	c(14)	25.00	53.85	57.14

Abbreviations: ACC: Accuracy; ANN: Artificial neural network; FNR: False negative rate; FPR: False positive rate.

## 6. Conclusion and future research

Data analytics based on four DL techniques (the Elman neural network, the Jordan neural network, the DNN-DBN, and regular DNN based on the four algorithms (“rprop+”, “rprop-“, “sag”, and “slr”) were conducted on a small dataset with unbalanced data of the LPBF. After z-score standardization was employed, the regular DNN could obtain a better ACC than the three other DL techniques (Elman, Jordan, and the DNN-DBN), while most of the relevant FPR and FNR values were much lower than those of the three DL techniques. Future research should consider DL-based data analytics and defect prediction of other defects (e.g., keyholes and cracks) while considering the material properties of LPBF. This will improve the DL model’s applicability and enable a more comprehensive defect classification in LPBF processes. DL-based data analytics on more AM datasets (small or big) and the prediction of related defects are also directions for future work.

## Acknowledgments

The author thanks the support from Mississippi State University, Mississippi, USA.

## Funding

None.

## Conflict of interest

The author declares no conflicts of interest.

## Author contributions

This is a single-authored article.

## Ethics approval and consent to participate

Not applicable.

## Consent for publication

Not applicable.

## Availability of data

The dataset in this paper is available from the author of reference<sup>10</sup> upon appropriate request.

## References

- Raihan AS, Harper A, Era IZ, *et al.* A data-efficient sequential learning framework for melt pool defect classification in laser powder bed fusion. *J Manuf Processes*. 2025;145:201-210.  
doi: 10.1016/j.jmapro.2025.03.118
- Ni C, Zhu J, Zhang B, *et al.* Recent advance in laser powder bed fusion of Ti-6Al-4V alloys: Microstructure, mechanical properties and machinability. *Virtual Phys Prototyp*. 2025;20(1):e2446952.  
doi: 10.1080/17452759.2024.2446952
- Nabavi SF, Dalir H, Farshidianfar A. A comprehensive review of recent advances in laser powder bed fusion characteristics modeling: Metallurgical and defects. *Int J Adv Manuf Technol*. 2024;132(5):2233-2269.  
doi: 10.1007/s00170-024-13491-1
- Ero O, Taherkhani K, Hemmati Y, Toyserkani E. An integrated fuzzy logic and machine learning platform for porosity detection using optical tomography imaging during laser powder bed fusion. *Int J Extrem Manuf*. 2024;6(6):065601.  
doi: 10.1088/2631-7990/ad65cd
- Gu Z, Mani Krishna KV, Parsazadeh M, *et al.* Deep learning-based melt pool and porosity detection in components fabricated by laser powder bed fusion. *Prog Addit Manuf*. 2025;10(1):53-70.  
doi: 10.1007/s40964-024-00603-2
- Zhao J, Yang Z, Chen Q, *et al.* Real-time detection of powder bed defects in laser powder bed fusion using deep learning on 3D point clouds. *Virtual Phys Prototyp*. 2025;20(1):e2449171.  
doi: 10.1080/17452759.2024.2449171
- Pouyanfar S, Sadiq S, Yan Y, *et al.* A survey on deep learning: Algorithms, techniques, and applications. *ACM Comput Surv (CSUR)*. 2018;51(5):1-36.  
doi: 10.1145/3234150
- Narasimharaju SR, Zeng W, See TL, Zhu Z, Scott P, Jiang X, Lou S. A comprehensive review on laser powder bed fusion of steels: Processing, microstructure, defects and control methods, mechanical properties, current challenges and future trends. *J Manuf Processes*. 2022;75:375-414.  
doi: 10.1016/j.jmapro.2021.12.033
- Ganta MG, Kurek M. Influence of post-processing methods on the fatigue performance of materials produced by selective laser melting (SLM). *Int J Adv Manuf Technol*. 2025;9:1-32.  
doi: 10.1007/s00170-024-14920-x
- Wang GW. *Microstructure and Mechanical Properties of Oxide Dispersion Strengthened Nickel-Based Superalloys by Laser Additive Manufacturing*. [Dissertation, Zhongnan University, China]; 2023. Available from: <https://www.cnki.net> [Last accessed on 2025 May 28].
- Bramer M. *Data for Data Mining. Principles of Data Mining*. London: Springer; 2016. p. 9-19.  
doi: 10.1007/978-1-4471-7307-6
- Alabdulwahab S, Moon B. Feature selection methods simultaneously improve the detection accuracy and model building time of machine learning classifiers. *Symmetry*. 2020;12(9):1424.  
doi: 10.3390/sym12091424
- Maseer ZK, Yusof R, Bahaman N, Mostafa SA, Foozy CF. Benchmarking of machine learning for anomaly based intrusion detection systems in the CICIDS2017 dataset. *IEEE Access*. 2021;9:22351-22370.  
doi: 10.1109/ACCESS.2021.3056614
- Mohammed JZ, Wagner M. *Data Mining and Analysis: Fundamental Concepts and Algorithms*. Cambridge: Cambridge University Press; 2014.
- Lewis ND. *Deep Learning Made Easy with R. A Gentle Introduction for Data Science*. South Carolina: CreateSpace Independent Publishing Platform; 2016.
- Elman JL. Finding structure in time. *Cogn Sci*. 1990;14(2):179-211.  
doi: 10.1207/s15516709cog1402\_1
- Jordan MI. Serial order: A parallel distributed processing approach. *Adv Psychol*. 1997;121:471-495.
- Jang H, Plis SM, Calhoun VD, Lee JH. Task-specific feature extraction and classification of fMRI volumes using a deep neural network initialized with a deep belief network: Evaluation using sensorimotor tasks. *Neuroimage*. 2017;145:314-328.  
doi: 10.1016/j.neuroimage.2016.04.003
- Ghasemi F, Mehridehnavi A, Fassihi A, Pérez-Sánchez H. Deep neural network in QSAR studies using deep belief network. *Appl Soft Comput*. 2018;62:251-258.  
doi: 10.1016/j.asoc.2017.09.040
- Hinton GE. Training products of experts by minimizing contrastive divergence. *Neural Comput*. 2002;14:1771-800.  
doi: 10.1162/089976602760128018
- Hinton G. A practical guide to training restricted Boltzmann

- machines. *Momentum*. 2010;9(1):926.
22. Fischer A, Igel C. Training restricted Boltzmann machines: An introduction. *Pattern Recognit*. 2014;47(1):25-39.  
doi: 10.1016/j.patcog.2013.05.025
23. Hann J, Pei J, Kamber M. *Data Mining: Concepts and Techniques*. Netherlands: Elsevier; 2011.
24. Chung H, Lee SJ, Park JG. Deep Neural Network using Trainable Activation Functions. In: *2016 International Joint Conference on Neural Networks (IJCNN)*. IEEE; 2016. p. 348-352.  
doi: 10.1109/IJCNN.2016.7727219

## Appendix

**Table A1. Acronyms**

AM	Additive manufacturing
ANN	Artificial neural network
ACC	Accuracy
CD	Contrastive divergence
CNN	Convolutional neural network
CT	Computed tomography
DBN	Deep belief network
DED	Directed energy deposition
DL	Deep learning
DNN	Deep neural network
DOE	Design of experiments
FN	False negative
FNR	False negative rate
FP	False positive
FPR	False positive rate
LOF	Lack of fusion
LPBF	Laser powder bed fusion
ML	Machine learning
MPC	Model predictive control
RBM	Restricted Boltzmann machine
RNNs	Recurrent neural networks
SLM	Selective laser melting
TN	True negative
TP	True positive

## ORIGINAL RESEARCH ARTICLE

# Automated fruit sorting system integrating image processing and support vector machine techniques

**Babatunde Olayinka Oyefeso<sup>1</sup>**, **Oluwaseun Emmanuel Oyewande<sup>1</sup>**,  
**and John Audu<sup>2\*</sup>**

<sup>1</sup>Department of Agricultural and Environmental Engineering, Faculty of Technology, University of Ibadan, Ibadan, Oyo State, Nigeria

<sup>2</sup>Department of Agricultural and Bio-systems Engineering, College of Engineering, Joseph Sarwuan Tarka, University Makurdi, Benue State, Nigeria

## Abstract

Traditional fruit grading methods are mostly time-consuming and subjective, thereby limiting efficiency in the agricultural sector. To address these problems, this paper presents the design and implementation of an automated fruit sorting system for classifying certain fruits, namely oranges, tomatoes, and mangoes, using image processing and support vector machine (SVM) techniques. An ESP32 camera was used to capture images of the fruits, which were later passed through algorithms in Python. Extracted features were then fed into a SVM model for the classification process of fruits. The model demonstrated excellent performance, achieving an accuracy of 100%, a precision of 96%, a recall of 92%, and an F1 score of 89%. The results indicated that incorporating multiple features significantly increases the accuracy of the classification. Moreover, the performance was optimized by selecting an appropriate regularization parameter during the training of the model and the use of polynomial kernel functions. Finally, the whole automated system was assembled to physically sort the classified fruits into different containers. This research highlights the potential of integrating image processing and machine learning technologies to revolutionize fruit classification processes, thereby improving both efficiency and quality control in agriculture.

**Keywords:** Image processing; Fruit classification; Support vector machine; Automated sorting; Feature extraction

### \*Corresponding author:

John Audu  
 (audu.john@uam.edu.ng)

**Citation:** Oyefeso BO, Oyewande OE, Audu J. Automated fruit sorting system integrating image processing and support vector machine techniques. *Int J AI Mater Design*. 2025;2(2):79-90. doi: 10.36922/IJAMD025150011

**Received:** April 8, 2025

**1st revised:** May 9, 2025

**2nd revised:** May 14, 2025

**3rd revised:** May 18, 2025

**Accepted:** May 22, 2025

**Published online:** June 20, 2025

**Copyright:** © 2025 Author(s). This is an Open-Access article distributed under the terms of the Creative Commons Attribution License, permitting distribution, and reproduction in any medium, provided the original work is properly cited.

**Publisher's Note:** AccScience Publishing remains neutral with regard to jurisdictional claims in published maps and institutional affiliations.

## 1. Introduction

Fruit image classification techniques are continually being developed due to their vital roles in agriculture and food analysis within the food industry. In the agricultural and food industries, imaging technology streamlines operations by enhancing quality control and optimizing the process. Mango production in Nigeria, the ninth most produced fruit globally, is hindered by several challenges resulting from outdated technology.<sup>1-9</sup>

It was reported in previous studies that the existing methods for manual classification of fruits are somewhat inefficient, ineffective, slow, and prone to bias.<sup>10-13</sup> Developments in image analysis have provided an efficient, reliable, and accurate system of fruit

categorization without causing much harm to the fruits.<sup>14-17</sup> In contrast, manual sorting of fruits by professional personnel undergoes physical handling, thus potentially damaging the fruits and affecting their value.<sup>18-21</sup> This research focuses on creating an image processing system for the classification of fruits through machine learning to enhance precision and productivity in the agriculture business as well as the food chain. Similar approaches utilizing image processing and machine learning to detect mangoes, tomatoes, and oranges were also performed by other researchers. Image processing methods and machine learning algorithms have been widely used to classify mangoes, tomatoes, and oranges, achieving classification accuracies ranging from 80% to 100% across these fruit types.<sup>22-37</sup> Research on fruit classification using image processing and machine learning is constrained due to its focus on single fruit type, small datasets, inconsistent image acquisition methods, and the lack of deep learning approaches. Future investigations should prioritize standardized data collection and the application of deep learning algorithms.

The proposed fruit classification system leverages image processing to achieve maximum accuracy and minimal time expenditure. It is trained on a large database comprising mangoes, tomatoes, and oranges. Such a classification system has significant potential to enhance the quality of both the agricultural sector and the food industry by monitoring product quality, minimizing wastage, and adding value to the product. Furthermore, it can be integrated into other automated systems and mobile applications.

The novel integration of real-time image processing with real-time mechanical fruit sorting, powered by artificial intelligence machine learning optimization techniques using Python programming, represents the novelty of this study.

## **2. Materials and methods**

### **2.1. Image processing system to process fruit images**

Four steps were included in developing the image processing system to classify fruits (mango, oranges, and tomatoes): Image acquisition, pre-processing, feature extraction, and feature selection. Each step played a key role in ensuring the accuracy and effectiveness of the classification system.

#### **2.1.1. Image acquisition**

This step was crucial to capture high-quality images of the fruits, which we needed for later analysis. Crucial factors to consider during image acquisition included:

- (i) Lighting conditions: Good lighting was vital in showing the visual traits of the fruits. An ESP32 camera provided the best lighting and clarity.
- (ii) Camera specifications: The camera's resolution and color accuracy had a big impact on image quality. We fine-tuned these factors to ensure the fruits' features were displayed accurately.

#### **2.1.2. Pre-processing**

Pre-processing prepared the captured images for feature extraction by enhancing important properties and reducing noise. The methods used include:

- (i) Resizing: The system resized all images to uniform dimensions while preserving their aspect ratio. This step was essential to ensure consistency across datasets and to enhance computational efficiency.
- (ii) Histogram equalization: This technique enhanced image contrast by spreading out pixel intensity values. It standardized the appearance of images, making key features more distinguishable during the later processing stage.
- (iii) Thresholding: Thresholding splits pixels into object and background areas based on a predefined value. It effectively isolated the fruit from the background and reduced noise, thereby improving feature extraction.

#### **2.1.3. Feature extraction**

At this point, the system extracted various features from the pre-processed images. These features included color, shape, texture, and size, which were essential in differentiating fruits.

#### **2.1.4. Feature selection**

After the features were extracted, the system evaluated the significance of each feature. The features that varied widely between fruit types were retained, while those with insignificant variation were excluded. This step enhanced the sorting system by focusing on the most distinctive features, which resulted in better accuracy and reduced computational work.

### **2.2. Support vector machine (SVM) model to classify fruit images**

The SVM model helped classify fruits by their appearances. This part explained the key steps in building the SVM model, which included standardizing the features, training the model, and applying different kernel functions.

#### **2.2.1. Standardizing the features**

Standardizing the features was a key step before starting the modeling process. It ensured that all the features selected for model creation contributed to the fruit-sorting process. In this study, normalization was used to scale all

feature values into the same range. This prevents any single feature from having too much influence over the model's performance.

### 2.2.2. Training the model

To train the model, the system splits the entire dataset into two parts: One for training and one for testing. It used 70% of the data in training the model and kept the other 30% to test the training efficiency. Then, the SVM model was trained using the selected features. The study also used kernel functions to transform the feature space, which helped the model capture non-linear relationships.

### 2.2.3. Kernel functions

Kernel functions play a crucial role in SVMs as they allow data to be transformed into higher dimensional spaces, where it can be linearly separable. The following kernel functions were implemented:

#### (i) Linear kernel

If the relationship between features was linearly separable, then the linear kernel was utilized. It is defined in Equation I<sup>38</sup>:

$$K(x, y) = x^T y \tag{I}$$

Where  $x$  and  $y$  are input feature vectors and  $x^T y$  represents the dot product of the transpose of  $x$  and  $y$ .

#### (ii) Polynomial kernel

The polynomial kernel enabled the SVM to handle non-linear relationships between features. It mapped the input data into a higher-dimensional feature space using polynomial functions, allowing SVM to learn more complex decision boundaries. The polynomial kernel is defined in Equation II<sup>39</sup>:

$$K(x, y) = (\gamma \times (x^T y) + r)^d \tag{II}$$

Where  $\gamma$  is the scaling factor,  $r$  is a constant, and  $d$  is the degree of polynomial.

#### (iii) Radial basis function (RBF) kernel

The RBF kernel was used to capture non-linear relationships in the data. It assigned lower weights to more distant points and higher weights to closer points, allowing the SVM to identify local patterns effectively. The RBF is defined in Equation III<sup>40</sup>:

$$K(x, y) = e^{(-\gamma \cdot \|x - y\|^2)} \tag{III}$$

Where  $\gamma$  is a constant,  $e$  is the base of the natural logarithm, and  $\|x - y\|^2$  is the Euclidean distance between  $x$  and  $y$ .

This is an established method of SVM model development, which ensures accuracy and efficacy in fruit classification using different kernel functions.

## 2.3. Comparison of kernel functions

The different kernel functions were benchmarked against each other based on their performance in efficiently classifying the fruits. This evaluation utilized several performance metrics, including accuracy, precision, recall, and F1 score, all derived from confusion matrix analyses.

### 2.3.1. Confusion matrix method

One of the most effective approaches for evaluating the performance of the trained classification model is the confusion matrix. In this study, the confusion matrix provided the number of correct and incorrect classifications among the three fruit classes: tomato, mango, and orange. A standard confusion matrix table is presented in Figure 1.

#### (i) Model accuracy

Model accuracy measured the proportion of correct predictions made by the classifier. It was calculated based on a ratio of total true predictions to the total prediction value, which provided a simple sense of the model's performance as indicated in Equation IV.<sup>41</sup>

$$\text{Accuracy} = \frac{TP + TN}{TP + TN + FP + FN} \tag{IV}$$

Where TP is true positive, TN is true negative, FP is false positive, and FN is false negative.

#### (ii) Model precision

Model precision measured the accuracy of positive predictions. In this study, it referred to the proportion of predicted positive instances that were actually positive. This provided insight into the reliability of the model in making positive classification, as shown in Equation V.<sup>42</sup>

$$\text{Precision} = \frac{TP}{TP + FP} \tag{V}$$

#### (iii) Model recall score

Model recall, also known as sensitivity, was used to evaluate the model's ability to correctly identify

		Predicted	
		Positive	Negative
Actual	Positive	True positive	False negative
	Negative	False positive	True negative

Figure 1. A typical confusion matrix table used to evaluate classification performance

positive instances. It indicated how many actual positive observations were correctly identified among all the true positives, thereby showing the model's effectiveness in capturing relevant cases, as shown in Equation VI.<sup>43</sup>

$$\text{Recall} = \frac{\text{TP}}{\text{TP} + \text{FN}} \quad (\text{VI})$$

(iv) Model F1 score

The F1 score is the harmonic mean of precision and recall, providing a balanced metric that considers both aspects. It was particularly useful for evaluating model performance on imbalanced datasets, as it offered a better overview than individual metrics. The F1 score was calculated using Equation VII.<sup>44</sup>

$$\text{F1} = \frac{2}{\frac{1}{\text{Precision}} + \frac{1}{\text{Recall}}} = \frac{2 \times (\text{Precision} \times \text{Recall})}{(\text{Precision} + \text{Recall})} \quad (\text{VII})$$

In such a structured approach, the performance metrics of different kernels were compared directly to identify the most effective kernel for fruit classification.

## 2.4. Model Optimization

It was essential to optimize a model for its performance and accuracy toward fruit classification. The techniques applied in model development were also used to tune the model, with a focus on the regularization parameter (C).

The C value controlled the trade-off between minimizing training error and testing error.

- (i) Impact of the value of C: A lower C value applied stronger regularization by shrinking the coefficients less aggressively, allowing a larger margin of error, which may result in higher misclassification rates. On the other hand, a higher C value reduced the error margin, thereby lowering misclassification rates.
- (ii) Optimal C by cross-validation: Cross-validation was utilized to identify the optimal value of C. This involved testing various C values using the model to determine which value achieved the best classification performance while avoiding overfitting.

## 2.5. Automated image sorting mechanism

The automated sorting mechanism played a crucial role in the fruit classification system. It physically sorted the classified fruits into their respective containers based on the output classifications identified by the SVM model. The system was designed to ensure efficient and accurate sorting of the fruits.

The process began by placing fruits on a slanting plane that acted as a conveyor. As the fruits rolled down

the inclined plane, images were captured by a camera for classification according to their classes, as implemented by the SVM model. The camera used was an ESP32-cam (Espressif Systems, China), controlled by the Arduino Uno R3 (Microchip, United States), with the entire setup powered by a 9 V battery. The captured images were transmitted to the processing unit for classification using the trained SVM model.

Based on the classification results, the Arduino board (Arduino, Italy) sent commands to three servo motors (MG996r, TowerPro, China). These motors controlled a mechanical arm responsible for guiding the fruits into different containers. Once the fruits reached the end of the inclined plane, the servo motors activated the mechanical arms to direct the fruits into their respective containers. Collection containers were placed at the base of the inclined plane to collect the sorted fruits.

In this project, an efficient and accurate automated sorting mechanism was developed. Figure 2A shows the conceptual drawing of the mechanism, Figure 2B shows the side view, and Figure 2C shows the front view of the mechanism, clearly depicting the system components and their arrangement. Figure 3 displays the complete experimental setup for the system, while Figure 4 illustrates the overall framework for the automated fruit sorting process.

This setup incorporated an automated sorting mechanism integrated into the Arduino board, which controlled the classification results from the SVM model and ensured efficient and accurate sorting of fruits into their respective containers. The system was specifically designed to handle the fruits with the least damage, thereby maintaining the quality of the fruits during the sorting process. All program codes that automated this system were displayed in Programs S1–S6 (in Supplementary File).

## 3. Results and discussion

### 3.1. Experimental results for model detection of fruit image features

Table 1 shows the results of the fruit classification system. The results highlight key differences in the efficacy of various features used in the image processing approach. This was evident in the performance metrics, including accuracy, precision, recall, and F1 score, all of which demonstrated that feature selection significantly impacts the overall results of classification.

One of the important metrics is accuracy, which represents the proportion of correct predictions made by the classifier. The accuracy obtained in this study was 90% with combined features. The result demonstrates

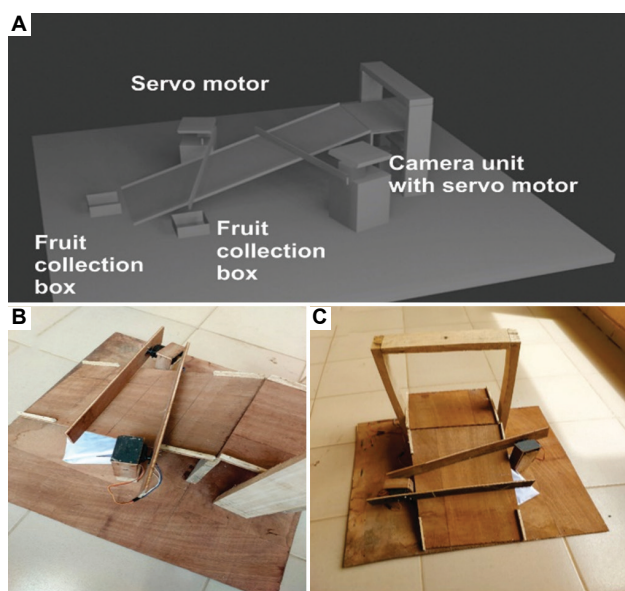


Figure 2. Automated fruit sorting system developed in this study. (A) The conceptual drawing of the system. (B) The fabricated side view of the system. (C) The fabricated front view of the system. Image produced by the authors.

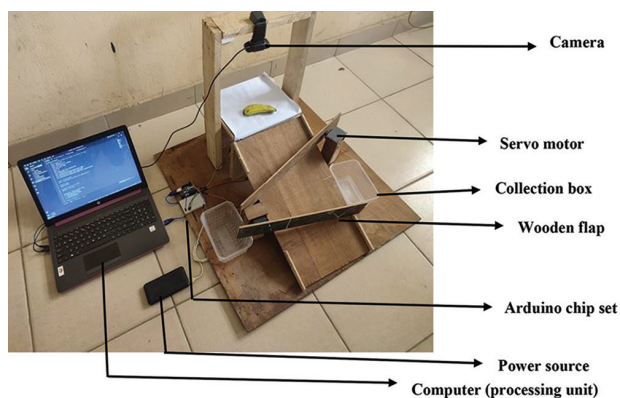


Figure 3. Complete experimental setup of the system. Image produced by the authors.

that combined features provide more comprehensive information about the fruit characteristics, leading to improved prediction outcomes.

The results were also favorable in terms of precision, which measures the accuracy of positive predictions. In this study, the model achieved a precision score of 88%, indicating high reliability in its positive classifications. The accuracy is particularly important in agricultural applications, where precise identification of fruit types can significantly influence sorting efficiency and marketing decisions.

Recall (or sensitivity) measures the effectiveness of a model in identifying relevant instances. In this study, using

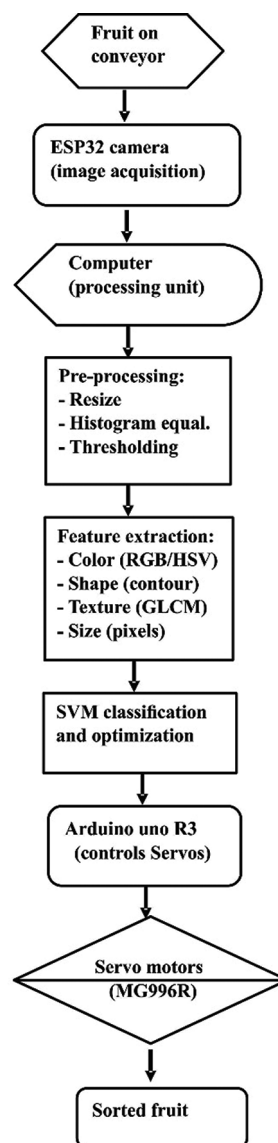


Figure 4. An overall framework of the method for the automated fruit sorting system. Abbreviation: SVM: Support vector machine.

Table 1. Summary of the experimental results for fruit classification models based on image features

Feature	Accuracy (%)	Precision (%)	F1 score (%)
Color feature	85.0	82.0	81.0
Shape feature	78.0	75.0	72.5
Texture feature	80.0	78.0	76.5
Size feature	76.0	74.0	73.0
Combined features	90.0	88.0	86.5

combined features, the model achieved a maximum recall score of 85%, efficiently capturing most of the true positive cases. This measure is important in ensuring that no fruit

is left unclassified by the system, thereby maximizing the efficiency of the sorting process.

The F1 score balances the measure between precision and recall, further underscores the performance of a model. Using combined features, an F1 score of 86.5% was observed, demonstrating an effective balance between precision and recall. This result highlights the robustness of the classification framework and its suitability for reliable fruit sorting.

In summary, the results show that the fruit classification system performed significantly better when using a comprehensive set of features. The findings underscore the importance of effective feature selection in achieving high accuracy, precision, recall, and F1 scores, all of which contribute to a reliable and efficient automated fruit sorting mechanism.

### 3.2. Confusion matrix for fruit classification

The confusion matrix shown in Table 2 indicates the performance of the model across the three fruit classes: Tomato, mango, and orange. The entries along the main diagonal represent correct classifications, while the off-diagonal entries indicate misclassification.

For example, of the 100 actual tomato instances, the model correctly classified 85 of them as tomatoes, misclassifying 10 of them as mangoes and five of them as oranges. The average model accuracy was calculated to be 86.67%, which aligned well with the experimental results of 90% accuracy when using combined features.

The confusion matrix provides an overview of the model's performance and highlights potential areas for improvement. For example, a higher misclassification rate between tomatoes and mangoes immediately indicates that these two fruit classes are similar. Therefore, additional or more distinctive features might be required to enhance the model's ability to distinguish between them.

### 3.3. Effectiveness comparison of the selected features on image processing system accuracy

This study critically assessed the effectiveness of each feature in enhancing the accuracy of the image processing system in fruit classification. Figure 5 shows the impact of each feature on the performance metrics, including accuracy, precision, recall, and F1 score.

The classification accuracy for the model using different features is shown in Figure 5. It can be seen that combined features improve the model in classifying fruits with reasonable accuracy. Other influential features were color, shape, and texture, with color features showing the highest score. This aligns with a previous study by Chithra and

Table 2. Confusion matrix for fruit classification

Fruit type	Predicted tomato	Predicted mango	Predicted orange
Actual tomato	85	10	5
Actual mango	12	85	3
Actual orange	8	2	90

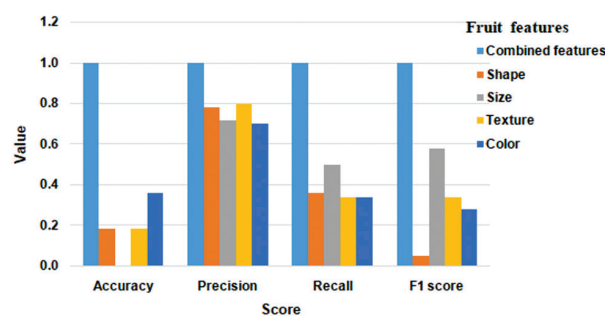


Figure 5. The score of each feature on the performance metrics

Henila,<sup>45</sup> which emphasized the necessity of changing the image format from Red, Green, and Blue to Hue, Saturation, and Intensity to acquire more quantifiable color values. In terms of precision scores, Figure 5 indicates that all features contribute positively to the model's precision score. However, the combination of features yields the highest precision score, confirming that the model is most reliable when using a combined feature set. Similarly, combined features resulted in the highest recall score, indicating the model's ability to capture the maximum proportion of true positive cases. This is particularly important in agricultural applications, where accurate identification of fruit types can directly impact sorting efficiency and marketing decisions. Finally, the combined features resulted in the best F1 score across all features, further reinforcing the conclusion that utilizing all available features significantly enhanced the overall performance of the classification system.

Hence, the comparison of selected features indicates that combined features improve the accuracy of this image-processing system. These findings further highlight the feature selection step in optimizing the performance of the fruit classification model to ultimately contribute to a reliable and efficient automated sorting mechanism.

### 3.4. Choice of the optimal regularization parameter value in SVM model

One of the most important steps to improve the performance of an SVM model for fruit classification is selecting an appropriate C value. This parameter controls the balance between minimizing training errors and testing errors. A smaller C value allows a greater margin

of error, which may lead to more misclassifications. In contrast, a higher C value reduces this margin, thereby reducing misclassification rates.

Figure 6 shows the performance scores for various C values. The results demonstrate that the optimal value of C is influenced by the numerical scale of the input feature values. For example, when feature values ranged from 0 to 100, a C value of 1 yielded strong model performance. In contrast, when the features were scaled between 100 and 1,000, optimal performance was achieved with much higher C values of 100.

This observation underlines the importance of tuning the C parameter in accordance with the scale of feature values. Through cross-validation, the study evaluated model performance across a range of C values to identify the optimal parameter that maximized the classification accuracy while minimizing the risk of overfitting. The results underscore that careful adjustment of the C value is a critical factor in optimizing the SVM model performance and improving accuracy in fruit classification.

This selection of optimum C value is a key part of the SVM training process. The results indicate that properly setting the C parameter with respect to the nature of the feature values is essential. It significantly enhances the efficiency of the image processing system used for fruit classification.

### 3.5. Comparative analysis of the accuracy of SVM owing to impacts of different kernels

The current research investigated whether significant differences exist in the performance of various kernel functions, aiming to identify the most effective kernel for SVM-based fruit classification. Figure 7 illustrates the accuracy scores for the SVM model using three kernel functions: Linear kernel, polynomial kernel, and RBF kernel.

These results clearly show that the accuracy of the model is highly dependent on the choice of the kernel function. Among them, the polynomial kernel achieved the highest accuracy score. This aligns with the fact that polynomial kernels are efficient in handling non-linear relationships within data, enabling the SVM to generate higher-order, non-linear decision boundaries. In contrast, while the linear kernel performs well on linearly separable data, it did not perform as effectively in this context. This outcome reflects the underlying complexity of the fruit classification task, where features can be non-linearly separable.

The RBF kernel also delivered strong performance, although slightly lower than that of the polynomial kernel. This may suggest that while the RBF kernel is effective in

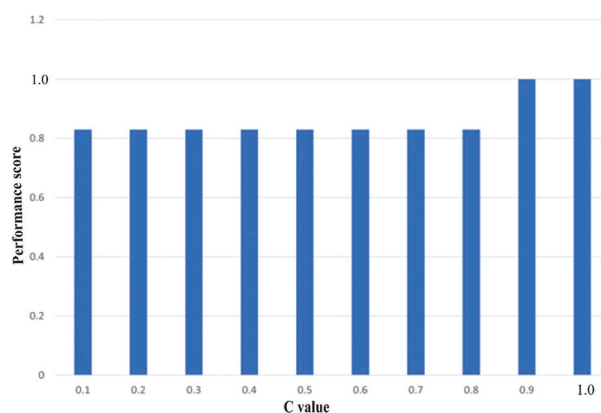


Figure 6. The score of the model across various C values

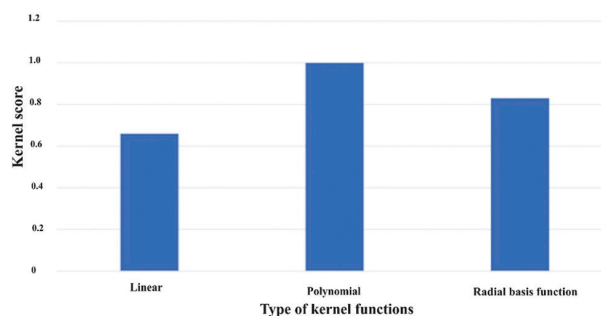


Figure 7. Effect of different kernels on the accuracy of the support vector machine model

capturing local patterns in the data, the polynomial kernel's strength in modeling non-linear relationships contributes to its superior accuracy.

The comparison underscores the importance of selecting a kernel function based on the specific nature of the data and classification task. The results support the conclusion that the polynomial kernel offers a significant advantage in improving accuracy for SVM-based fruit classification applications.

### 3.6. Hyperplanes constructed from the classification of selected fruits

A critical aspect of the SVM model's functionality lies in its ability to generate a classifying hyperplane to distinguish between fruit classes. Figures 8 and 9 illustrate examples using tomato, mango, and orange data to train the SVM model in generating hyperplanes for their classification.

Figure 8 shows a separating hyperplane in a two-dimensional feature space. This example demonstrates how the model distinguishes between fruit classes within a two-dimensional feature space. The hyperplane serves as a decision boundary, and the clear separation of classes suggests that the

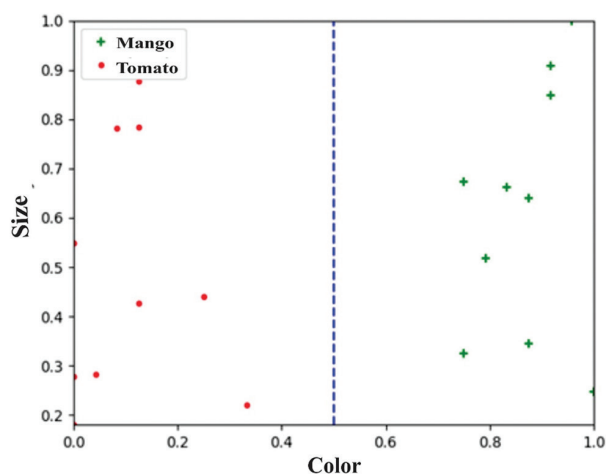


Figure 8. Scatter plot of fruit classification between mango and tomato

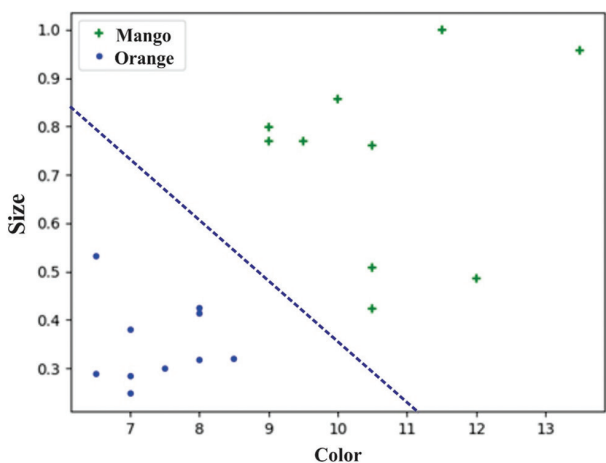


Figure 9. Scatter plot of fruit classification between mango and orange

SVM model efficiently captures the underlying patterns in the data, enabling accurate classification.

Figure 9 provides another visualization of hyperplanes in a two-dimensional feature space. In contrast to Figure 8, where there is a distinct separation between mango and tomato based on the color feature but not size, resulting in a vertical hyperplane. Figure 9 shows a clear separation between mango and orange. Here, both color and size features contribute to the distinction, resulting in a diagonal hyperplane.

### 3.7. Performance of the SVM model

The performance of the SVM model was evaluated using several standard metrics, as depicted in Figure 10, which shows the model's accuracy, precision, recall, and F1 score in the context of fruit classification.

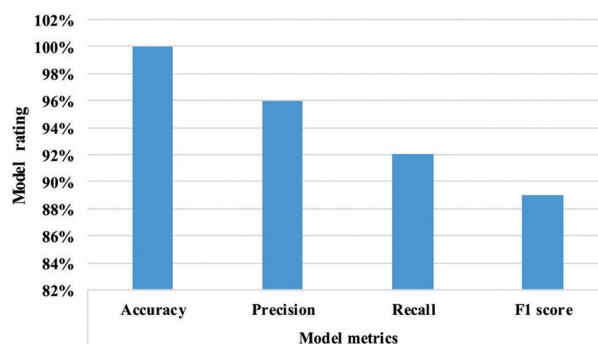


Figure 10. Results obtained from different feature metrics evaluated on the system

The results indicate that the SVM model performed well in classifying the fruits, achieving high scores across all metrics. This is attributed to the effective feature extraction, the selection of an optimal kernel, and careful tuning of the C value.

Therefore, the performance evaluation has identified the capability of the SVM model to classify fruits with reasonably high accuracy using only visual features. This reinforces the potential of image-processing techniques in agricultural applications. The findings also emphasize the importance of selecting appropriate kernels, optimizing model parameters, and use of comprehensive feature sets to further improve the classification accuracy of the system.

## 4. Discussion

The use of image processing techniques in fruit classification solves all the problems associated with the traditional method of classification, such as subjectivity in classification and potential damage to the fruit. Various features can be utilized in the classification system; while some features allow highlighting the differences across fruit classes easily and accurately, the selection of the most impactful features helps reduce the computational power required.

There are various machine learning models available. Naskar and Bhattacharya<sup>46</sup> utilized artificial neural networks and achieved an accuracy above 90%. Similarly, Bahaghighat *et al.*<sup>47</sup> proposed the use of neural networks and reported reasonable results. Bahaghighat *et al.*<sup>47</sup> demonstrate that the SVM model is comparable in effectiveness to other models while offering the advantage of requiring a significantly smaller dataset.

The SVMs are primarily designed for linearly separable data. However, when dealing with non-linear data, a kernel function can be applied. The kernel effectively projects the

input data into a higher-dimensional feature space, where the data are considered linearly separable.<sup>48</sup>

According to Yekkehkhany *et al.*,<sup>48</sup> the linear kernel is the simplest and fastest to process, but the polynomial kernel, though more time-consuming and complicated, often yields more accurate and reliable results. In this study, the polynomial kernel achieved a much greater accuracy than a linear kernel. This suggests that when more than two features are used for fruit classification, utilizing the linear kernel may negatively affect the results obtained.

Color features played a significant role in the classification of the fruits. As such, the quality of the camera and the lighting conditions during image capture are crucial. Poor image quality or inconsistent lighting may distort color representation, particularly due to background interference, which may affect classification results.

## 5. Conclusion

This paper presents an image processing system developed for classifying selected fruits, including oranges, tomatoes, and mangoes. This system demonstrated tremendous potential in enhancing both the efficiency and accuracy of fruit sorting within associated processes. The system achieved impressive performance metrics, with an accuracy of 100%, precision of 96%, recall of 92%, and F1 score of 89%, as shown in [Figure 10](#). These results demonstrate the effectiveness of the implemented techniques and the robustness of the model in accurately classifying fruits.

The findings highlight the importance of feature selection in the classification process. With the inclusion of multiple features, the accuracy of the system increased significantly. This indicates that certain features contribute more strongly to overall classification performance compared to others. For the SVM model, various kernel functions were evaluated. The results show that the polynomial kernel outperformed both the linear kernel and the RBF kernel, demonstrating its effectiveness in handling non-linear relationships within the data.

Furthermore, it is essential to optimize the C value. This study suggests that the optimal C value is tightly connected with the various features' values. This indicates the need for dataset-specific parameter tuning to achieve optimal performance.

The integration of the Arduino board with the automated sorting mechanism, guided by the classification results from the SVM model, sorted all fruits into their respective containers. This integration of image processing

with mechanical sorting provides a proof of concept for a fully automated fruit classification and sorting system.

The image processing system developed in the study demonstrates a reliable and efficient approach to fruit classification, with the potential to enhance quality control and reduce labor costs in the agricultural sector. The findings further emphasize the potential of advanced technologies to replace or improve traditional fruit classification methods. Future research should focus on extending the system to accommodate a wider variety of fruits, along with the integration of machine learning algorithms for real-time fruit classification and sorting.

## Acknowledgments

None.

## Funding

None.

## Conflict of interest

The authors declare that they have no competing interests.

## Author contributions

*Conceptualization:* All authors

*Data curation:* Oluwaseun Emmanuel Oyewande, John Audu

*Formal analysis:* All authors

*Investigation:* Oluwaseun Emmanuel Oyewande

*Methodology:* All authors

*Project administration:* Babatunde Olayinka Oyefeso, John Audu

*Resources:* All authors

*Software:* Oluwaseun Emmanuel Oyewande, John Audu

*Supervision:* Babatunde Olayinka Oyefeso, John Audu

*Validation:* Babatunde Olayinka Oyefeso, John Audu

*Visualization:* Oluwaseun Emmanuel Oyewande, John Audu

*Writing – original draft:* Oluwaseun Emmanuel Oyewande

*Writing – review & editing:* John Audu

## Ethics approval and consent to participate

Not applicable.

## Consent for publication

Not applicable.

## Availability of data

The code, analysis scripts, and datasets supporting this article have been included as part of the supplementary material.

## References

- Ibeawuchi II, Okoli NA, Alagba RA, *et al.* Fruit and vegetable crop production in Nigeria: The gains, challenges and the way forward. *J Biol Agric Healthc.* 2015;5:194-208.
- Tian H, Wang T, Liu Y, Qiao X, Li Y. Computer vision technology in agricultural automation-a review. *Inf Process Agric.* 2020;7(1):1-19.  
doi: 10.1016/j.inpa.2019.09.006
- Li D, Song Z, Quan C, Xu X, Liu C. Recent advances in image fusion technology in agriculture. *Comput Electron Agr.* 2021;191:106491.  
doi: 10.1016/j.compag.2021.106491
- Gupta S, Tripathi AK. Fruit and vegetable disease detection and classification: Recent trends, challenges, and future opportunities. *Eng Appl Artif Intell.* 2024;133:108260.  
doi: 10.1016/j.engappai.2024.108260
- Kaushal S, Tammineni DK, Rana P, Sharma M, SridharK, Chen H. Computer vision and deep learning-based approaches for detection of food nutrients/nutrition: New insights and advances. *Trends Food Sci Technol.* 2024;146:104408.  
doi: 10.1016/j.tifs.2024.104408
- Pauzi NAM, Mustaza SM, Zainal N, Zaman MHM, Moubark AM. Artificial Intelligence in precision agriculture: A review. *J Kejuruter.* 2025;37(2):1025-1047.  
doi: 10.17576/jkukm-2025-37(2)-38
- Iano Y. Image processing-based via agridrones for agriculture fields. In: *Intelligent Designs, Innovations and Sustainability in Agriculture 4.0.* United States: CRC Press; 2025. p. 214.  
doi: 10.1201/9781003380801
- Amin R, Amin S. Machine learning techniques for increasing the productivity of high-quality food products. In: *Artificial Intelligence in the Food Industry.* United States: CRC Press; 2025. p. 239-259.  
doi: 10.1201/9781032633602
- Kheiralipour K, Kazemi A. A new method to determine morphological properties of fruits and vegetables by image processing technique and non-linear multivariate modeling. *Int. J. Food Prop.* 2020;23(1):368-374.  
doi: 10.1080/10942912.2020.1729177
- Han B, Lu Z, Dong L, Zhang J. Lightweight non-destructive detection of diseased apples based on structural re-parameterization technique. *Appl Sci.* 2023;14(5):1907.  
doi: 10.3390/app14051907
- Wang W, Zhu A, Wei H, Yu L. A novel method for vegetable and fruit classification based on using diffusion maps and machine learning. *CRFS.* 2024;8:100737.  
doi: 10.1016/j.crfs.2024.100737
- Shen C, Wang R, Nawazish H, Wang B, Cai K, Xu B. Machine vision combined with deep learning-based approaches for food authentication: An integrative review and new insights. *Compr Rev Food Sci Food Saf.* 2024;23(6):e70054.  
doi: 10.1111/1541-4337.70054
- Usman U, Yunita F, Ridha MR. Improving classification accuracy of local coconut fruits with image augmentation and deep learning algorithm convolutional neural networks (CNN). *JADS.* 2025;6(1):1-19.  
doi: 10.47738/jads.v6i1.389
- Safari Y, Nakatumba-Nabende J, Nakasi R, NakibuuleR. A Review on automated detection and assessment of fruit damage using machine learning. *IEEE Access.* 2024;12:21358-21381.  
doi: 10.1109/ACCESS.2024.3362230
- Anjali JA, Bamola A, Mishra S, *et al.* State-of-the-art non-destructive approaches for maturity index determination in fruits and vegetables: Principles, applications, and future directions. *Food Prod Process Nutr.* 2024;6(1):56.  
doi: 10.1186/s43014-023-00205-5
- Ercan U, Kabas O, Kabaş A, Moiceanu G. Classification of dragon fruit varieties based on morphological properties: Multi-class classification approach. *Sustainability.* 2024;17(6):2629.  
doi: 10.3390/su17062629
- Barbosa JMR, Santos RGD, Sales LDA, Vargas RBS, Deltisid A, Oliveira LPD. Image-based and ML-driven analysis for assessing blueberry fruit quality. *Heliyon.* 2025;11(3):e42288.  
doi: 10.1016/j.heliyon.2025.e42288
- Pathare PB, Opara UL, editors. *Mechanical Damage in Fresh Horticultural Produce: Measurement, Analysis and Control.* Germany: Springer Nature; 2024.  
doi: 10.1007/978-981-99-7096-4
- Hofman PJ, Bower J, Woolf A, Defilippi BG, Olivares D, Garcia-Rojas M. Harvesting, packing, postharvest technology, transport and processing. In: *The Avocado: Botany, Production and Uses.* United Kingdom: CABI; 2024. p. 622-683.  
doi: 10.1079/9781800621824.0015
- Khatun T, Nirob MAS, Bishshash P, Akter M, Uddin MS. A comprehensive dragon fruit image dataset for detecting the maturity and quality grading of dragon fruit. *Data in Brief.* 2024;52:109936.  
doi: 10.1016/j.dib.2023.109936
- Dutta SK, Bhutia B, Misra T, Mishra VK, Singh SK, Patel VB. Application and prospects of artificial intelligence (AI)-

- based technologies in fruit production systems. *Appl Fruit Sci.* 2025;67(1):1-18.  
doi: 10.1007/s10341-024-01223-4
22. Supekar AD, Wakode M. Multi-parameter based mango grading using image processing and machine learning techniques. *NFOCOMP JCS.* 2020;19(2):175-187.
  23. Worasawate D, Sakunasinha P, Chiangga S. Automatic classification of the ripeness stage of mango fruit using a machine learning approach. *AgriEngineering.* 2022;4(1):32-47.  
doi: 10.3390/agriengineering4010003
  24. Doan TN, Le-Thi DN. A Novel mango grading system based on image processing and machine learning methods. *IJACSA.* 2023;14(5):1118-1129.  
doi: 10.14569/IJACSA.2023.01405115
  25. Tripathi MK, Neelakantappa M, Mahalle PN, Channappattana SV, Deshmukh G, Prashant G. Detection and classification of mango fruit-based on feature extraction applying optimized hybrid LA-FF algorithms. In: *Data-Centric Artificial Intelligence for Multidisciplinary Applications.* Boca Raton, FL, USA: Chapman and Hall/CRC; 2024. p. 177-185.  
doi: 10.1201/9781003461500
  26. Kiran PR, Aradwad P, Arunkumar TV, Parray RA. Enhancing mango quality control: A novel approach to spongy tissue inspection through image clustering and machine learning models via X-ray imaging. *J. Food Process Eng.* 2024;47(6):e14664.  
doi: 10.1111/jfpe.14664
  27. Azeez TB. An automatic mango quality grading system in smart agriculture using novel adaptive feature vector and ensemble learning. *Multimed Tools Appl.* 2025;84:1-26.  
doi: 10.1007/s11042-025-20688-3
  28. Siddiquee A, Islam MS, Ud Dowla MY, Rezaul KM, Grout V. Detection, quantification and classification of ripened tomatoes: A comparative analysis of image processing and machine learning. *IET Image Processing.* 2020;14(11):2442-2456.  
doi: 10.1049/iet-ipr.2019.0738
  29. Ropelewska E, Piecko J. Discrimination of tomato seeds belonging to different cultivars using machine learning. *Eur Food Res Technol.* 2022;248:685-705.  
doi: 10.1007/s00217-021-03920-w
  30. Bai Y, Mao S, Zhou J, Zhang B. Clustered tomato detection and picking point location using machine learning-aided image analysis for automatic robotic harvesting. *Precis Agric.* 2023;24(2):727-743.  
doi: 10.1007/s11119-022-09972-6
  31. Vo HT, Mui KC, Thien NN, Tien PP. Automating tomato ripeness classification and counting with YOLOv9. *Int J Adv Comput Sci Appl.* 2024;15(4):1120-1128.
  32. Moya V, Quito A, Pilco A, Vásconez JP, Vargas C. Crop detection and maturity classification using a yolov5-based image analysis. *Emerg Sci J.* 2024;8(2):496-512.  
doi: 10.28991/ESJ-2024-08-02-08
  33. Bhargava A, Bansal A. Automatic detection and grading of multiple fruits by machine learning. *Food Anal Methods.* 2020;13:751-761.  
doi: 10.1007/s12161-019-01690-6
  34. Ismail N, Malik OA. Real-time visual inspection system for grading fruits using computer vision and deep learning techniques. *Inf Process Agric.* 2022;9(1):24-37.  
doi: 10.1016/j.inpa.2021.01.005
  35. Chakraborty SK, Subeesh A, Dubey K, et al. Development of an optimally designed real-time automatic citrus fruit grading-sorting machine leveraging computer vision-based adaptive deep learning model. *Eng Appl Artif Intell.* 2023;120:105826.  
doi: 10.1016/j.engappai.2023.105826
  36. Raza SM, Raza A, Babeker MIA, Haq ZU, Islam MA, Li S. Efficient citrus fruit image classification via a hybrid hierarchical CNN and transfer learning framework. *J Food Meas Charact.* 2025;19(1):356-377.  
doi: 10.1007/s11694-024-02973-1
  37. Huong PT, Hien LT, Son NM, Tuan HC, Nguyen TQ. Enhancing deep convolutional neural network models for orange quality classification using MobileNetV2 and data augmentation techniques. *J Algorithms Comput Technol.* 2025;19:1-22.  
doi: 10.1177/17483026241309070
  38. Lord M. Validation of an invariant embedding method for Fredholm integral equations. *Appl Math Comput.* 1980;7(1):1-7.  
doi: 10.1016/0096-3003(80)90030-2
  39. Nantomah K, Ege I. A lambda analogue of the gamma function and its properties. *Res Math.* 2022;30(2):18-29.  
doi: 10.15421/242209
  40. Coulembier K. Homological kernels of monoidal functors. *Sel Math New Ser.* 2023;29(2):24.  
doi: 10.1007/s00029-023-00829-y
  41. Singh P, Singh N, Singh KK, Singh A. Diagnosing of disease using machine learning. In: *Machine Learning and the Internet of Medical Things in Healthcare.* United States: Academic Press; 2020. p. 89-111.  
doi: 10.1016/B978-0-12-821229-5.00003-3
  42. Obi JC. A comparative study of several classification metrics and their performances on data. *WJAETS.* 2023;8(1):308-314.  
doi: 10.30574/wjaets.2023.8.1.0054

43. Sathyanarayanan S, Tantri BR. Confusion matrix-based performance evaluation metrics. *Afr J Biomed Res.* 2024;27:4023-4031.  
doi: 10.53555/AJBR.v27i4S.4345
44. Humphrey A, Kuberski W, Bialek J, *et al.* Machine-learning classification of astronomical sources: estimating F1-score in the absence of ground truth. *MNRAS Lett.* 2022;517(1):L116-L120.  
doi: 10.1093/mnrasl/slac120
45. Chithra PL, Henila M. Fruits classification using image processing techniques. *IJCSE.* 2019;7(5):131-135.  
doi: 10.26438/ijcse/v7si5.131135
46. Naskar S, Bhattacharya T. A fruit recognition technique using multiple features and artificial neural network. *Int J Comput Appl.* 2015;116:20.  
doi: 10.5120/20453-2808
47. Bahaghighat M, Abedini F, S'hoyan M, Molnar AJ. Vision inspection of bottle caps in drink factories using convolutional neural networks. In: *2019 IEEE 15<sup>th</sup> International Conference on Intelligent Computer Communication and Processing (ICCP).* United States: IEEE; 2019. p. 381-385.  
doi: 10.1109/ICCP48234.2019.8959737
48. Yekkehkhany B, Safari A, Homayouni S, Hasanlou M. A comparison study of different kernel functions for SVM-based classification of multi-temporal polarimetry SAR data. *ISPRS Arch.* 2014;40:281-285.  
doi: 10.5194/isprsarchives-XL-2-W3-281-2014, 2014

## OUR JOURNALS



*Tumor Discovery* is a peer-reviewed and open-access journal that aims to present new cancer research with strong emphasis on fundamental and translational studies. *Tumor Discovery* covers topics, including but not limited to the following:

- Etiology and pathogenesis of cancer
- Mechanisms and molecular pathways underlying cancer initiation and progression
- Tumor metastasis
- Tumor evolution and heterogeneity
- Tumor microenvironment and tumor-host interactions
- Cancer genetics and genomics
- Cancer characterization using omics approaches
- Discovery and validation of cancer biomarker
- Discovery of new therapeutic targets
- New approaches of diagnostic and treatment modalities
- Statistical methods in cancer research

*Global Translational Medicine* is a quarterly journal that focuses on medicine, biological sciences, and biomaterials engineering. The goal of *Global Translational Medicine* is to provide a platform to researchers for showcasing their latest research works in translational medicine so as to advance the field towards the betterment of human health. Despite the advancement of omics and new technologies, the process of transforming these technologies and scientific research results into effective therapies and putting them into clinical use still has a long way to go. *Global Translational Medicine* provides a platform to fill the gaps in preclinical and inter-disciplinary research, to promote clinical translation of scientific research results, and to contribute to the conception of new and improved preventive measures as well as diagnostic and therapeutic techniques of diseases.

*Global Translational Medicine* covers the following themes: cardiovascular disease, metabolism/diabetes/obesity, neuroscience/neurology, cancer, biomaterials and their applications in medicine, proteomics/metabolomics, pharmacogenomics, biomarkers, bioinformatics and data mining, animal and clinical research, and medical methods arising from interdisciplinary crossover.



### Start a new journal

Write to us via email if you are interested to start a new journal with AccScience Publishing. Please attach your CV, professional profile page and a brief pitch proposal in your email. We shall inform you of our decision whether we are interested to collaborate in starting a new journal.

**Contact:** [info@accscience.com](mailto:info@accscience.com)

<https://accscience.com/journal/IJAMD>



Contact

[www.accscience.com](http://www.accscience.com)

9 Raffles Place, Republic Plaza 1 #06-00 Singapore 048619

E-mail: [editorial@accscience.com](mailto:editorial@accscience.com)

Phone: +65 8182 1586